الجمهورية الجزائرية الديمقراطية الشعبية
People's Democratic Republic of Algeria
وزارة التعليم العالي والبحث العلمي
Ministry of Higher Education and Scientific Research

Mohamed Khider University of Biskra
Faculty of Science and Technology
Departement : **Industrial Chemistry**
Ref:.....

جامعة محمد خيضر بسكرة
كلية العلوم والتكنولوجيا
قسم: الكيمياء الصناعية
المرجع:.....

Thesis presented for obtaining the degree of

Doctorate in: Process Engineering

Specialty (Option): Chemical Engineering

Experimental and machine learning approaches of adsorption of pharmaceutical compounds onto various adsorbents

Presented by :
Imane AKACHA

Thesis defended publicly on : 01/07/2026

The jury members

Pr. Elhachmi Guettaf Temam	Professor	Chairman	University of Biskra
Pr. Abdelkrim Merzougui	Professor	Supervisor	University of Biskra
Dr. Khadidja Bouzid	MRA	Co-Supervisor	CRSTRA
Dr. Sihem Djebabra	MCA	Examiner	University of Biskra
Dr. Djenette Elbar	MRA	Examiner	CRSTRA

Academic year : 2025/2026

Acknowledgments

First and foremost, I wish to express my sincere gratitude to **Allah**, who has granted me the health, patience, determination, and strength to accomplish this work. I would like to express my deepest gratitude to my beloved parents for their unwavering moral. I am also thankful to my family for their help, For their dedicated efforts in supporting me throughout the completion of this thesis.

I wish to express my deep gratitude and high regard to my supervisor, Pr. **Abdelkrim MERZOUGUI**, professor at the University of Biskra, for accepting to oversee my research. His invaluable guidance, insightful feedback, generosity, and unwavering encouragement have been instrumental throughout the course of my doctoral studies. I am equally grateful to my co-supervisor, Dr. **Khadidja BOUZID**, researcher at the Scientific and Technical Research Center on Arid Regions Omar El-Bernaoui, Biskra, for her constant assistance and direction, which greatly contributed to the development of this thesis.

I sincerely appreciate Pr. **Elhachmi GUETTAF TEMAM,** professor at the University of Biskra for graciously accepting the honor of chairing my thesis defense jury. I would like to extend my profound gratitude to Dr. **Sihem DJEBABRA** Senior Lecturer A at the University of Biskra and Dr. **Djannet ALBARR**, Reserchер at the Scientific and Technical Research Center on Arid Regions Omar El-Bernaoui, Biskra, for the honor of serving as examiners of this thesis. I am especially thankful for their valuable insights, constructive remarks, and expertise, which have enriched and strengthened this work.

I would like to express my sincere thanks to all those who, directly or indirectly, contributed to the completion of this work. It was carried out at the University of Biskra, within the Laboratory of Civil Engineering, Hydraulics, Sustainable Development and Environment 'LARGHYDE' under the direction of Mr. **Abdelhafid OUNIS**, and at the Scientific and Technical Research Center on Arid Regions 'CRSTRA,' under the direction of Mr. **Mohamed KECHEBAR**

I wish to extend my sincere gratitude to Mrs. **Radia NAILI**, Lab Engineer at the Industrial Chemistry Laboratory of Mohamed Khider University–Biskra; Mrs. **Saliha BENAOUNE**, Mrs. **Narimene BOUZIDI**, and Mr. **Tarik OTHMANE**, Lab Engineers at the Scientific and Technical Research Center on Arid Regions (Omar El-Bernaoui, Biskra), for their kindness, valuable support, and assistance.

I am grateful to my loved ones for their constant support, encouragement, and motivation throughout this work.

Dedication

With all my heart and deepest gratitude, I dedicate this work to:

My father, my first pillar of strength and unwavering support. This achievement bor from your faith in me.

My mother, the source of endless love and guidance this achievement is born from your faith, prayers, and patience.

My sister WAFA, my support, my companion, and the voice that speaks when I cannot.

My brother ABDALLAH, my support and refuge in every challenge, and the voice of reassurance in my moments of doubt.

My aunt, my second mother, your love and support have shaped this success.

My friends by my side through every step Hadjer, Khadidja, Loubna, Rima, Rania, Djihad, Loubna, Hayat, Amani, your companionship and the memories we created together made this journey joyful.

My entire family**, Akacha** and **Lanabi,** your love and support have been the foundation of this success.

All my esteemed teachers, who taught me even a single letter, and to my colleagues throughout my studies who encouraged me with love in difficult moments.

Imane

Contents

Acknowledgments i

Dedication ii

Contents iii

Figures list ix

Tables list xii

Nomenclature xiii

General introduction 1

Part I: Bibiographical part

Chapter 1: Pharmaceutical residues in the aquatic environment

I.1.1. Introduction 6

I.1.2. Pharmaceutical contaminant 6

I.1.3. Sources of pharmaceutical contaminants into the environment 7

I.1.3.1. Pharmaceutical manufacturing 7

I.1.3.2. Human and animal excretion 7

I.1.3.3. Agriculture and aquaculture 8

I.1.3.4. Improper disposal of medications 8

I.1.4. Occurence of pharmaceuticals contaminants 8

I.1.4.1. Surface waters 8

I.1.4.2. Groundwater 9

I.1.4.3. Drinking Water 9

I.1.4.4. Wastewater 9

I.1.5. Effects of pharmaceuticals contaminants on the environment 10

I.1.6. Removal methods for pharmaceutical contaminants 11

I.1.6.1. Biological treatment methods 11

I.1.6.2. Chemical advanced oxidation processes 11

I.1.6.3. Physical treatment methods 12

I.1.6.3.1. Adsorption 12

I.1.6.3.2. Membrane Separation Process 12

I.1.7. Pharmaceuticals used in this study 12

I.1.7.1. Paracetamol 12

I.1.7.2. Diclofenac 13

I.1.8. Conclusion 14

References 15

Chapter 2: Theory and modeling of adsorption process

I.2.1. Introduction 19

I.2.2. Definition 19

I.2.3. Types of adsorption 20

I.2.3.1. Physical adsorption or physisorption 20

I.2.3.2. Chemical adsorption or chemisorption 20

I.2.4. Mass transport mechanism in the adsorption process 21

I.2.5. Factors influencing the adsorption phenomenon 22

I.2.5.1. Influence of adsorbent properties 22

I.2.5.1.1. Adsorbents particle size 22

I.2.5.1.2. Specific surface area (SSA) 22

I.2.5.1.3. Pore size distribution 22

I.2.5.1.4. Surface functional groups 22

I.2.5.2. Influence of adsorbate properties 23

I.2.5.3. Influence of solution chemistry 23

I.2.5.3.1. Solution pH 23

I.2.5.3.2. Solution temperature 23

I.2.5.3.3 Ionic strength 23

I.2.5.3.4. Dosage of adsorbent and contact time 24

I.2.6. Adsorption kinetics 24

I.2.7. Adsorption isotherms 25
I.2.7.1. Giles classification 25
I.2.7.2. Brunauer, Emmett and Teller classification 26
I.2.7.3. Modeling of adsorption isotherms 28
I.2.7.3.1. Langmuir isotherm 28
I.2.7.3.2. Freundlich isotherm 28
I.2.7.3.3. Temkin isotherm 29
I.2.8. Adsorption thermodynamics 29
I.2.9. Adsorption on Carbonaceous materials 31
I.2.9.1. Biochar 32
I.2.9.2. Activated carbon 32
I.2.9.2.1. Activated carbon production through physical activation 32
I.2.9.2.2. Activated carbon production through chemical activation 33
I.2.10. Conclusion 33
References 34

Part II: Experimental part

Chapter 1: Synthesis and characterization of adsorbents

II.1.1. Introduction 38
II.1.2. Cypress tree 38
II.1.3. Characterization of Cypress cones biomass 39
II.1.3.1. Fourier Transform Infrared (FT-IR) 39
II.1.3.2. Scanning Electron Microscopy coupled with Energy Dispersive Spectroscopy 40
II.1.3.3. X-Ray Diffraction (XRD) 40
II.1.3.4. Brunauer -Emmett-Teller (BET) 41
II.1.3.5. Thermogravimetric analysis (TGA) 42
II.1.4. Synthesis of different adsorbents 42
II.1.5. Adsorbents characterization 43

II.1.5.1. Fourier Transform Infrared (FT-IR) 43

II.1.5.2. Scanning Electron Microscopy coupled with Energy Dispersive Spectroscopy 45

II.1.5.3. X-Ray Diffraction (XRD) 47

II.1.5.4. Brunauer -Emmett-Teller (BET) 48

II.1.5.5. pH point of zero charge 50

II.1.6.Conclusion 51

References 52

Chapter 2: Adsorption of Paracetamol and Diclofenac onto CCB-650

II.2.1. Introduction 57

II.2.2. Preparation of synthetic solutions 57

II.2.3. Investigation of Operational Conditions Influencing PCM and DCF Adsorption 57

II.2.3.1. Investigation of Adsorption Kinetics 58

II.2.3.2. Effect of adsorbent dosage 61

II.2.3.3. Effect of pH medium 62

II.2.3.4. Effect of ionic strength 63

II.2.3.5. Investigation of the adsorption isotherm 64

II.2.3.6.Thermodynamic study 65

II.2.4. Conclusion 67

References 68

Chapter 3: Adsorption of Paracetamol and Diclofenac onto CC-$ZnCl_2$-AC

II.3.1. Introduction 70

II.3.2. Investigation of Operational Conditions Influencing PCM and DCF Adsorption 70

II.3.2.1. Investigation of Adsorption Kinetics 70

II.3.2.2. Effect of adsorbent dosage 73

II.3.2.3. Effect of pH medium 74

II.3.2.4. Effect of ionic strength 76

II.3.2.5. Investigation of the adsorption isotherm 76

II.3.2.6. Thermodynamic study 78

II.3.3. Conclusion 79

References 80

Chapter 4: Adsorption of Paracetamol and Diclofenac onto CC-$ZnCl_2$-AC in binary mixture

II.4.1. Introduction 83

II.4.2. Binary experiments 83

II.4.3. Investigation of Operational Conditions Influencing PCM and DCF Adsorption 84

II.4.3.1. Effect of contact time 84

II.4.3.2. Effect of adsorbent dosage 87

II.4.3.3. Effect of pH medium 88

II.4.3.4. Effect of ionic strength 89

II.4.3.5. Effect of concentration 91

II.4.3.6. Thermodynamic study 91

II.4.4. Conclusion 93

References 94

Chapter 5: Machine learning approaches of adsorption of pharmaceutical compounds

II.5.1. Introduction 96

II.5.2. Types of Machine Learning Techniques 96

II.5.2.1. Supervised learning 96

II.5.2.2. Unsupervised learning 96

II.5.2.3. Semi-supervised learning 97

II.5.2.4. Reinforcement learning 97

II.5.3 Adsorption modeling of data via machine learning 97

II.5.3.1. Artificial Neural Networks (ANNs) Algorithm 98

II.5.3.2. Random Forest Regression (RFR) 98

II.5.4. Data collection, model development, and performance evaluation 98

II.5.5. Conclusion 103

References 104

General conclusion 106

Abstract

Resumé

ملخص

annex

Figures list

Figure I.2.1. Schematic depiction of adsorption and desorption processes	19
Figure I.2.2. Adsorption mass transfer steps	21
Figure I.2.3. Classification of adsorption equilibrium isotherms according to Giles	26
Figure I.2.4. Different types of adsorption isotherms	27
Figure I.2.5. Schematic activated carbon model	31
Figure II.1.1. Cypress tree	38
Figure II.1.2. FTIR specta of the raw material CC	39
Figure II.1.3. SEM micrographand EDS analysis of the raw material CC	40
Figure II.1.4. XRD pattern of the raw material CC	41
Figure II.1.5. Nitrogen adsorption isotherm for raw material CC	41
Figure II.1.6. Geographical localization map of the study area	42
Figure II.1.7. Preparation steps of adsorbents	43
Figure II.1.8. FTIR spectra of CCB-450, CCB-550, CCB-650, CC-$ZnCl_2$-AC	44
Figure II.1.9. SEM micrograph and EDS analysis of CCB-450	46
Figure II.1.10. SEM micrograph and EDS analysis of CCB-550	46
Figure II.1.11. SEM micrograph and EDS analysis of CCB-650	46
Figure II.1.12. SEM micrograph and EDS analysis of CC-$ZnCl_2$-AC.	46
Figure II.1.13. XRD pattern of CCB-450, CCB-550, CCB-650, CC-$ZnCl_2$-AC	47
Figure II.1.14. The nitrogen adsorption/desorption isotherms of (a) CCB-650 and (b) CC-$ZnCl_2$-AC	49
Figure II.1.15. The pore size distribution of (a) CCB-650 and (b) CC-$ZnCl_2$-AC	49
Figure II.1.16. pH point of zero charge (pH_{pzc}) of CCB-650 and CC-$ZnCl_2$-AC	51
Figure II.2.1. Typical UV-Vis spectrum of each single solution of PCM and DCF	57
Figure II.2.2. Comparison between the evolutions of the adsorption efficiency of paracetamol and diclofenac on the prepared biochars as a function of time	58

Figure II.2.3. Kinetics of paracetamol adsorption (Nonlinear fitting and Linear fitting of Weber-Morris model)	59
Figure II.2.4. Kinetics of diclofenac adsorption (Nonlinear fitting and Linear fitting of Weber-Morris model)	59
Figure II.2.5. Effect of CCB-650 dose on a) the adsorption capacity and b) the removal efficiency of paracetamol and diclofenac	61
Figure II.2.6. a) Effect of pH medium, b) Effect of ionic stength on the removal of paracetamol and diclofenac onto CCB-650	63
Figure II.2.7. Paracetamol and diclofenac adsorption isothers onto CCB-650	64
Figure II.2.8. Van't Hoff plot for paracetamol and diclofenac removal on CCB-650	66
Figure II.3.1. Kinetics of paracetamol adsorption (Nonlinear fitting and Linear fitting of Weber-Morris model)	71
Figure II.3.2. Kinetics of diclofenac adsorption (Nonlinear fitting and Linear fitting of Weber-Morris model)	71
Figure II.3.3. Effect of CC-$ZnCl_2$-AC dose on a) the adsorption capacity and b) the removal efficiency of paracetamol and diclofenac	74
Figure II.3.4. a) Effect of pH medium, b) Effect of ionic stength on the removal of paracetamol and diclofenac on CC-$ZnCl_2$-AC	75
Figure II.3.5. Paracetamol and diclofenac adsorption isotherms onto CC-$ZnCl_2$-AC	77
Figure II.3.6. Van't Hoff plot for paracetamol and diclofenac removal on CC-$ZnCl_2$-AC	79
Figure II.4.1. Calibration curves of paracetamol and diclofenac at $\lambda_{max\ 1}$ and $\lambda_{max\ 2}$	84
Figure II.4.2. Effect of contact time on the adsorption behavior of diclofenac and paracetamol in binary mixture onto CC-$ZnCl_2$-AC at different concentration ratios	85
Figure II.4.3. Effect of CC-$ZnCl_2$-AC dose on the removal efficiency and the adsorption capacity ofdiclofenac and paracetamol in binary mixture at different concentration ratios	88
Figure II.4.4. Effect of pH medium on the removal of diclofenac and paracetamol onto CC-$ZnCl_2$-AC in binary mixture at different concentration ratios	89
Figure II.4.5. Effect of ionic strength on the removal of diclofenac and paracetamol onto CC-$ZnCl_2$-AC in binary mixture at different concentration ratios	90
Figure II.4.6. Effect of concentration on the removal of diclofenac and paracetamol onto CC-$ZnCl_2$-AC in binary mixture	91
Figure II.4.7. Van't Hoff plot for diclofenac and paracetamol removal onto CC-$ZnCl_2$-AC in binary mixture	92
Figure II.5.1. Predicted versus experimental values for the removal efficiency of PCM and DCF adsorption systems	100

Figure II.5.2. Predicted versus experimental values for the adsorption capacity of PCM and DCF adsorption systems 101

Figure II.5.3. Error deviation plots for PCM and DCF removal prediction model 103

Tables list

Table I.1.1. Characteristics of Diclofenac and Paracetamol	14
Table I.2.1. General characteristics of physisorption and chemisorption	20
Table I.2.2. Equations of kinetic modeling	25
Table I.2.3. Thermodynamic parameters and their interpretations in adsorption studies	30
Table II.1.1. The chemical elements present on the surface of the raw material CC	40
Table II.2.1. Kinetic model parameters for the adsorption of paracetamol and diclofenac on CCB-650	60
Table II.2.2. Parameters of isotherm for paracetamol and diclofenac adsorption onto CCB-650	65
Table II.2.3. Thermodynamic parameters of paracetamol and diclofenac adsorption on CCB-650	67
Table II.3.1. Kinetic model parameters for the adsorption of paracetamol and diclofenac on CC-$ZnCl_2$-AC	73
Table II.3.2. Parameters of isotherm for paracetamol and diclofenac adsorption onto CC-$ZnCl_2$-AC	77
Table II.3.3. Thermodynamic parameters of paracetamol and diclofenac adsorption on CC-$ZnCl_2$-AC	79
Table II.4.1. Kinetic model parameters for the adsorption of paracetamol and diclofenac in binary mixture onto CC-$ZnCl_2$-AC at different concentration ratios	86
Table II.4.2. Thermodynamic parameters of diclofenac and paracetamol adsorption onto CC-$ZnCl_2$-AC in binary mixture.	93
Table II.5.1. Performance evaluation of ANN and RFR models using statistical parameters for PCM and DCF adsorption	99

Nomenclature

ECs: Emerging contaminants

PhCs: Pharmaceuticals

CC: Cypress cones

CCB-650: Cypress cones biochar carbonized at 650 °C

CC-$ZnCl_2$-AC: Cypress cones activated carbon using $ZnCl_2$

APAP/PCM: Paracetamol

DCF: Diclofenac de sodium

UV: Ultraviolet

FTIR: Fourier Transform Infrared

BET: Brunauer -Emmett-Teller

XRD: X-Ray Diffraction

SEM: Scanning Electron Microscopy

pH : Potential of hydrogen

pH_{PZC} : The pH of point zero charge

q_m : Maximum adsorption capacity

q_e : Equilibrium adsorption capacity

C_e : Equilibrium concentration

K_L, K_F, K_T : Langmuir, Freundlich, et Temkin isotherm constants

K_1, K_2: first-order /second order adsorption reaction rate constants

K_{int}: The constant of the Intraparticle diffusion (IPD) model

S_{BET}: Surface BET

PFO: Pseudo-premier ordre

PSO: Pseudo-second-ordre

$\Delta G°$: Gibbs free energy

$\Delta H°$: Change in Enthalpy

$\Delta S°$: Change in Entropy

ML: Machine Learning

ANN: Artificial Neural Network

RFR: Random Forest Regression

General introduction

General introduction

Water is a fundamental component of our planet, forming the basis of life and playing a key role in maintaining the stability and proper functioning of Earth's ecological systems. It is a vital resource, necessary for drinking as well as for numerous everyday developmental and sustenance-related activities (Ali and Gupta 2006). The accelerating demand for clean water, coupled with its declining availability, has become a global concern, driven by factors such as rapid industrialisation, population expansion, prolonged droughts, urbanisation, agricultural practices, and various geological, environmental, and climatic shifts. To address this growing need, numerous practical measures have been implemented to develop sustainable water supplies. Examples include harvesting rainwater for daily use and enhancing stormwater catchment capacity, which can offer short-term relief. In arid regions with intense sunlight, scarce rainfall, and persistent drought, both water authorities and governments face the pressing challenge of identifying reliable, long-term water sources (Chong, Jin et al. 2010).

Water supply systems are increasingly contaminated by emerging contaminants, including pesticides, artificial fertilisers, industrial chemicals such as dyes, toxic heavy metals, pharmaceuticals, hormones, personal care products, and cleaning agents (Mustafa and Hassan 2024). Over the past few decades, numerous substances, both entirely human-made and naturally occurring, have been detected in aquatic environments, raising concerns about the health of the planet's ecosystems and surface waters. In natural settings, the majority of these pollutants are organic compounds, usually present in extremely low concentrations, ranging from parts per trillion (ppt or ng/L) to parts per billion (ppb or μg/L). These substances are commonly referred to as "emerging contaminants (ECs)," micropollutants, emerging pollutants, contaminants of emerging concern, or trace organic compounds (Kumar, Qureshi et al. 2022).

Pharmaceuticals play a crucial role in preventing and treating diseases in both humans and animals, yet their extensive use has led to a growing presence in the environment. As a result, the detection of these compounds and their potential impacts on human health and ecosystems has become a significant focus of current research. Medications used for medical and veterinary purposes are often released into the environment. It is important to recognise

that municipal wastewater, regardless of its source, will inevitably contain pharmaceutical residues stemming from metabolic excretion, improper disposal, or industrial activities, while the specific types, concentrations, and proportions of these substances vary from one region to another (Jelić, Gros et al. 2012; Abd El-Fattah, Maged et al. 2023).

Given growing concerns about pharmaceutical contamination, many researchers have focused on developing biological, physical, and chemical methods to eliminate or degrade these substances in water (Serna-Galvis, Arboleda-Echavarría et al. 2024). In addressing this challenge, sorption processes can offer notable benefits, including high efficiency, simplicity, low cost and sustainability (Li, Taggart et al. 2019). Carbon-based materials are regarded as highly efficient adsorbents for eliminating pollutants and treating wastewater, owing to their large surface area and unique physical and chemical characteristics (Nazal 2020).

With the rapid growth of technology and population, vast quantities of agricultural and food waste are being produced worldwide. Traditionally, such waste was either burned or left to decompose in fields, practices that pose serious environmental risks. Hence, new strategies for their utilisation, recycling, and processing are essential to promote sustainable feedstock use and minimise pollution. Agricultural residues are primarily composed of cellulosic fibres, which are rich in fixed carbon and functional groups. Their notable features, such as high strength, eco-friendliness, low cost, wide availability, and reusability, make them valuable materials. Owing to these properties, agricultural waste has been extensively studied for wastewater treatment (Rao and Rathod 2019).

The development of computational science, especially machine learning provides a powerful tool to reveal the complex nonlinear relationship in the adsorption process. These empirical modelling techniques are characterized by total knowledge independence regarding the phenomenological nature of the process considered, being capable of mapping non-linear relationships between a group of input and output variables. Several algorithms have been used in the development of empirical models for adsorption(Soares, de Oliveira Carvalho et al. 2020; Zhang, Chen et al. 2023)

The objective of this study is to explore the valorization of Cypress cones as a low-cost and eco-friendly biosorbent for the decontamination of water polluted with pharmaceutical compounds, with particular emphasis on the removal of paracetamol and

diclofenac. This process was modelled using a machine learning algorithm Random Forest (RFR) and compared with the traditional Artificial Neural Networks (ANN) approach.

This study has dual environmental significance: first, the development of efficient, low-cost adsorbents derived from natural, locally available agricultural waste precursors, specifically cypress cones; and second, the treatment of pharmaceutical-contaminated water through adsorption in single- and binary-batch systems. The adsorbents investigated include biochars synthesised at different pyrolysis temperatures (450–650 °C), designated CCB-450, CCB-550, and CCB-650, and a chemically modified carbon (CC-$ZnCl_2$-AC).

To examine each point outlined in the introduction in greater depth, the thesis is organised into two subsequent parts, each further divided into several chapters.

The first part of this work comprises two chapters that present a literature review of pharmaceutical residues in the environment and the adsorption process. The first chapter focuses on the occurrence of pharmaceutical products in the aquatic environment, tracing their sources and their detrimental impacts on the ecosystem, while also examining the principal treatment processes employed to remove these pollutants. The second chapter offers a general overview of the adsorption process, presenting its fundamental principles, the various types of adsorption, the modelling equations related to adsorption kinetics and isotherms, and the thermodynamic equations. Furthermore, a review of carbon-based adsorbents applied in water treatment is provided.

The second part will be divided into five chapters. In the first chapter, the preparation methods and characterisation results (BET, FTIR, MEB, DRX, and pH_{PZC}) of different adsorbents derived from cypress cones, CCB-450, CCB-550, CCB-650, and CC-$ZnCl_2$-AC, are presented. The second chapter will present the results of adsorption experiments on the two pharmaceutical products in synthetic solutions using CCB-650, the best adsorbent among the prepared biochars. Subsequently, the third chapter will present the results of adsorption experiments on paracetamol and diclofenac in synthetic solutions, in a single-component system, using CC-$ZnCl_2$-AC. The fourth chapter will present the results obtained for binary systems of (PCM + DCF) in synthetic solutions using the best-prepared adsorbent, CC-$ZnCl_2$-AC. Lastly, Chapter 5 discusses the use of machine learning approaches for predicting the adsorption performance of CC-$ZnCl_2$-AC toward PCM and DCF.

References

Abd El-Fattah, H., A. Maged, et al. (2023). "Recent technologies for the elimination of pharmaceutical compounds from aqueous solutions: A review." Frontiers in Scientific Research and Technology **5**(1) DOI: 10.21608/FSRT.2023.173676.1074.

Ali, I. and V. Gupta (2006). "Advances in water treatment by adsorption technology." Nature protocols **1**(6): 2661-2667 DOI: https://doi.org/10.1038/nprot.2006.370.

Chong, M. N., B. Jin, et al. (2010). "Recent developments in photocatalytic water treatment technology: a review." Water research **44**(10): 2997-3027 DOI: https://doi.org/10.1016/j.watres.2010.02.039.

Jelić, A., M. Gros, et al. (2012). Occurrence and elimination of pharmaceuticals during conventional wastewater treatment. Emerging and priority pollutants in rivers: Bringing science into river management plans, Springer**:** 1-23.

Kumar, R., M. Qureshi, et al. (2022). "A review on emerging water contaminants and the application of sustainable removal technologies." Case Studies in Chemical and Environmental Engineering **6**: 100219 DOI: https://doi.org/10.1016/j.cscee.2022.100219.

Li, Y., M. A. Taggart, et al. (2019). "Utilizing low-cost natural waste for the removal of pharmaceuticals from water: Mechanisms, isotherms and kinetics at low concentrations." Journal of Cleaner Production **227**: 88-97 DOI: https://doi.org/10.1016/j.jclepro.2019.04.081.

Mustafa, B. M. and N. E. Hassan (2024). "Water contamination and its effects on human health: A review." Journal of Geography, Environment and Earth Science International **28**(1): 38-49 DOI: DOI: 10.9734/JGEESI/2024/v28i1743.

Nazal, M. K. (2020). "An overview of carbon-based materials for the removal of pharmaceutical active compounds." Carbon-Based Material for Environmental Protection and Remediation DOI: http://dx.doi.org/10.5772/intechopen.82334.

Rao, P. and V. Rathod (2019). "Valorization of food and agricultural waste: a step towards greener future." The chemical record **19**(9): 1858-1871 DOI: https://doi.org/10.1002/tcr.201800094.

Serna-Galvis, E. A., J. Arboleda-Echavarría, et al. (2024). "Removal and elimination of pharmaceuticals in water using zeolites in diverse adsorption processes and catalytic advanced oxidation technologies—a critical review." Environmental Science and Pollution Research **31**(55): 63427-63457 DOI: https://doi.org/10.1007/s11356-024-35204-7.

Soares, A. P. d. M. R., F. de Oliveira Carvalho, et al. (2020). "Random Forest as a promising application to predict basic-dye biosorption process using orange waste." Journal of environmental chemical engineering **8**(4): 103952 DOI: https://doi.org/10.1016/j.jece.2020.103952

Zhang, W., R. Chen, et al. (2023). "Synthesis optimization and adsorption modeling of biochar for pollutant removal via machine learning." Biochar **5**(1): 25 DOI: https://doi.org/10.1007/s42773-023-00225-x.

Part I :

Bibiographical part

Chapter I:

Pharmaceutical residues in the aquatic environment

I.1.Pharmaceutical residues in the aquatic environment

I.1.1. Introduction

With the rapid emergence of various metabolic and multiple-drug-resistant infectious diseases, new pharmaceuticals are continuously being introduced in the market. The excess production and use of pharmaceuticals, and their untreated/unmetabolised release into the environment, contaminate aquatic ecosystems and thus compromise the environment and human health (Sharma, Joshi et al. 2022). In recent years, the occurrence and fate of pharmaceutically active compounds in the aquatic environment have been recognised as an emerging issue in environmental chemistry (Heberer 2002). The primary objective of this chapter is to provide an overview of pharmaceutical products, Sources of pharmaceutical contaminants into the environment, the occurrence of pharmaceuticals in aquatic systems, and the adverse effects associated with these compounds.

I.1.2. Pharmaceutical contaminant

Pharmaceutical compounds include a wide range of chemicals with diverse structures, functions, behaviours, and activities (Al Qarni, Collier et al. 2016). Pharmaceuticals, considered one of the most significant milestones in the development of science for humanity, have expanded life spans, cured many from lethal ailments and significantly refined the standards of our lives (Gupta, Kumar et al. 2024). In the last two decades, pharmaceuticals have been considered emerging pollutants in the aquatic environment due to their high persistence, low biodegradability, and harmful effects on human and animal health and on aquatic life. These compounds contain various groups, including antibiotics, anti-inflammatory agents, lipid regulators, and steroidal hormones. Pharmaceutical industries, personal hygiene products, hospital waste, and animal or human excretion via urine or faeces are some of the primary sources of these pollutants in water. They can indirectly enter the human food chain through other sources, such as fertilisers. Pharmaceutical compounds have been detected in all aquatic environmental matrices, including drinking water, surface water (rivers, lakes, etc.), groundwater, and wastewater treatment plant effluents, in many different countries, posing a major environmental problem (Karimi-Maleh, Ayati et al. 2021). PhCs can be toxic, persistent, and capable of bioaccumulating in organisms at different trophic levels, thereby posing a hazard to wildlife. As PhCs are designed to exert specific biological activity, they can cause immediate effect (acute toxicity) towards the organism. Then, long-term

exposure of the PhCs towards organisms, even in sub-inhibitory concentrations, is potentially associated with chronic toxicity (Lee, Goh et al. 2020).

I.1.3. Sources of pharmaceutical contaminants into the environment

Drug residues in the environment are perhaps the most recognisable indicators of how everyday human actions, activities, and behaviours can directly impact the environment.

I.1.3.1. Pharmaceutical manufacturing

The first significant source of pharmaceutical pollution is the industry itself, which produces these compounds on a massive scale. Despite rigorous regulations, manufacturing plants often discharge effluents directly into wastewater streams. These effluents, laden with APIs, enter aquatic environments when proper treatment protocols are not in place or are ineffective. This issue is exacerbated in regions with a high concentration of pharmaceutical production, resulting in severe localised pollution (Ashiwaju, Uzougbo et al. 2024).

I.1.3.2. Human and animal excretion

The second prominent source of pharmaceutical pollution is much more diffuse and extends to virtually every household. Pharmaceutical substances (such as antibiotics, anti-anxiety agents, analgesic anti-inflammatories, hormones, antiepileptics, etc.) are discharged into the public wastewater system either through improper disposal in toilets or sinks, or following human consumption via urine and faeces. In the latter case, scientific studies have shown that the human body does not fully absorb all ingested pharmaceutical compounds. A significant portion is excreted either in its original form or as metabolites, ultimately reaching wastewater treatment plants for processing (Kheira 2023). The excretion of pharmaceutical residues by humans and animals. Not all active pharmaceutical ingredients consumed are fully metabolised by the body; significant quantities are expelled via urine and faeces, which eventually enter sewage systems. This issue is magnified with the use of veterinary pharmaceuticals, where residues can be directly introduced into the environment through the application of manure on agricultural land. Such contributions make human and animal excretion a widespread and challenging source of pharmaceutical pollution to tackle (Ashiwaju, Uzougbo et al. 2024).

I.1.3.3. Agriculture and aquaculture

Pharmaceuticals are widely used in agriculture and aquaculture. Antibiotics and steroids are among the most widely used in agriculture and aquaculture. Though the pharmaceuticals used for humans are similar to those used for animals, the quantity of drugs used in agriculture is enormous. Thus, the residues entering the environment at higher concentrations have the potential to cause ecological damage. In aquaculture, drugs are introduced directly into the environment. Highly toxic drugs like chloramphenicol, nitrofurazone and furazolidone are used at high concentrations, which results in accumulation in seafood. These antibiotics can easily enter the food chain if consumed by humans and exert adverse effects. Antibiotic-treated animals' excretory products are used as manure, and pharmaceutical residues enter the soil. These residues are accumulated in the roots and stems of the plants (Kumar, Lakkaboyana et al. 2023).

I.1.3.4. Improper disposal of medications

Improper disposal of leftover or expired medications has become a serious threat to environmental well-being. In many cases, unused drugs are thrown away with household waste or washed down sinks and toilets. Such actions allow pharmaceutical substances to flow directly into landfill leachate or wastewater systems, often without undergoing any treatment or breakdown, enabling them to infiltrate various environmental compartments. Though this may appear trivial on an individual level, the cumulative effect across worldwide medication consumption creates a widespread and persistent source of pharmaceutical contamination (Ashiwaju, Uzougbo et al. 2024).

I.1.4. Occurence of pharmaceuticals contaminants

Measurable concentrations of pharmaceuticals can be found today in surface water, ground water, effluents and even drinking water, usually in the range of $\mu g.L^{-1}$ to $ng.L^{-1}$.

I.1.4.1. Surface waters

Pharmaceutical contamination has a pronounced impact on surface waters, mainly because many wastewater treatment facilities discharge their treated effluents directly into rivers. This direct discharge leaves these aquatic systems highly susceptible to human-derived pollutants, particularly active pharmaceutical ingredients. Compounds that are both extensively used (such as paracetamol and aspirin) and resistant to degradation (such as carbamazepine and diclofenac) are among the most commonly identified. In many cases, their

concentrations surpass 100 ng·L^{-1}, highlighting the considerable exposure risk and fragility of these freshwater environments (Thiebault 2015).

I.1.4.2. Groundwater

Groundwater resources are considered sensitive due to their diverse uses. Two primary uses can remobilise pollutants and bring them back to the surface. The first is the use of groundwater for crop irrigation, which may have possible health implications in certain practices, such as market gardening, or lead to the contamination of agricultural soils in general. The second is its use for drinking water, often abstracted from aquifers that, in some regions, are relatively shallow and therefore vulnerable. Understanding the types and levels of pollution present in groundwater is therefore essential for guiding the utilisation of this resource while minimising associated risks (Thiebault 2015). The occurrence of pharmaceuticals was widely detected in the groundwaters, and it was found that pharmaceuticals in groundwater mainly came from the infiltration of landfill leachate (Tang, Yin et al. 2019)

I.1.4.3. Drinking Water

The presence of pharmaceuticals in drinking water has become a pressing worldwide issue because of the potential dangers they pose to both human health and the environment. The detection of antibiotics in these water sources is particularly alarming, as it can drive the emergence of antibiotic-resistant strains in both disease-causing organisms and environmental microbes. Such resistance undermines the effectiveness of antibiotic treatments, creating significant challenges for global healthcare systems. In addition, these substances can disrupt natural microbial populations, leading to shifts in biodiversity and impairing essential ecosystem processes (Patterton 2013; Nnamso D. Ibuotenang and Fatunla 2025).

I.1.4.4. Wastewater

Wastewater is defined as a reservoir of pharmaceutical products discharged through various drainage and sanitation systems. The influent entering wastewater treatment plants contains substantial amounts of both organic and inorganic pollutants, including biodegradable and non-biodegradable compounds. While a significant portion of these contaminants is removed during the different treatment processes within the plant, a fraction persists due to their low biodegradability (CHEBBI 2024).

I.1.5. Effects of pharmaceuticals contaminants on the environment

Studies have revealed that numerous widely used pharmaceuticals persist in the environment due to their resistance to natural breakdown processes. As a result, traces of these compounds, ranging from the order of micrograms per litre to nanograms per litre, are now commonly detected in both aquatic systems and soil environments. The ongoing release of insufficiently treated wastewater introduces these substances into ecosystems, where their interaction with other environmental pollutants may trigger unpredictable and potentially harmful ecological consequences.

Fish are among the species most susceptible to elevated levels of pharmaceutical contaminants. Research indicates that substances such as Diclofenac and 17α-ethinylestradiol can cause tissue damage in organs such as the kidneys and intestines, as well as disrupt gene expression associated with essential metabolic functions. Prolonged exposure to these compounds may compromise fish survival and reproductive capabilities. Furthermore, evidence suggests that the impact of Diclofenac on fish organs may resemble those observed in mammals, including humans (Li 2014). Feminisation of river fish is also observed in the presence of endocrine disruptors, such as ethinylestradiol. This alteration of the male-to-female ratio can pose a threat to the survival of affected species by reducing their viability and disturbing the balance of the aquatic ecosystem (Kheira 2023). Pharmaceuticals have harmful effects not only on fish but also on algae and microorganisms in aquatic ecosystems. Increased concentrations of drugs such as Carbamazepine, Diclofenac, and Sulfamethoxazole can damage chloroplasts in algae, impairing photosynthesis and fatty acid synthesis, both of which are vital for plant growth and survival. These substances can also cause chronic toxicity to algae's photosynthetic systems. As a result, algae mortality increases, leading to secondary environmental impacts such as eutrophication, food chain disruption, and ecosystem imbalance (Li 2014). The widespread presence of antibiotics in the environment promotes the development and spread of antimicrobial resistance. This leads to the emergence of resistance genes in microbial communities, creating reservoirs of resistant bacteria in water, soil, and food. Such contamination alters natural microbial ecosystems and can disrupt the human microbiome through exposure. As a result, it reduces the effectiveness of antibiotics, posing serious risks to both environmental and public health (Chaturvedi, Shukla et al. 2021). (Wang, Xi et al. 2021) Explain how certain pharmaceuticals, depending on their physicochemical properties and slow biotransformation rates, can persist in aquatic organisms and magnify through successive trophic levels.

I.1.6. Removal methods for pharmaceutical contaminants

Pharmaceutical removal techniques can generally be grouped into biological, physical, and chemical approaches. In biological systems, the activated sludge method, based on microbial breakdown, is the predominant option and typically serves as a secondary stage in wastewater treatment. Physical techniques most frequently involve adsorption or membrane filtration. In the realm of chemical treatments, advanced oxidation processes are extensively applied, particularly in tertiary treatment stages (Loganathan, Vigneswaran et al. 2023).

I.1.6.1. Biological treatment methods

This method relies on microorganisms (primarily bacteria) to break down wastewater contaminants through biochemical reactions, ultimately producing stable end products. Biological treatment techniques are typically classified as aerobic or anaerobic, depending on whether dissolved oxygen is present during the process (Reddy, Sandeep et al. 2014).

At present, microbial degradation is the primary means of eliminating organic pollutants, favoured for its affordability and straightforward operation. Microorganisms can metabolise these contaminants either as single species or in mixed communities, breaking them down and reducing their toxicity through enzyme-mediated reactions. In conventional wastewater treatment plants, the activated sludge process is commonly employed for the removal of Pharmaceuticals. The efficiency of this method varies with the configuration and capacity of the sludge bioreactor, as well as operational parameters such as pH, hydraulic retention time, and the chemical characteristics of the specific compounds being treated (Loganathan, Vigneswaran et al. 2023).

I.1.6.2. Chemical advanced oxidation processes

Advanced oxidation processes are a group of methods that operate in the aqueous phase, in which highly reactive species degrade the target pollutant. Advanced oxidation processes involve using potent oxidising agents like ozone and peroxide, and/or catalysts like Iron, Manganese, or Titanium dioxide, usually in combination with high-energy radiation such as UV irradiation, and produce a potent, non-selective oxidising species: the hydroxyl radical (•OH). Once these radicals are formed, they oxidise the organic pollutants, producing biodegradable intermediates that are then mineralised to water, carbon dioxide, and inorganic salts. Hydroxyl radicals formed in advanced oxidation processes react principally via mechanisms such as hydrogen abstraction, electrophilic addition to π systems, and electron transfer reactions (Karungamye 2020). The most important processes of advanced oxidation

treatment are Photolysis, Ozonation, Fenton oxidation, photocatalysis, and Electrochemical oxidation.

I.1.6.3. Physical treatment methods

Physical methods exhibit high removal efficiency, ease of operation, and more straightforward implementation, making them suitable for various water treatment applications (Gupta, Kumar et al. 2024).

I.1.6.3.1. Adsorption

Solid-based adsorption is considered a highly effective technique for removing various pharmaceutical contaminants from both water and wastewater. Research has shown that carbon-based materials can serve as a cost-effective option for removing pharmaceutical contaminants from wastewater. These adsorbents are generally grouped into two categories: natural and industrial. Natural adsorbents such as coal, clay minerals, zeolites, and mud are inexpensive, widely available, and can be modified to enhance their adsorption performance. Industrial adsorbents, on the other hand, are derived from diverse sources including agricultural by-products, household refuse, industrial residues, sanitation waste, polymer-based materials, and various metallic wastes. Examples include residues from fertiliser and sugar production, algae, red clay, sediments, and untreated soil (Taha and Ahmed 2024).

I.1.6.3.2. Membrane Separation Process

Membrane separation is a method for isolating compounds or molecules by passing them through minute pores or narrow channels in a semipermeable membrane. This approach is classified by the membrane's pore size and the operating pressure. In principle, it works by exerting external pressure to drive water from a solution with high solute concentration (and high osmotic pressure) through the membrane toward a solution with lower solute concentration (and lower osmotic pressure). Standard techniques include microfiltration, ultrafiltration, nanofiltration, and reverse osmosis, arranged from larger to smaller pore sizes and from lower to higher pressure demands (Lee, Goh et al. 2020).

I.1.7. Pharmaceuticals used in this study

I.1.7.1. Paracetamol

Paracetamol (APAP), also referred to as acetaminophen, is extensively utilised worldwide for its properties as a painkiller, fever reducer, and anti-inflammatory agent, with annual consumption reaching approximately (1.45 × 105 tons/year) (Hassani, Eghbali et al.

2020). Paracetamol belongs to a group of organic pollutants that are persistently released into aquatic ecosystems through sources such as hospital discharge, household usage, improper disposal, and pharmaceutical production (Montaseri and Forbes 2018). Due to its low absorption rate in the human body (approximately 5%–15%) and high water solubility (~12–14 g/L at 20 °C), it has been detected at notable concentrations (6.8–8.6 µg/L) in surface waters (Hassani, Eghbali et al. 2020). Additionally, it is frequently present in municipal wastewater effluents, where its concentration can range from 0.1 to 10 mg/L (Yanyan, Kurniawan et al. 2018). Even at low concentrations, paracetamol has been linked to several harmful effects, such as both acute and chronic toxicity in aquatic organisms and suppression of cell growth in human cells. Although it is not environmentally persistent, its constant release and rapid transformation in aquatic systems can still lead to long-term adverse impacts(Montaseri and Forbes 2018).

I.1.7.2. Diclofenac

Diclofenac, chemically known as 2-(2,6-dichloranilino) phenylacetic acid (DCF), is a widely prescribed non-steroidal anti-inflammatory drug (NSAID) recognised for its potent effects. It stands out among NSAIDs for having the most significant level of acute toxicity. This compound is frequently utilised in managing pain and inflammation associated with conditions such as rheumatoid arthritis (de Franco, de Carvalho et al. 2018; Samah, Sánchez-Martín et al. 2018). Diclofenac enters the environment primarily via discharge from sewage treatment plants, which are often not equipped to break it down effectively. As a result, its elimination efficiency in these facilities is typically low, with removal rates frequently falling below 20% (Viotti, Moreira et al. 2019; Salomão, Américo-Pinheiro et al. 2021). Owing to their biological activity, diclofenac and similar pharmaceuticals have emerged as environmental pollutants. Their lipophilic properties and resistance to biodegradation contribute to their tendency to accumulate in living organisms and remain in ecosystems for extended periods (Salomão, Américo-Pinheiro et al. 2021). Even at minimal concentrations, the presence of diclofenac has been linked to various harmful effects, including disruption of microbial functions, the emergence of resistant microbial strains, interference with hormonal systems, and a decline in overall biodiversity (Viotti, Moreira et al. 2019). Additionally, it can cause toxicity to aquatic organisms and plants by altering their normal physiological processes, such as inducing feminisation and disrupting the balance of natural food chains (Salomão, Américo-Pinheiro et al. 2021).

Table I.1.1. Characteristics of Diclofenac and Paracetamol.

	Paracetamol	Diclofenac sodium
Chemical stucture	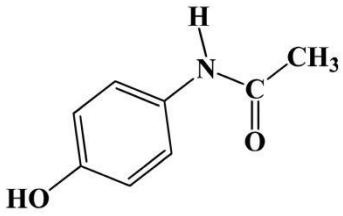	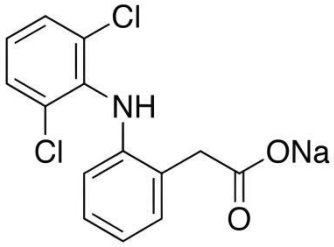
IUPAC name	N-(4-hydroxyphenyl)acetamide	2-[2-[(2,6-dichlorophenyl)amino]-phenyl]acetate
Type	Non-steroid anti-inflammatory drug	Non-steroid anti-inflammatory drug
Molecular formula	$C_8H_9NO_2$	$C_{14}H_{10}Cl_2NNaO_2$
Molecular weight	151.163 g/mol	318.13 g/mol
λ_{max}	241 nm	276 nm
pK_a	9.39	4.15
Log K_w	0.46	0.70

I.1.8. Conclusion

In conclusion, the literature study shows that pharmaceutical pollutants are a new class of contaminants that pose serious environmental risks. Because of their persistence, bioaccumulation capacity, and detrimental impacts on ecosystems and human health, their continuous release into aquatic environments poses serious concerns. Investigating alternative, more effective techniques is necessary because conventional treatment methods often fall short of eliminating harmful chemicals.

References

Al Qarni, H., P. Collier, et al. (2016). "Investigating the removal of some pharmaceutical compounds in hospital wastewater treatment plants operating in Saudi Arabia." Environmental Science and Pollution Research **23**: 13003-13014 DOI: https://doi.org/10.1007/s11356-016-6389-7.

Ashiwaju, B. I., C. G. Uzougbo, et al. (2024). "Environmental impact of pharmaceuticals: a comprehensive review." Matrix Science Pharma **7**(3): 85-94 DOI: 10.4103/mtsp.mtsp_15_23.

Chaturvedi, P., P. Shukla, et al. (2021). "Prevalence and hazardous impact of pharmaceutical and personal care products and antibiotics in environment: A review on emerging contaminants." Environmental Research **194**: 110664 DOI: https://doi.org/10.1016/j.envres.2020.110664.

CHEBBI, M. (2024). Valorisation des matériaux locaux pour l'élimination des produits pharmaceutiques par procédés physico-chimiques de traitement, Faculté Science et technologie.

De Franco, M. A. E., C. B. de Carvalho, et al. (2018). "Diclofenac removal from water by adsorption using activated carbon in batch mode and fixed-bed column: isotherms, thermodynamic study and breakthrough curves modeling." Journal of Cleaner Production **181**: 145-154 DOI: https://doi.org/10.1016/j.jclepro.2018.01.138.

Gupta, A., S. Kumar, et al. (2024). "Pharmaceutically active micropollutants: Origin, hazards and removal." Frontiers in Microbiology **15**: 1339469 DOI: https://doi.org/10.3389/fmicb.2024.1339469.

Hassani, A., P. Eghbali, et al. (2020). "Acetaminophen removal from aqueous solutions through peroxymonosulfate activation by CoFe2O4/mpg-C3N4 nanocomposite: insight into the performance and degradation kinetics." Environmental Technology & Innovation **20**: 101127 DOI: https://doi.org/10.1016/j.eti.2020.101127.

Heberer, T. (2002). "Occurrence, fate, and removal of pharmaceutical residues in the aquatic environment: a review of recent research data." Toxicology letters **131**(1-2): 5-17 DOI: https://doi.org/10.1016/S0378-4274(02)00041-3.

Karimi-Maleh, H., A. Ayati, et al. (2021). "Recent advances in using of chitosan-based adsorbents for removal of pharmaceutical contaminants: A review." Journal of Cleaner Production **291**: 125880 DOI: https://doi.org/10.1016/j.jclepro.2021.125880.

Karungamye, P. N. (2020). "Methods used for removal of pharmaceuticals from wastewater: A review." Applied Journal of Environmental Engineering Science **6**(4): & al./Appl. J. Envir. Eng. Sci. 6 N° 4 (2020) 2412-2428 DOI: https://doi.org/10.48422/IMIST.PRSM/ajees-v6i4.23828.

Kheira, A. (2023). "Élimination des polluants pharmaceutiques sur des Argiles naturelles et synthétiques." Université Dr Yahia Farès de Médéa.

Kumar, V., S. K. Lakkaboyana, et al. (2023). "A critical assessment of technical advances in pharmaceutical removal from wastewater–a critical review." Case Studies in Chemical and Environmental Engineering **8**: 100363 DOI: https://doi.org/10.1016/j.cscee.2023.100363.

Lee, W., P. Goh, et al. (2020). "Removal of pharmaceutical contaminants from aqueous medium: a state-of-the-art review based on paracetamol." Arabian Journal for Science and Engineering **45**(9): 7109-7135 DOI: https://doi.org/10.1007/s13369-020-04446-1.

Li, W. C. (2014). "Occurrence, sources, and fate of pharmaceuticals in aquatic environment and soil." Environmental pollution **187**: 193-201 DOI: https://doi.org/10.1016/j.envpol.2014.01.015.

Loganathan, P., S. Vigneswaran, et al. (2023). "Treatment trends and combined methods in removing pharmaceuticals and personal care products from wastewater—a review." Membranes **13**(2): 158 DOI: https://doi.org/10.3390/membranes13020158.

Montaseri, H. and P. B. Forbes (2018). "Analytical techniques for the determination of acetaminophen: A review." TrAC Trends in Analytical Chemistry **108**: 122-134 DOI: https://doi.org/10.1016/j.trac.2018.08.023.

Nnamso D. Ibuotenang, P. O. A., Solomon E. Shaibu, Utibe A. Ofon, Opeyemi K. and O. A. A. Fatunla (2025). "Pharmaceuticals in Drinking Water: Assessing human Exposure and Environmental Contamination." Asian Journal of Science and Technology **16**(02): 13449-13457.

Patterton, H.-G. (2013). Scoping study and research strategy development on currently known and emerging contaminants influencing drinking water quality: main Report, Water Research Commission Pretoria, South Africa.

Reddy, B. V., P. Sandeep, et al. (2014). "Water treatment process in pharma industry-A review." International Journal of Pharmacy and Biological Sciences **4**(2): 7-18.

Salomão, G. R., J. H. P. Américo-Pinheiro, et al. (2021). "Diclofenac removal in water supply by adsorption on composite low-cost material." Environmental Technology **42**(13): 2095-2111 DOI: https://doi.org/10.1080/09593330.2019.1692078.

Samah, N. A., M.-J. Sánchez-Martín, et al. (2018). "Molecularly imprinted polymer for the removal of diclofenac from water: Synthesis and characterization." Science of The Total Environment **631**: 1534-1543 DOI: https://doi.org/10.1016/j.scitotenv.2018.03.087.

Sharma, J., M. Joshi, et al. (2022). "Pharmaceutical residues: One of the significant problems in achieving 'clean water for all'and its solution." Environmental Research **215**: 114219 DOI: https://doi.org/10.1016/j.envres.2022.114219.

Taha, A. A. A.-R. and S. H. Ahmed (2024). "Removal Pharmaceutical Contaminants from Water and Wastewater: A review." Al-Rafidain Journal of Engineering Sciences: 53-66 DOI: 10.61268/ge8d4h64.

Tang, Y., M. Yin, et al. (2019). "Emerging pollutants in water environment: Occurrence, monitoring, fate, and risk assessment." Water Environment Research **91**(10): 984-991 DOI:

Thiebault, T. (2015). L'adsorption des produits pharmaceutiques par interactions organo-minérales: Processus et Applications environnementales, Université d'Orléans.

Viotti, P. V., W. M. Moreira, et al. (2019). "Diclofenac removal from water by adsorption on Moringa oleifera pods and activated carbon: Mechanism, kinetic and equilibrium study." Journal of Cleaner Production **219**: 809-817 DOI: https://doi.org/10.1016/j.jclepro.2019.02.129.

Wang, H., H. Xi, et al. (2021). "Ecotoxicological effects, environmental fate and risks of pharmaceutical and personal care products in the water environment: A review." Science of The Total Environment **788**: 147819 DOI: https://doi.org/10.1016/j.scitotenv.2021.147819.

Yanyan, L., T. A. Kurniawan, et al. (2018). "Enhanced removal of acetaminophen from synthetic wastewater using multi-walled carbon nanotubes (MWCNTs) chemically modified

with NaOH, HNO_3/H_2SO_4, ozone, and/or chitosan." Journal of Molecular Liquids **251**: 369-377 DOI: https://doi.org/10.1016/j.molliq.2017.12.051.

Chapter 2:

Theory and modeling of adsorption process

I.2. Theory and modeling of adsorption process

I.2.1. Introduction

Adsorption is a mass transfer process that removes pollutants from the liquid phase to the solid adsorbent. Adsorption is one of the most widely used technologies in water and wastewater treatment because it offers many advantages, such as simple design, low cost, easy maintenance, and high efficiency (Wang and Guo 2020). The objective of this chapter is to present general information on adsorption to define its importance better. An overview of modelling adsorption kinetics and isotherms will be provided. Attention will also be given to the presentation of the calculation of the thermodynamic parameters of adsorption. It also contains a basic theory on carbon-based adsorbent materials, their definitions, and their preparation by both physical and chemical methods.

I.2.2. Definition

The term adsorption was first used by Heinrich Kayser in 1881(Salih 2017). Adsorption is a physicochemical phenomenon that results in a particular modification of concentration at the interface between two immiscible phases. It is a surface phenomenon in which gas or liquid molecules attach to the solid surfaces of adsorbents (Hadjer 2019) through interactions with the adsorbent surface. The type and strength of these interactions depend on the characteristics of both the adsorbent and the adsorbate, as well as on solution conditions, such as pH, temperature, and ion strength (Piai 2021). We call desorption the inverse transformation of adsorption, by which the adsorbed molecules or atoms detach themselves from the substrate (Hadjer 2019) (See Figure I.2.1).

- Adsorbate: the chemical entity that adsorbs.
- Adsorbent: the solid on which the adsorbate adsorbs.

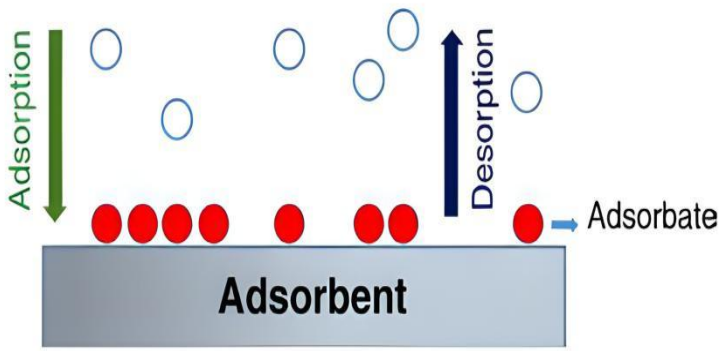

Figure I.2.1. Schematic depiction of adsorption and desorption processes (Kecili and Hussain 2018).

I.2.3. Types of adsorption

The removal efficiency of any adsorption process depends on selectivity and affinity. According to the type of adsorbent and adsorbate bonds formed, adsorption can be classified into:

I.2.3.1. Physical adsorption or physisorption

The bonding between adsorbate and adsorbent is a weak Van der Waals force; no changes in chemical structure for both (Alqabreh 2021). Physical adsorption is usually fast and reversible. This is because the physical adsorption process involves the formation of weak bonds between the adsorbate and adsorbent; thus, the adsorption bonds are easily formed and broken (Salih 2017).

I.2.3.2. Chemical adsorption or chemisorption

Chemisorption is characterized by the formation of strong chemical bonds between molecules or ions of the adsorbate and the adsorbent surface, generally due to electron exchange (Mustafa T. Yagub 2014). A chemisorption process is usually slow and irreversible. This is because the chemical adsorption process involves the formation of strong bonds between the adsorbate and adsorbent and can change both the surface and adsorbate chemical character (Salih 2017).

Table I.2.1. General characteristics of physisorption and chemisorption

Properties	Physisorption	Chemisorption
Binding type	Weak interaction : Electrostatic bonding Van der Waals bond Hydrogen bond	Strong interaction : Chemical bond Covalent bond Complexation bond Ion exchange
Heat of adsorption	≤ 40 KJ/mole	> 40 KJ/mole
Individuality of molecules	The individuality of molecules is preserved	Destraction of individuality of molecules
Desorption	Easy	Difficult
Kinetics	Fast	Slow

Formation type	Multi-layer and mono layer	Mono-layer

I.2.4. Mass transport mechanism in the adsorption process

Adsorption describes fluid phase molecules attaching to a solid phase. It involves several steps (see Figure I.2.2):

- Solute transport in the bulk fluid phase
- Film diffusion (external diffusion): transport of the adsorbate present in the solution to the external surface of the adsorbent.
- Pore diffusion (intraparticle diffusion): transport of the adsorbate from the surface of the adsorbent into the pores.
- Surface reaction: fixation of the adsorbate on the surface of the adsorbent pores involving weak van der Waals interactions, hydrogen bonding, charge-transfer complexes, electrostatic attractions, and sometimes strong chemical bonds and electron transfers creating electrostatic attractions (Quesada, Cusioli et al. 2019) (Patel, Kumar et al. 2019).

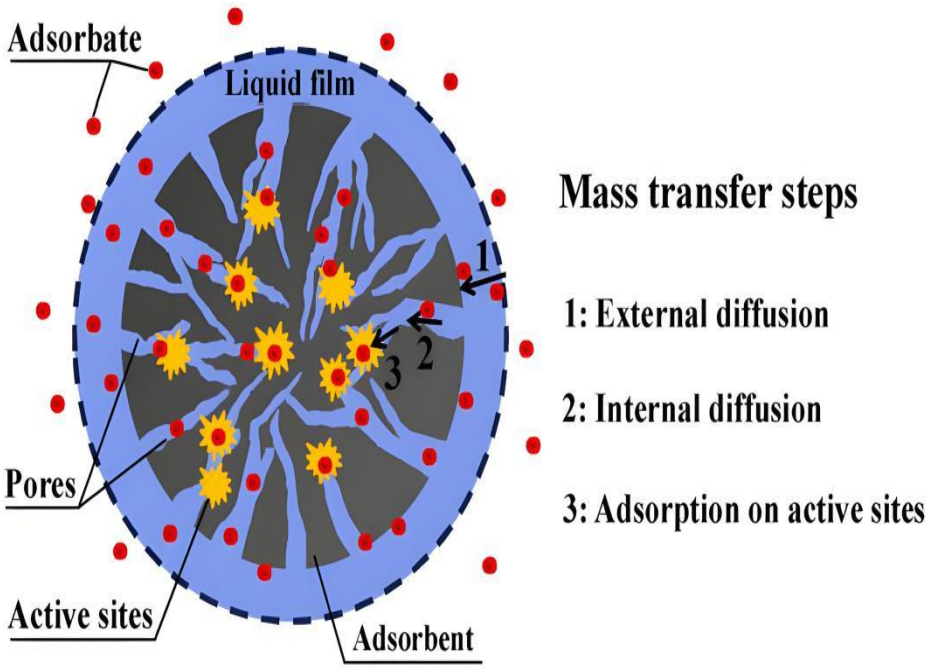

Figure I.2.2. Adsorption mass transfer steps (Wang and Guo 2020).

I.2.5. Factors influencing the adsorption phenomenon

I.2.5.1. Influence of adsorbent properties

I.2.5.1.1. Adsorbents particle size

The particle size of the adsorbents significantly affects the final solute concentration and, consequently, the overall performance of the adsorption process. A larger particle size will reduce final uptake due to the lower specific surface area. When the surface area of the adsorbent increases, new active sites are formed, thus allowing more binding of solute molecules (Samira Karimia 2019).

I.2.5.1.2. Specific surface area (SSA)

Generally, SSA indicates the degree of porosity available for adsorption, and higher SSA can provide more active adsorption sites. However, adsorbents with relatively low SSA have also been shown to effectively remove contaminants, as the expanding adsorbent in water diffuses the adsorbate into the solid structure. Therefore, the role of SSA in the adsorption removal of organic pollutants by biochar varies depending on the specific situation (Zirui Luo 2022)

I.2.5.1.3. Pore size distribution

Pore-size distribution is another factor that significantly affects the adsorption of organic contaminants. Biochar with a highly porous structure facilitates the removal of organic contaminants of similar molecular weight. The SSA of activated carbon is larger than that of biochar, but the latter is more adsorbable because its pore size distribution is broader than that of activated carbon. The presence of a large number of high-energy adsorption sites in the micropore could enhance adsorption strength. Besides that, the steric hindrance occurs when the pores are too narrow to cause the adsorbate molecules to diffuse to deep micropore sites rapidly (Zirui Luo 2022).

I.2.5.1.4. Surface functional groups

The chemical properties of activated carbon mainly depend on its surface functional groups, heteroatoms, and compounds. More specifically, the materials generated during the preparation of AC contain multiple surface groups, such as hydroxyl, carbonyl, carboxyl, amino, and alkyl groups, in addition to aromatic rings. Due to these different functional groups, the chemical characteristics of the AC surface vary and can range from acidic to alkaline, oxidizing to reducing, and hydrophilic to hydrophobic. In terms of the functional

groups, these can be divided into oxygen-containing and nitrogen-containing groups. Many oxygen-containing groups are acidic, increasing the surface's hydrophilicity. If the AC surface is hydrophilic, hydrophilic carbon-based gases are easily absorbed (Wang, Cheng et al. 2022).

I.2.5.2. Influence of adsorbate properties

Depending on the type of pollutant (pharmaceutical contaminants, dyes, heavy metals, or pesticides…), its chemical structure, molecular weight, molecular size and polarity should also be taken into account (Eszter Rápó 2021).

I.2.5.3. Influence of solution chemistry

I.2.5.3.1. Solution pH

One of the most important factors affecting the adsorbent capacity in wastewater treatment is solution pH. The efficiency of adsorption is dependent on the solution pH, since variation in pH leads to a variation in the degree of ionization of the adsorptive molecule and the surface properties of the adsorbent (Mustafa T. Yagub 2014).

I.2.5.3.2. Solution temperature

Temperature is also a significant physico-chemical factor, as it affects the treatment process by shifting the reaction from endothermic to exothermic, or vice versa. Moreover, it has a strong effect on adsorption, as it can increase or decrease the amount adsorbed. The temperature can affect sorption efficiency differently depending on the adsorbent and the pollutant. In general, it enhances biosorption of adsorption impurities by increasing the surface activity and kinetic energy of the adsorbate, but it can also damage the physical structure of the biosorbent.

- As the temperature rises, the rate of chemical reaction also increases, so if the sorption process is chemisorption ($\Delta H_{chemisorption} = -200$ kJ/mol), then higher sorption efficiency will be seen at higher temperatures (this would eventually reach equilibrium).
- On the other hand, if the process is physical adsorption ($\Delta H_{physisorption} \approx -20$ kJ/mol), then a higher temperature will reduce adsorption. Temperature can chemically alter the adsorbent, its adsorption sites and activity (Eszter Rápó 2021).

I.2.5.3.3 Ionic strength

The effect of ionic strength on the adsorption process is varied and depends on the physicochemical characteristics of the adsorbent and adsorbate (Valentina Bernal 2020). Wastewater contains several compounds, such as dissolved inorganic contaminants in cationic,

anionic, or neutral forms, as ions, atoms, or molecules of any element of the periodic table. Water quality parameters often include cations and anions such as Na^{+}, CO_3^{2-}, Ca^{2+}, Mg^{+2}, and Cl^{-}, underscoring the frequency and importance of these ions in surface waters. Ionic strength can affect the hydrophobic and electrostatic interactions between the adsorbate and the adsorbent, due to the competition between the ions and the molecules of the contaminant for the active sites of the solid (Quesada, Cusioli et al. 2019)

I.2.5.3.4. Dosage of adsorbent and contact time

In general, the extent of adsorption of a solute increases with the increase in the concentration of an adsorbent because the increase in adsorbent concentration translates into increased active exchangeable adsorption sites. However, the overall solute adsorption per unit weight of an adsorbent can decrease following the increase in adsorbent concentration due to interference caused by the interaction of active sites of an adsorbent. The contact time significantly affects the adsorption process. Also, contact time can influence both the economic efficiency of the process and the adsorption kinetics. Therefore, contact time is another performance governing factor in the adsorption process (Iftekhar, Ramasamy et al. 2018).

I.2.6. Adsorption kinetics

The kinetics of adsorption involves studying how the concentration of the adsorbate in the solution changes over time when it comes into contact with the adsorbent. Investigating adsorption kinetics provides insights into the adsorption rate, assesses the efficiency of the adsorbent material, and helps clarify the mechanisms underlying mass transport during adsorption. A clear grasp of adsorption kinetics is fundamental to the development and optimisation of adsorption processes (Wang and Guo 2020).

The kinetic description of adsorption processes and the removal efficiency have been frequently evaluated using several mathematical models, most of which are empirical equations. The standard kinetics models (pseudo-first order, pseudo-second order, intra-particle diffusion kinetic, and Elovich), which were used to fit experimental data (see Table I.2.2) (Raji, Karim et al. 2023).

Table I.2.2. Equations of kinetic modeling.

	Linear form	Non-linear form
Pseudo-first order	$\ln(q_e - q_t) = lnq_e - K_1 t$ **Eq.I.2.1**	$q_t = q_e(1 - e^{-K_1 t})$ **Eq.I.2.5**
Pseudo-second order	$\frac{t}{q_e} = \left(\frac{1}{K_2 q_e^2}\right) + \left(\frac{1}{q_e}\right) t$ **Eq.I.2.2**	$q_t = \frac{q_e^2 K_2 t}{1 + q_e K_2 t}$ **Eq.I.2.6**
Elovich	$q_t = \frac{1}{\beta}\ln(\alpha\beta) + \frac{1}{\beta}\ln(t)$ **Eq.I.2.3**	$q_t = \frac{1}{\beta}\ln(1 + (\alpha\beta t))$ **Eq.I.2.7**
Intra-particle diffusion	$q_t = K_{int} t^{1/2} + C$ **Eq.I.2.4**	/

With:

q_t and **q_e** (mg.g^{-1}): The amount of pollutant adsorbed at a specific time and at equilibrium respectively.

K_1 (min^{-1}), **K_2** (g (min^{-1}mg^{-1})), **K_{int}** (mg.g^{-1}.min$^{0.5}$): The constants of PFO, PSO and intraparticle diffusion model respectively.

α (mg.g^{-1}.min^{-1}): The Elovich initial rate constant.

β (mg.g^{-1}): The desorption constant.

C (mg.g^{-1}): constant related to the thickness of the boundary layer.

I.2.7. Adsorption isotherms

The amount of material absorbed by a substrate is often expressed as a function of the equilibrium concentration at a constant temperature in a process known as the Adsorption Isotherm. The study of adsorption isotherms is essential for gaining insight into the design and operation of adsorption systems (Ehiomogue, Ahuchaogu et al. 2021). The role of temperature is to determine a model that describes the adsorption process between the sorbent and the adsorbate and the effect of temperature on it, whether favourable or not.

I.2.7.1. Giles classification

Adsorption isotherms were classified into four main groups as illustrated in Figure I.2.3**.** The classification depends on the lower part of the curve when the adsorbate solution is very dilute.

- **S-type isotherm (Sigma)**

Indicates cooperative adsorption, which works when the adsorbate-adsorbate interaction is stronger than the adsorbate-adsorbent interaction. Consequently, clustering of

adsorbate molecules is favoured at the surface because they interact strongly with each other than with the surface.

- **L-type isotherm (Langmuir)**

Indicates a high affinity of the adsorbate for the adsorbent, suggesting chemisorption. This kind of isotherm occurs when the adsorbate-solution interaction is weaker than the adsorbate-adsorbent interaction.

- **H-type isotherm (High affinity)**

It is an extended case of L-type, which suggests extremely high affinity of the adsorbate for the adsorbent, so in a dilute solution, the adsorbate is almost completely adsorbed

- **C-type isotherm (score unchanged)**

indicates a constant proportional affinity of the adsorbate molecules for the adsorbent and is always noticed only at a low range of adsorbate concentration (Alqabreh 2021)

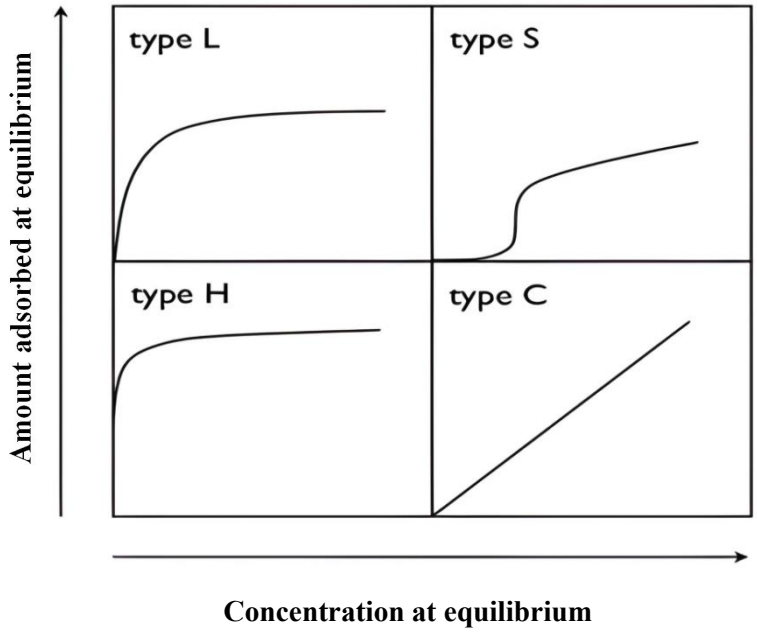

Figure I.2.3. Classification of adsorption equilibrium isotherms according to Giles (Guemaz 2025).

I.2.7.2. Brunauer, Emmett and Teller classification

According to the classification proposed by Brunauer, Emmett, and Teller, adsorption–desorption isotherms are divided into six distinct types, as shown in Figure I.2.4.

- **Type one (I) adsorption isotherm** is for tiny pores or microporous adsorbents. In this case, adsorption occurs by filling the micropores. The adsorbate adsorption rate depends on the available micropore volume rather than the total interior surface area.
- **Type two (II) and type four (IV) adsorption isotherms** they were detected for non-porous or macroporous adsorbents with unlimited monolayer-multilayer adsorption. First, the adsorption volume quickly increases at low relative pressures due to contact of the adsorbate molecules with the higher energetic section, followed by the interaction with the less energetic section (Abebe, Murthy et al. 2018).
- **Type III isotherms** can be observed when the fluid does not completely wet the surface due to weak interactions between fluid molecules and the (pore) wall. In this case, the molecules form clusters around preferred adsorption sites on the adsorbent owing to stronger interactions between fluid molecules than between fluid molecules and the adsorbent..
- **Type V isotherms** molecular clustering is followed by pore filling. For instance, type V isotherms are observed for water adsorption in hydrophobic microporous and mesoporous adsorbents.
- **Type IV isotherms** these characteristics are typical of fluid adsorption in mesopores. In fact, the definition of micro- and mesopore size ranges is somewhat arbitrary, and the detailed adsorption mechanism depends on the ratio between molecular size and pore size (Thommes and Schlumberger 2021).

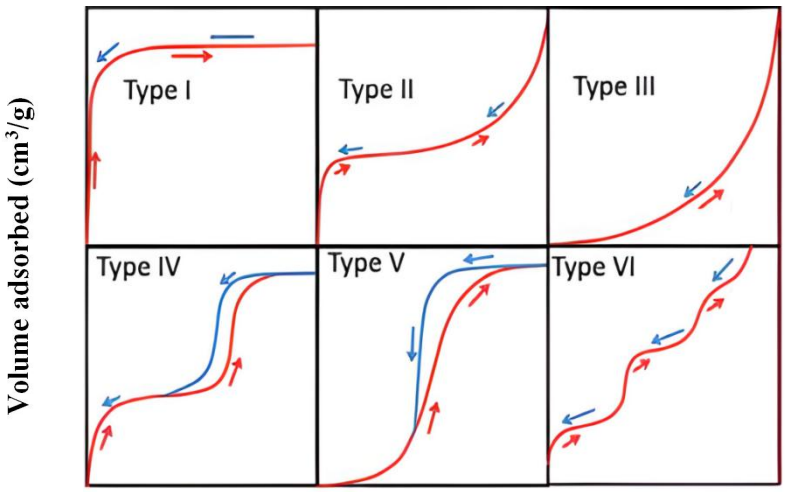

Figure I.2.4. Different types of adsorption isotherms **(**Ehiomogue, Ahuchaogu et al. 2021).

I.2.7.3. Modeling of adsorption isotherms

The most widely used isotherms for liquid/solid phase systems are the Langmuir and the Freundlich Isotherms. There are also Redlich–Peterson, Temkin, Dubinin–Radushkevich, Harkins, and Halsey, and BET (Brunauer, Emmett, and Teller) are used to get detailed information about the interactions between the surface of the adsorbents and molecules to be adsorbed (Kecili and Hussain 2018)

I.2.7.3.1. Langmuir isotherm

In 1932, Irving Langmuir proposed the Langmuir adsorption model (Kecili and Hussain 2018). The assumption of the Langmuir isotherm is based on the fact that the attainment of equilibrium is achieved when there is saturation of the adsorbent by the monolayer adsorbate substances (Ugwu, Tursunov et al. 2020). The Langmuir isotherm is shown thus:

$$q_e = \frac{Q_{max} K_L C_e}{1 + K_L C_e} \quad \textbf{Eq.I.2.8}$$

The linearized form of the Isotherm is:

$$\frac{C_e}{q_e} = \frac{1}{K_L q_L} + \frac{C_e}{q_L} \quad \textbf{Eq.I.2.9}$$

Where:

q_e (mg/g): Equilibrium adsorption capacity.

Q_{max} (mg/g): Maximum adsorption capacity of Langmuir.

C_e (mg/l): The adsorbate equilibrium concentration.

K_L (L/mg): Langmuir isotherm constant.

q_L(mg/g): Maximum adsorption capacity.

I.2.7.3.2. Freundlich isotherm

The Freundlich isotherm is an empirical model that accounts for the adsorbent monolayer interference with the solute. Nevertheless, it is based on the assumption that the adsorbent has a heterogeneous surface, with binding sites that are not similar (Ugwu, Tursunov et al. 2020). The Freundlich isotherm is shown thus:

$$Q_e = K_F C_e^{\,1/n_f} \quad \textbf{Eq.I.2.10}$$

The linear form of the Isotherm is:

$$\ln q_e = \ln K_F + \frac{1}{n} \ln C_e \quad \textbf{Eq.I.2.11}$$

q_e (mg/g): Equilibrium adsorption capacity.

C_e (mg/l): The adsorbate equilibrium concentration.

K_L [$(mg.g^{-1}) / (mg.L^{-1})^{1/n}$]: Freundlich isotherm constant.

n: dimensionless Freundlich parameter of intensity.

I.2.7.3.3. Temkin isotherm

The Temkin isotherm ignores the extremely low and high concentration values (Ehiomogue, Ahuchaogu et al. 2021). This model accounts for the influence of adsorption enthalpy, which diminishes progressively as surface coverage increases. This reduction in adsorption energy arises from intermolecular interactions among the adsorbed species on the adsorbent surface (Kecili and Hussain 2018). It is described as:

$$q_e = B.ln\,(K_T C_e) \qquad \textbf{Eq.I.2.12}$$

The linear form of the isotherm is:

$$q_e = B\,ln\,K_T + B\,ln\,C_e \qquad \textbf{Eq.I.2.13}$$

Thus:

B: is related to the thermal adsorption energy and is defined as B = $\frac{RT}{b_T}$, where R: is the universal gas constant (8.314 J/mol·K), T: is the absolute temperature (K), and b_T is the Temkin constant

associated with the sorption heat (J/mol).

q_e (mg/g): Equilibrium adsorption capacity.

C_e (mg/L): The adsorbate equilibrium concentration.

K_T (L/mg): The Temkin constant

I.2.8. Adsorption thermodynamics

Thermodynamic parameters derived from adsorption processes provide essential insights into chemical engineering applications and the overall adsorbent capacity to capture the adsorbate. They also serve as valuable indicators for understanding the underlying adsorption mechanisms. Moreover, analyzing these thermodynamic parameters is a common and effective approach for optimizing and modifying adsorption processes (Doke and Khan 2013).

Thermodynamic factors such as Gibbs free energy change ($\Delta G°$), enthalpy ($\Delta H°$) and entropy ($\Delta S°$) were calculated to check the influence of temperature on the adsorption process from the following well-known expressions (Sajid, Bari et al. 2022):

$$K_C = \frac{q_e}{C_e} \quad \textbf{Eq.I.2.14}$$

$$\Delta G° = -RT \ln K_c \quad \textbf{Eq.I.2.15}$$

$$\Delta G° = \Delta H° - T\Delta S° \quad \textbf{Eq.I.2.16}$$

The values of $\Delta H°$ and $\Delta S°$ were calculated from the slope and intercept of the plot of ln K_C against 1/T to the van't Hoff equation wich is given in Eq.I.2.17 :

$$\ln K_C = -\frac{\Delta H°}{R} \times \frac{1}{T} + \frac{\Delta S°}{R} \quad \textbf{Eq.I.2.17}$$

Where:

K_C (L g^{-1}): The thermodynamic equilibrium constant.

q_e (mg g^{-1}) : The adsorption equilibrium capacity.

C_e (mg L^{-1}): The equilibrium adsorbate concentration.

R: The universal gas constant (8.314 J mol^{-1} K^{-1}) and T (°K) is the absolute temperature.

Table I.2.3. Thermodynamic Parameters and Their Interpretations in Adsorption Studies.

Parameters	Indicates	Interpretation	
ΔG°	Spontaneity	ΔG°< 0	The process is spontaneous
		ΔG°> 0	The process is not spontaneaous
ΔH°	Heat change	ΔH°< 0	Exothermic process
		ΔH°>0	Endothermic process
		2-40 KJ/mol	Physisorption
		40-400 KJ/mol	Chemisorption

ΔS°	Disorder	ΔS°< 0	Increased randomness
		ΔS°> 0	Decreased randomness

I.2.9. Adsorption on Carbonaceous materials

Generally, carbonaceous materials have long been recognized as effective adsorbents for a wide range of organic pollutants (Kyriakopoulos and Doulia 2006), securing their significance in adsorption processes. These substances are primarily made up of carbon along with additional elements, offering outstanding attributes such as environmental friendliness, strong thermal and chemical resistance, excellent conductivity (both thermal and electrical), and robust mechanical strength. They come in diverse forms, including activated carbon with high porosity, biochar, carbon molecular sieves, carbon nanotubes, and graphene. These materials are typically inexpensive, naturally abundant, and are characterized by a large surface area, high pore volume, and low mass density (Abd, Naji et al. 2020).

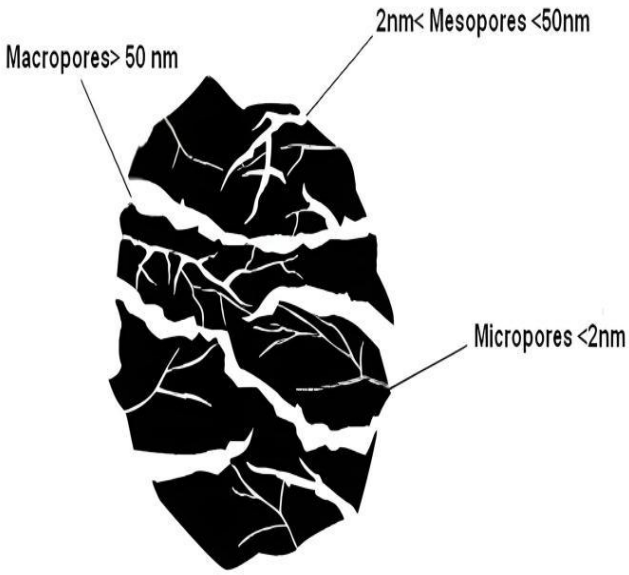

Figure I.2.5. Schematic activated carbon model (Baccar Ep Yangui, Sarrà i Adroguer et al. 2014).

I.2.9.1. Biochar

Biochar, produced by pyrolysis of carbon-rich biomass under limited oxygen conditions, possesses a fibrous, multi-layered, porous structure. These distinctive features have made it a subject of growing interest among researchers. Biochar can be produced through three primary pyrolysis methods, which are classified based on the operating temperature: fast pyrolysis occurs at temperatures above 500 °C, moderate pyrolysis takes place between 300 and 500 °C, while slow pyrolysis is carried out at temperatures below 300 °C. Owing to its distinctive physicochemical attributes such as elevated pH, high carbon concentration, substantial cation exchange capacity, large specific surface area, and aromatic structure biochar has been extensively employed in fields including metallurgy, chemical processing, pharmaceuticals, electronics, and bioenergy. Its environmentally sustainable nature and economic feasibility further enhance its appeal across these disciplines. In recent years, it has played an increasingly important role in environmental protection, particularly in the adsorption and elimination of diverse organic contaminants from various environmental media (Luo, Yao et al. 2022).

I.2.9.2. Activated carbon

Activated carbon generally refers to highly porous carbonaceous materials (Figure I.2.5). It is the most popular amongst adsorbents owing to its large surface area which ranges from 500 to 3000 m^2g^{-1}, low cost and good charge-holding capacity and the ability for various functional groups to be generated, which may be responsible for the effective elimination of a variety of contaminants from aqueous or gaseous media. Activated carbon has different structures, like granular, powdery and fibrous physical forms, which are generally applied for water cleanup procedures (Sabzehmeidani, Mahnaee et al. 2021).

I.2.9.2.1. Activated carbon production through physical activation

Commercially applied physical activation generally proceeds through a sequential two-stage approach: first, the raw material undergoes thermal decomposition (carbonization) in an inert environment, followed by an activation phase in the presence of oxidizing gases such as steam, carbon dioxide, nitrogen-carbon dioxide blends, or air at elevated temperatures ranging between 800 and 1100 °C. This technique facilitates the formation of activated carbon with a well-developed porous architecture and robust mechanical stability. It is cost-effective and environmentally sustainable because it does not use chemical reagents. Nonetheless, the process is hindered by extended activation durations, relatively modest adsorption

performance of the resulting carbon, and significant energy demands, which limit its efficiency (Heidarinejad, Dehghani et al. 2020).

I.2.9.2.2. Activated carbon production through chemical activation

Chemical activation involves incorporating chemical agents, typically dehydrating compounds, into the raw material to enhance pyrolysis and suppress the formation of tarry or volatile intermediates. This process generally entails impregnating the biomass with activating substances such as alkaline hydroxides (e.g., NaOH, KOH), acids (e.g., HCl, H_2SO_4), or salts (e.g., $ZnCl_2$, K_2CO_3) through thorough mixing and stirring. Though typically carried out in a single thermal step, the process may sometimes begin with carbonization to generate a char, which is then chemically treated and thermally activated under an inert nitrogen atmosphere. Unlike physical activation, chemical activation operates at comparatively moderate temperatures (typically 400-800 °C), making it suitable for lignocellulosic feedstocks. In many cases, the raw material is directly blended with the chemical agent prior to pyrolysis, with the impregnation ratio being a critical parameter for optimizing pore development. The efficacy of the activating agent varies with the precursor's chemical structure and the specific activation conditions. Additionally, a two-stage activation approach can be employed, where preformed biochar is impregnated with the chemical reagent and subsequently re-heated to enhance porosity (Ukanwa, Patchigolla et al. 2019).

I.2.10. Conclusion

In this chapter, a literature review was conducted to elucidate the adsorption process on carbonaceous materials. This bibliography shows that adsorption is a sustainable, environmentally friendly technology that offers significant advantages over conventional treatment methods. Adsorption is a surface phenomenon, which may occur through either physical or chemical interactions. Its efficiency is influenced by a variety of factors related to the adsorbent, the adsorbate, and the surrounding medium. To gain deeper insight into adsorption mechanisms, a range of kinetic and isotherm models has been developed. Furthermore, the study of adsorption thermodynamics is a critical step in predicting these mechanisms, as it relies on calculated thermodynamic parameters. This section also highlights the importance of carbon-based adsorbents for removing pollutants through adsorption.

References

Abd, A. A., S. Z. Naji, et al. (2020). "Carbon dioxide removal through physical adsorption using carbonaceous and non-carbonaceous adsorbents: a review." Journal of environmental chemical engineering **8**(5): 104142 DOI: https://doi.org/10.1016/j.jece.2020.104142.

Abebe, B., H. A. Murthy, et al. (2018). "Summary on adsorption and photocatalysis for pollutant remediation: mini review." Journal of encapsulation and adsorption sciences **8**(4): 225-255 DOI: https://doi.org/10.4236/jeas.2018.84012.

Alqabreh, M. (2021). "Adsorption Phenomena: Definition, Mechanisms, and Adsorption Types: Short Review." Green and Applied Chemistry **Vol. 13, 2021, pp. 43~51** DOI: https://doi.org/10.48419/IMIST.PRSM/rhazes-v13.28283.

Baccar Ep Yangui, R., M. Sarrà i Adroguer, et al. (2014). Removal of water pollutants by adsorption on activated carbon prepared from olive-waste cakes and by biological treatment using ligninolytic fungi, Universitat Autònoma de Barcelona.

Doke, K. M. and E. M. Khan (2013). "Adsorption thermodynamics to clean up wastewater; critical review." Reviews in Environmental Science and Bio/Technology **12**(1): 25-44 DOI: https://doi.org/10.1007/s11157-012-9273-z.

Ehiomogue, P., I. I. Ahuchaogu, et al. (2021). "Review of Adsorption Isotherms Models." Acta Technica Corviniensis-Bulletin of Engineering **14**(4) DOI:

Eszter Rápó, S. T. (2021). "Factors Affecting Synthetic Dye Adsorption; Desorption Studies: A Review of Results from the Last Five Years (2017–2021)." DOI: https://doi.org/10.3390/molecules26175419.

Guemaz, N. (2025). Synthèse, Caractérisation, propriétés adsorbants et activité antimicrobiennes d'un nouveau polymère fonctionnel : (Polystyrène-ohydroxy acétophénodiéthylènetriamine.

Hadjer, Z. (2019). Etude de l'adsorption des colorants sur un matériau poreux ‹‹charbon actif››, Université Larbi Ben M'hidi Oum-El-Bouaghi.

Heidarinejad, Z., M. H. Dehghani, et al. (2020). "Methods for preparation and activation of activated carbon: a review." Environmental Chemistry Letters **18**(2): 393-415 DOI: https://doi.org/10.1007/s10311-019-00955-0.

Iftekhar, S., D. L. Ramasamy, et al. (2018). "Understanding the factors affecting the adsorption of Lanthanum using different adsorbents: a critical review." Chemosphere **204**: 413-430 DOI: https://doi.org/10.1016/j.chemosphere.2018.04.053.

Kecili, R. and C. M. Hussain (2018). Mechanism of adsorption on nanomaterials. Nanomaterials in chromatography, Elsevier**:** 89-115.

Kyriakopoulos, G. and D. Doulia (2006). "Adsorption of pesticides on carbonaceous and polymeric materials from aqueous solutions: a review." Separation & Purification Reviews **35**(3): 97-191 DOI: https://doi.org/10.1080/15422110600822733.

Luo, Z., B. Yao, et al. (2022). "Novel insights into the adsorption of organic contaminants by biochar: A review." Chemosphere **287**: 132113 DOI: https://doi.org/10.1016/j.chemosphere.2021.132113.

Mustafa T. Yagub , T. K. S., Sharmeen Afroze , H.M. Ang (2014). "Dye and its removal from aqueous solution by adsorption: A review." Advances in Colloid and Interface Science DOI: https://doi.org/10.1016/j.cis.2014.04.002.

Patel, M., R. Kumar, et al. (2019). "Pharmaceuticals of emerging concern in aquatic systems: chemistry, occurrence, effects, and removal methods." Chemical reviews **119**(6): 3510-3673 DOI: https://doi.org/10.1021/acs.chemrev.8b00299.

Piai, L. M. e. (2021). Micropollutants removal with activated carbon: adsorption and regeneration by biodegradation, Wageningen University and Research.

Quesada, H. B., L. F. Cusioli, et al. (2019). "Acetaminophen adsorption using a low‐cost adsorbent prepared from modified residues of Moringa oleifera Lam. seed husks." Journal of Chemical Technology & Biotechnology **94**(10): 3147-3157 DOI: https://doi.org/10.1002/jctb.6121.

Raji, Z., A. Karim, et al. (2023). Adsorption of heavy metals: mechanisms, kinetics, and applications of various adsorbents in wastewater remediation—a review. Waste, MDPI.

Sabzehmeidani, M. M., S. Mahnaee, et al. (2021). "Carbon based materials: A review of adsorbents for inorganic and organic compounds." Materials Advances **2**(2): 598-627 DOI: https://doi.org/10.1039/D0MA00087F.

Sajid, M., S. Bari, et al. (2022). "Adsorption characteristics of paracetamol removal onto activated carbon prepared from Cannabis sativum Hemp." Alexandria Engineering Journal **61**(9): 7203-7212 DOI: https://doi.org/10.1016/j.aej.2021.12.060.

Salih, A. M. (2017). The purification of industrial wastewater to remove heavy metals and investigation into the use of zeolite as a remediation tool, University of Wolverhampton.

Samira Karimia, M. T. Y., Rama Rao Karric (2019). "A comprehensive review of the adsorption mechanisms and factors influencing the adsorption process from the perspective of bioethanol dehydration." Renewable and Sustainable Energy Reviews DOI: https://doi.org/10.1016/j.rser.2019.03.025.

Thommes, M. and C. Schlumberger (2021). "Characterization of nanoporous materials." Annual review of chemical and biomolecular engineering **12**(1): 137-162 DOI: https://doi.org/10.1146/annurev-chembioeng-061720-081242.

Ugwu, E., O. Tursunov, et al. (2020). Adsorption mechanisms for heavy metal removal using low cost adsorbents: A review. IOP Conference Series: Earth and Environmental Science, IOP Publishing.

Ukanwa, K. S., K. Patchigolla, et al. (2019). "A review of chemicals to produce activated carbon from agricultural waste biomass." Sustainability **11**(22): 6204 DOI: https://doi.org/10.3390/su11226204.

Valentina Bernal, L. G., Juan Carlos Moreno-Piraján (2020). "Thermodynamic analysis of acetaminophen and salicylic acid adsorption onto granular activated carbon: Importance of chemical surface and effect of ionic strength." Thermochimica Acta DOI: https://doi.org/10.1016/j.tca.2019.178467.

Wang, J. and X. Guo (2020). "Adsorption kinetic models: Physical meanings, applications, and solving methods." Journal of hazardous materials **390**: 122156 DOI: https://doi.org/10.1016/j.jhazmat.2020.122156.

Wang, X., H. Cheng, et al. (2022). "Key factors and primary modification methods of activated carbon and their application in adsorption of carbon-based gases: A review." Chemosphere **287**: 131995 DOI: https://doi.org/10.1016/j.chemosphere.2021.131995.

Zirui Luo , B. Y., Xiao Yang , Lingqing Wang , Zhangyi Xu , Xiulan Yan ,Lin Tian , Hao Zhou , Yaoyu Zhou (2022). "Novel insights into the adsorption of organic contaminants

by biochar:A review." Chemosphere DOI: https://doi.org/10.1016/j.chemosphere.2021.132113.

Part II:

Experimental part

Chapter 1:

Synthesis and characterization of adsorbents

II.1. Synthesis and characterization of adsorbents

II.1.1. Introduction

This chapter presents the preparation and characterization results of different adsorbents derived from cypress cones (CC). The materials were examined for their textural and structural properties, surface functional groups, and morphology using Fourier-transform infrared spectroscopy (FTIR), X-ray diffraction (XRD), scanning electron microscopy coupled with energy-dispersive spectroscopy (SEM/EDS), and Brunauer–Emmett–Teller (BET) surface area analysis. The influence of pyrolysis temperature and the activating agent (zinc chloride) on these properties is discussed in detail. Additionally, the point of zero charge of the adsorbents was determined and is also reported herein

II.1.2. Cypress tree

Cupressus sempervirens (Mediterranean cypress) is a species native to the Mediterranean region. It is one of the most widespread trees in Algeria. Its natural distribution comprises the Aegean islands (Greece), Cyprus, Turkey (South Anatolia), North-east Africa (Libya, Algeria and Tunisia), and the Middle East (Iran, Jordan, Lebanon and Syria). A slender tree can grow up to 25 m in height. The leaves are small and thin; they are used in the extraction of essential oils and natural extracts. The galbule or Cypress nut is the cone formed by the female flowers. The seed cones are ovoid or oblong, 25–40 mm long, with 10-14 scales, green at first, maturing to brown about 20–24 months after pollination (Ialeff, Debib et al. 2021) (Bouguenoun, De Pauw-Gillet et al. 2016). Once cypress cones fall to the ground, they are usually considered common forest waste.



Figure II.1.1. Cypress tree.

II.1.3. Characterization of Cypress cones biomass

II.1.3.1. Fourier Transform Infrared (FT-IR)

The FTIR spectrum of the untreated material, shown in Figure II.1.2, provides important insights into the surface functional groups on CC. The broad absorption band observed at 3384.40 cm^{-1} is associated with O–H stretching vibrations, which may originate from hydroxyl functionalities in alcohols, phenols, or carboxylic groups, as well as from water adsorbed on the surface (Benaoune, Merzougui et al. 2025). The absorption peak appearing at 2939.53 cm^{-1} is attributed to the stretching vibrations of C–H bonds (Larous and Meniai 2016) formed from CH_2 groups, and these are assigned to the presence of lignin components in the biomass (Nampeera, Recepoğlu et al. 2024). The bands observed near 1600 cm-1 are associated with the asymmetric stretching vibrations of C=O bonds characteristic of carboxylic (–COOH) groups (Gupta, Gupta et al. 2018). The absorption peak observed at 1269.22 cm^{-1} is mainly associated with the C-O bond of lactones and phenolic compounds (Bounaas, Bouguettoucha et al. 2019). The band at 1050.88 cm^{-1} indicates the presence of cellulose, as evidenced by the stretching vibrations of C–O–C bonds (El-Kelany, Radwan et al. 2024). Additional peaks at 780.84 cm^{-1} and 628.18 cm^{-1} correspond to out-of-plane bending vibrations of –CH groups (Azzaz, Jellali et al. 2019).

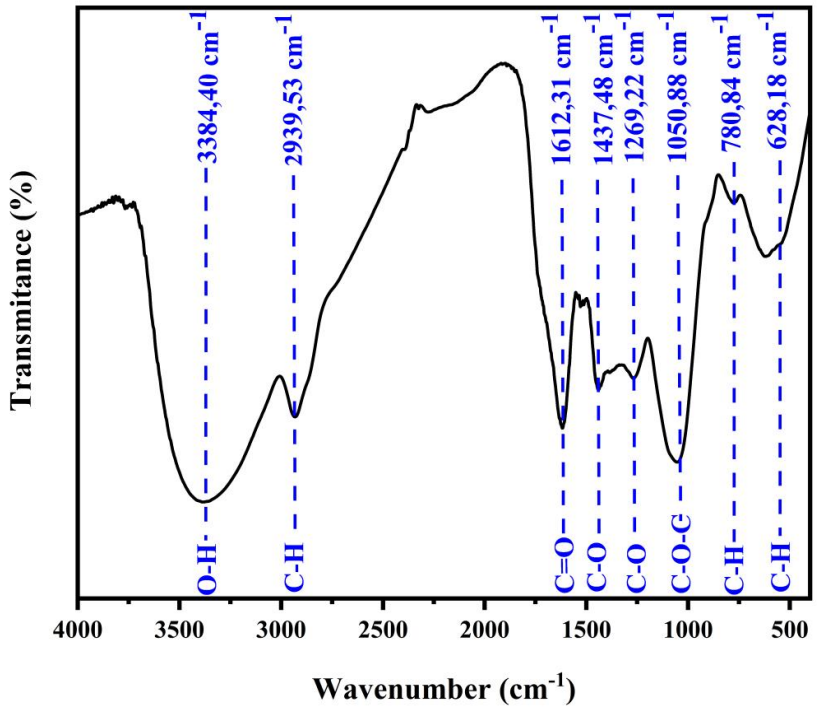

Figure II.1.2. FTIR specta of the raw material CC.

II.1.3.2. Scanning Electron Microscopy coupled with Energy Dispersive Spectroscopy (SEM/EDS)

The SEM analysis presented in Figure II.1.3 was performed using a Thermo Scientific Prisma E instrument. The CC sample exhibited an indistinct morphology characterized by irregular, disorganized edges and a rough, non-porous surface. The EDS analysis identified several chemical elements, including carbon (C), oxygen (O), stibium (Sb), and aluminium (Al), as listed in Table II.1.1.

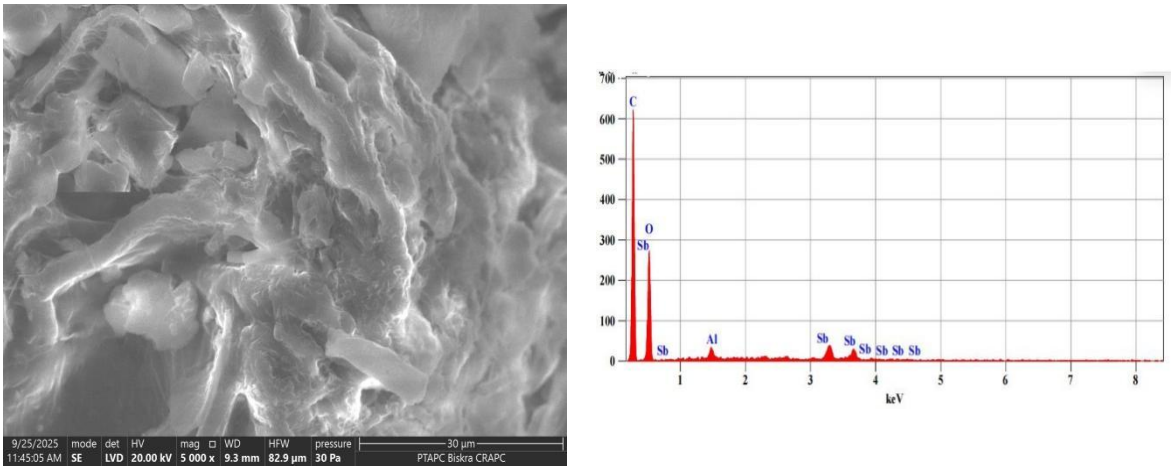

Figure II.1.3. SEM micrograph and EDS analysis of the raw material CC.

Table II.1.1. The chemical elements present on the surface of the raw material CC.

Elements	C	O	Sb	Al
Weight %	57.79	36.44	5.20	0.57

II.1.3.3. X-Ray Diffraction (XRD)

In this section, X-ray diffraction (XRD) was employed to evaluate the crystalline and amorphous characteristics of *Cypress cone* biomass. The XRD pattern of the raw cypress cones shows a broad diffraction peak around 2θ =22–24° , indicating that the material is predominantly amorphous (Hadey, Allouch et al. 2022). The lack of well-defined crystalline peaks suggests a low crystallinity, which is typical of untreated lignocellulosic biomass composed of cellulose, hemicellulose, and lignin.

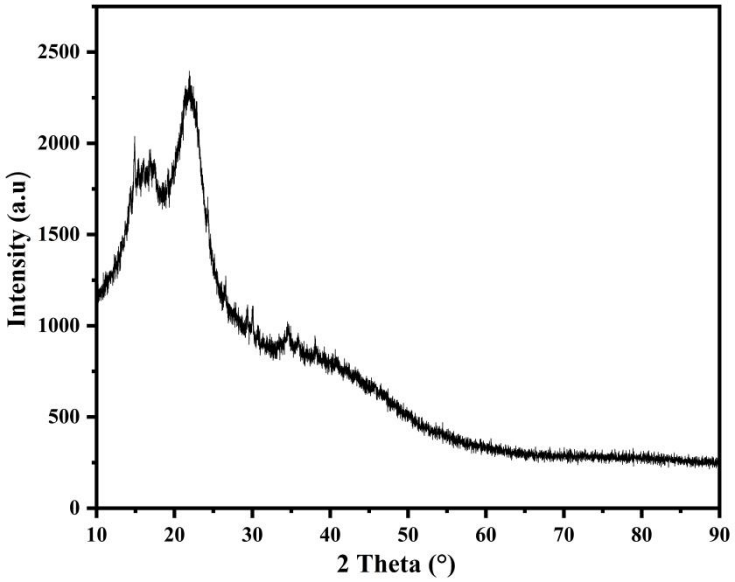

Figure II.1.4. XRD pattern of the raw material CC.

II.1.3.4. Brunauer -Emmett-Teller (BET)

The BET analysis of the raw CC yielded a specific surface area of 1.4000 m^2/g and a pore volume of 0.000569 cm^3/g. These values indicate a low specific surface area, which may be attributed to the non-porous nature of the structures. Compared with similar studies such as tea factory waste (1.3196 m2/g) (Wasewar, Atif et al. 2008), raw rice husk (0.1403 m^2/g) (Kolar and Jin 2019), Peanut Shells 1.7 m^2/g (Almeida-Naranjo, Frutos et al. 2024) Walnut shell powder (2.505 $m^2/$ g) (Uddin and Nasar 2020) it becomes evident that raw lignocellulosic materials generally exhibit low specific surface areas.

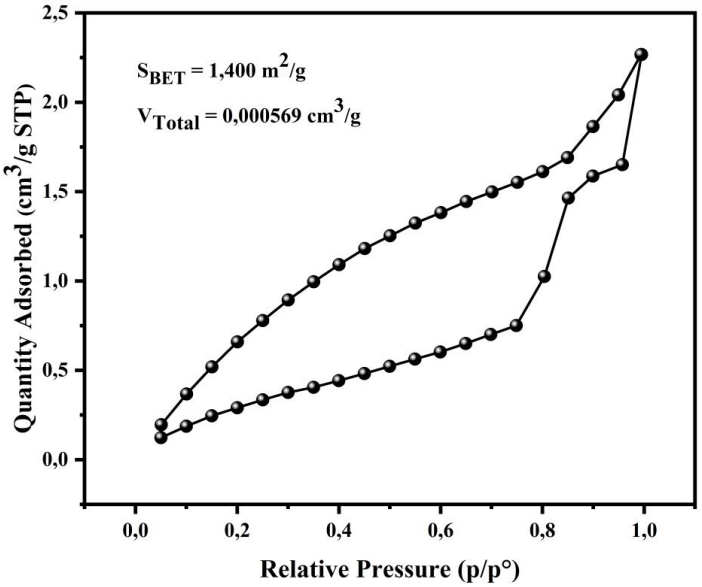

Figure II.1.5. Nitrogen adsorption isotherm for raw material CC.

II.1.3.5. Thermogravimetric analysis (TGA)

According to the thermogravimetric analysis reported by (Hamadneh, Al-Mobydeen et al. 2021), cypress cones biomass undergoes a two-step thermal degradation process. A slight mass reduction of about 4% appears between 60 °C and 220 °C, primarily reflecting the release of physically bound water. The main devolatilization phase follows between roughly 350 °C and 650 °C, during which approximately 70% of the material breaks down as organic constituents decompose. After this stage, the remaining solid residue accounts for 25.35% of the initial mass, corresponding to an overall mass loss of 74.65%.

II.1.4. Synthesis of different adsorbents

The raw material, cypress cones (CC), was collected from El-Kantara-Biskra, south-east of Algeria (Figure II.1.1). The CC was washed numerous times with tap water to remove contaminants, then with distilled water, before being dried for 12 h at 105 °C to reduce moisture content. After that, we crushed them into a fine powder. The amount of material obtained was divided into four fractions. The first three were pyrolysed at 450 °C, 550 °C, and 650 °C in a muffle furnace for 3 h, washed with 0.1 M HCl and agitated for 30 minutes, then cleaned with deionized water to achieve a neutral pH and remove chloride. This sample is labelled cypress cones biochar (CCB-450, CCB-550, CCB-650). The fourth part was treated with 40 ml of $ZnCl_2$ (0.5 M) and stirred for 1 h. The mixture was then dried for 12 h at 105 °C and carbonized for 3 h at 650 °C. The next step was washed with distilled water to remove chloride and achieve a neutral pH. Finally, the washed material was oven-dried at 105 °C for 24 h and designated as cypress cone activated carbon (CC-$ZnCl_2$-AC). Figure II.1.7 illustrates the different steps of adsorbent preparation.

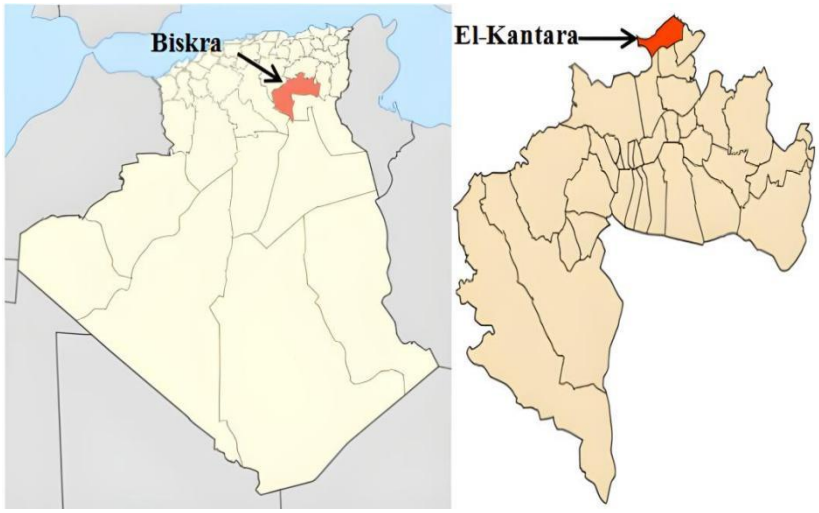

Figure II.1.6. Geographical localization map of the study area.

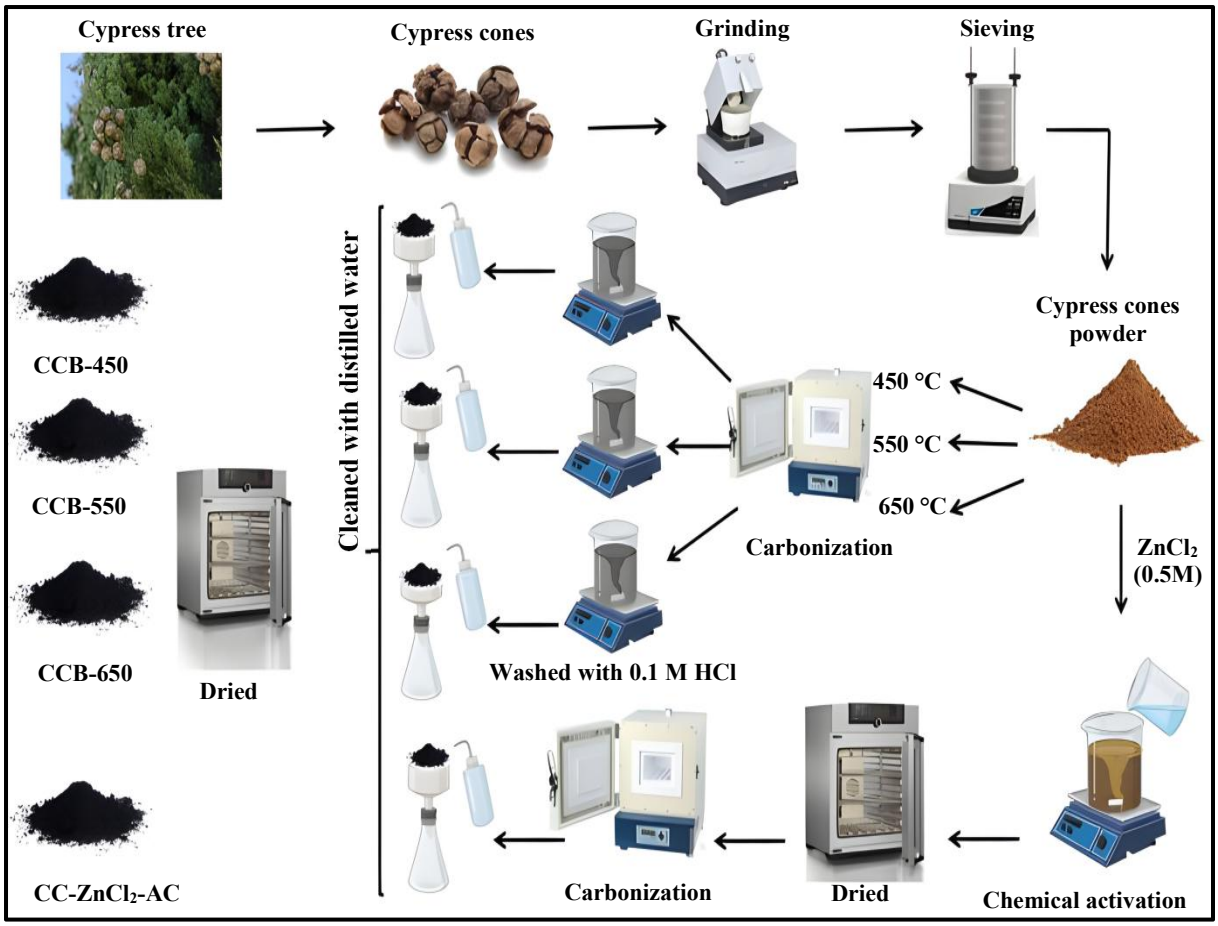

Figure II.1.7. Preparation steps of adsorbents.

II.1.5. Adsorbents characterization

Various techniques are employed to characterize the physical and chemical properties of each prepared adsorbent, including: Brunauer-Emmett-Teller (BET), Fourier Transform Infrared (FT-IR), Scanning Electron Microscopy coupled with Energy Dispersive Spectroscopy (SEM/EDS), X–Ray Diffraction(XRD), and the measurement of the point of zero charge.

II.1.5.1. Fourier Transform Infrared (FT-IR)

Fourier Transform Infrared Spectroscopy (FTIR) was used to characterize the surface functional groups of our adsorbents before the adsorption of pharmaceutical contaminants, in the wavenumber range of 400–4000 cm^{-1}.

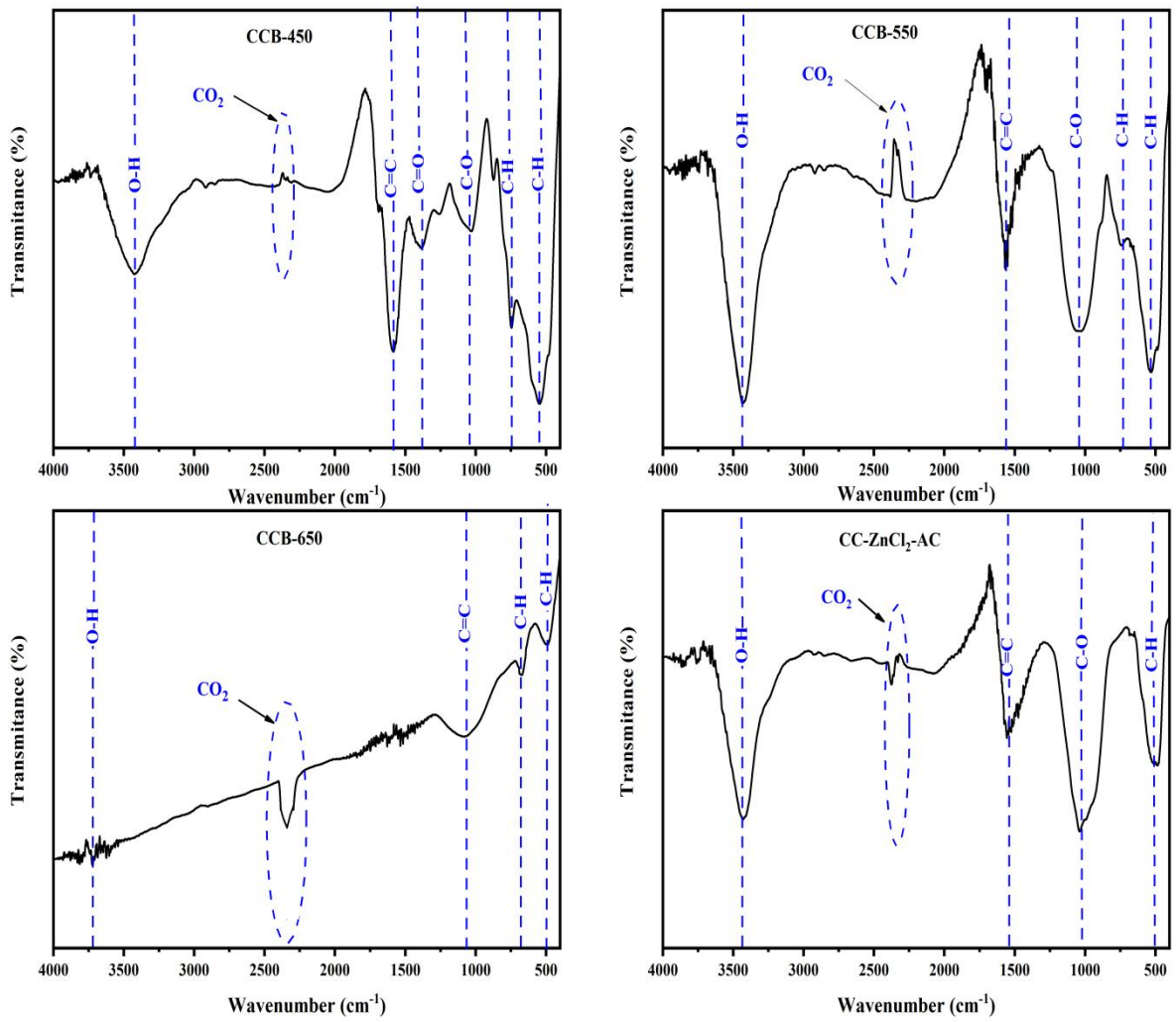

Figure II.1.8. FTIR spectra of CCB-450, CCB-550, CCB-650, CC-$ZnCl_2$-AC.

FTIR spectroscopy confirmed the presence of distinct functional groups, with notable variations in their intensities across the different adsorbents. A broad band observed around 3290-3650 cm^{-1} suggested O–H stretching vibrations, potentially from water, carboxylic acids, phenols, or alcohols (Mazen S. F. Al-Hazeef 2024). However, this peak is nearly absent in the CCB-650 spectrum. This absence can be ascribed to the intensified dehydration reactions in the biomass as pyrolysis temperature increases (Kim, Kim et al. 2012), In contrast, its presence in CC-$ZnCl_2$-AC may be due to the chemical modification applied during treatment. The minor band observed at 2367 cm^{-1} is attributed to atmospheric CO_2, as reported by (Hamida, Rehali et al. 2024). Furthermore, the appearance of a band at 1576 cm^{-1} is attributed to vibrations of the C=C bond (Salem, Ouakouak et al. 2023). In CCB-650, the marked reduction in the intensity of the prominent C=C peak indicates that, at elevated temperatures, the volatile carbon was eliminated, leaving behind only structural carbon (Chebbi, Ounoki et al. 2023). C–O vibrations of phenolic or carboxylate groups were

identified by the band appearing at 1051 cm^{-1} (Lima, Hosseini-Bandegharaei et al. 2019; Yanan, Srour et al. 2023). The intensity of this bond decreased in CCB-650. Peaks below 700 cm^{-1} in the wave counts indicate the presence of C-H functional groups (Saied, Shaban et al. 2024).

II.1.5.2. Scanning Electron Microscopy coupled with Energy Dispersive Spectroscopy (SEM/EDS)

A scanning electron microscope (SEM) was used to visualize the surface morphology of the prepared adsorbents. The figure shows scanning electron micrographs of the three prepared biochars at different pyrolysis temperatures: CCB-450, CCB-550, and CCB-650. The micrographs clearly show that changes in pyrolysis temperature have a pronounced effect on the surface morphology. At the lower temperature of 450 °C, the CCB-450 sample looked to show minor damage (Abubakar, Saeed et al. 2024). As the pyrolysis temperature increased, greater volatile gas evolution from the biomass led to the rupture of surface vesicles on CCB-550 (Zhao, Ta et al. 2017). This transformation led to the development of a porous morphology characterized by numerous macropores. Figure II.1.11 illustrates the morphological characteristics of CCB-650. The surface exhibits a heterogeneous, irregular texture, characterised by randomly distributed pores and cavities of varying geometries and sizes. The emergence of these porous structures is likely attributed to the thermal decomposition of volatile organic constituents in the biomass, notably lignin and cellulose, during pyrolysis (Melliti, Touihri et al. 2024). Additionally, the intensified and accelerated carbonization process may have further contributed to the extensive pore development observed (Elnour, Alghyamah et al. 2019). An increase in porosity is observed when transitioning from the raw material (Figure II.1.3) to the pyrolysed samples. Simultaneously, the CC-$ZnCl_2$-AC exhibited pores with diverse shapes and dimensions Figure II.1.12. This finding aligns with earlier studies (Ma, Wang et al. 2015; Mazen S. F. Al-Hazeef 2024; Saied, Shaban et al. 2024), which highlighted the important influence of $ZnCl_2$ in markedly improving the surface area, porosity, and adsorption performance of carbon-based materials. These cavities were generated during the chemical activation and carbonization processes, resulting from the emission of volatile gases released by the precursor material.

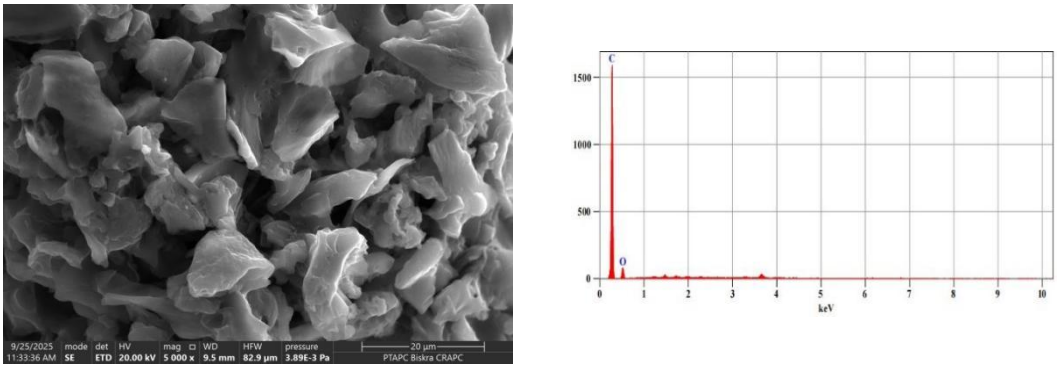

Figure II.1.9. SEM micrograph and EDS analysis of CCB-450.

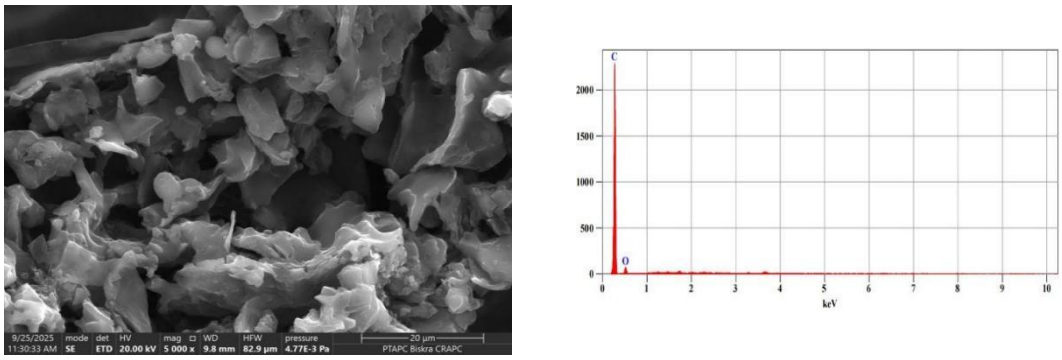

Figure II.1.10. SEM micrograph and EDS analysis of CCB-550.

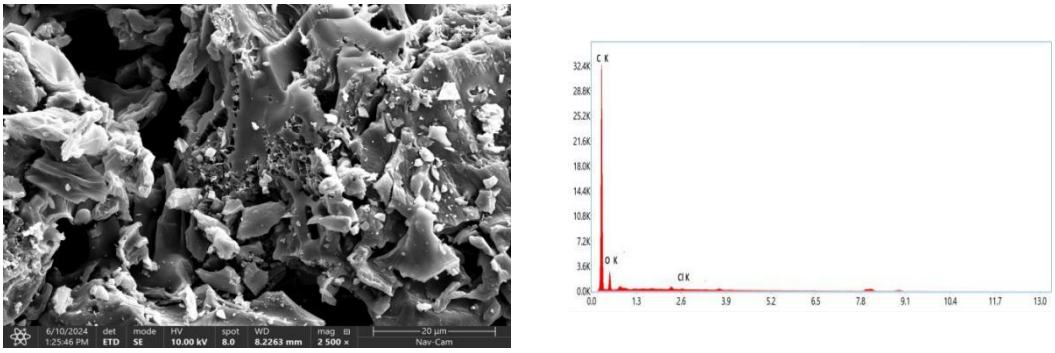

Figure II.1.11. SEM micrograph and EDS analysis of CCB-650.

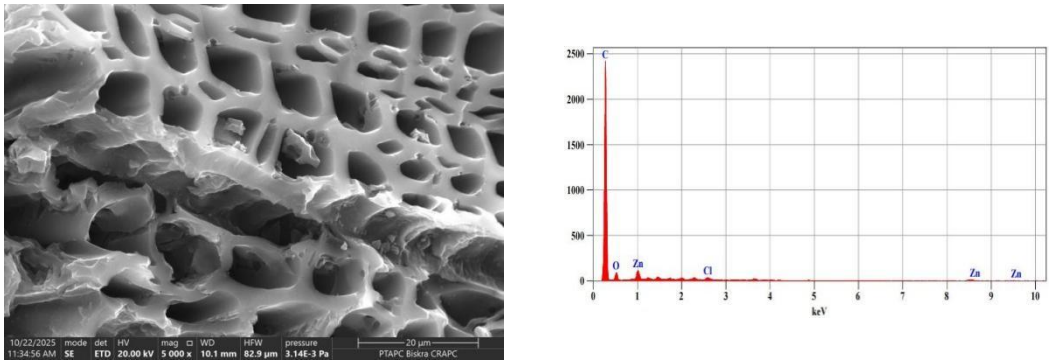

Figure II.1.12. SEM micrograph and EDS analysis of CC-$ZnCl_2$-AC.

The results of the energy-dispersive spectroscopy (EDS) analysis of the samples reveal that increasing pyrolysis temperature led to a progressive increase in carbon content, accompanied by a decline in oxygen levels, consistent with carbon enrichment of the material. This finding implies that the degree of carbonization intensified with increasing pyrolysis temperature. The elimination of volatile compounds at elevated temperatures led to a higher carbon concentration, particularly of aromatic carbon species, thereby enhancing both the structural stability and adsorption performance of the material (Kim, Kim et al. 2012; Sathyabama and Firdous 2025). The reduction in oxygen content can be attributed to the cleavage of weak bonds within the biochar matrix, resulting from the dehydration of organic matter and the release of volatile constituents (Abubakar, Saeed et al. 2024).

The results of EDS indicate that carbon (C) is the predominant element in all samples, with the highest content observed in the sample activated with $ZnCl_2$ (CC-$ZnCl_2$-AC). This elevated carbon content suggests enhanced retention of carbonaceous matter, likely due to $ZnCl_2$'s high efficiency in promoting deep activation (khadidja 2025). Trace amounts of Cl were detected in the CCB-650 sample, suggesting incomplete removal of residual chloride species during post-washing with distilled water. The activated carbon (CC-$ZnCl_2$-AC) is also characterized by the presence of a small amount of zinc (0.65%) and chlorine (1.12%), confirming the successful impregnation of the activating agent and suggesting specific surface properties of the activated material.

II.1.5.3. X-Ray Diffraction (XRD)

X-ray diffraction (XRD) was the analytical technique used for phase identification of the prepared materials. The XRD pattern of the synthesized adsorbents are presented in Figure II.1.13.

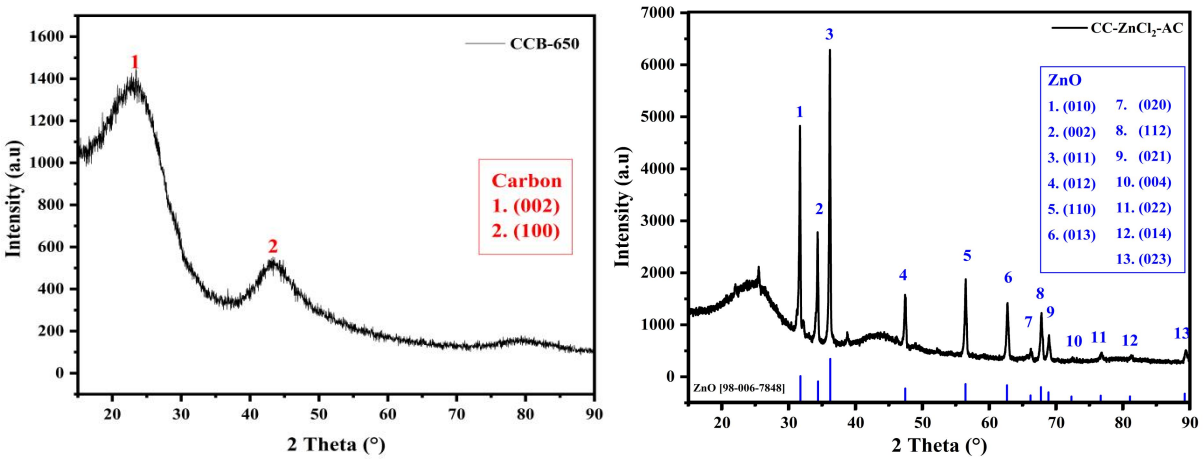

Figure II.1.13. XRD pattern of CCB-650 and CC-$ZnCl_2$-AC.

The XRD pattern of CCB-650 shows a broad diffraction feature near 2θ ≈ 23.3°, attributed to the (002) planes of graphitic-type carbon domains within the biochar. A weak and diffuse signal around 43.5° assigned to the (100) reflection, suggests the presence of small, partially ordered graphene-like regions, consistent with previous findings in the literature (Tang, Yan et al. 2017; Bedin, Cazetta et al. 2018; Tran, Tomul et al. 2020; Naima, Ammar et al. 2022; Saied, Shaban et al. 2024). Due to the absence of sharp peaks, the prepared biochar is highly amorphous. These observations highlight the efficiency of the one-step carbonization process employed in this research for degrading the cellulose and lignin in the biomass, generating a highly graphitic carbon product (Islam, Nazal et al. 2024).

The X-ray diffraction (XRD) pattern of the activated carbon obtained through impregnation with $ZnCl_2$ and carbonized at 650 °C shows a predominantly crystalline carbon structure, along with the presence of crystalline inorganic phases. A broad diffraction band observed in the range of 2θ ≈ 25.55° is characteristic of disordered carbon, indicating that the obtained material lacks a well-developed graphitic structure and is mainly amorphous. Additionally, several sharp and intense diffraction peaks were observed at 2θ values of approximately 31.70°, 34.36°, 36.18°, 47.48°, 56.50°, 62.75°, 66.28°,67.86°, 72.47°, 76.85°, 81.29°, 89.39° which were indexed to the (010), (002), (011), (012), (110), (013), (020), (112), (021), (004), (022), (014), and (023) crystal planes, respectively, in good agreement with the standard ICSD card [98-006-7848]. These diffraction peaks confirm the successful formation of highly crystalline hexagonal ZnO during the carbonization process. The high intensity and sharpness of these peaks indicate a good degree of crystallinity of the ZnO particles embedded within the carbon matrix. This suggests that the activation process not only developed porosity within the carbon structure but also resulted in the formation of a ZnO/carbon composite, which may contribute to enhanced adsorption properties.

II.1.5.4. Brunauer -Emmett-Teller (BET)

The textural characteristics of the prepared adsorbents can be experimentally determined using the BET (Brunauer-Emmett-Teller) method. The nitrogen adsorption–desorption method at 77 K is necessary for determining specific surface area, pore volume, and pore diameter, and for evaluating the adsorption potential of materials.

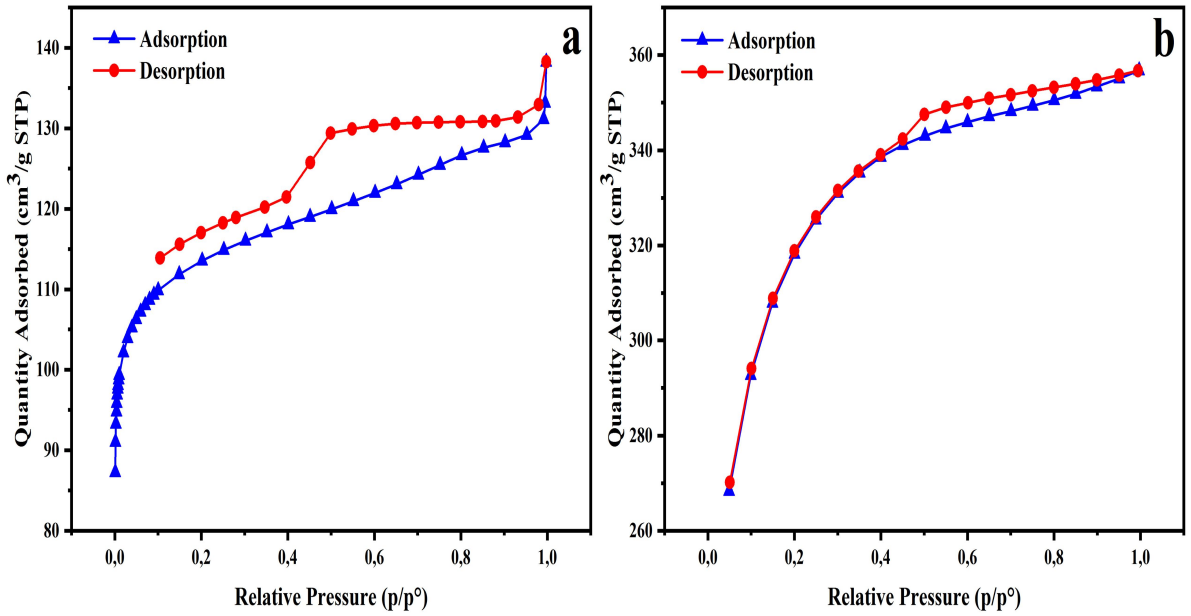

Figure II.1.14. The nitrogen adsorption/desorption isotherms of (a) CCB-650 and (b) CC-$ZnCl_2$-AC.

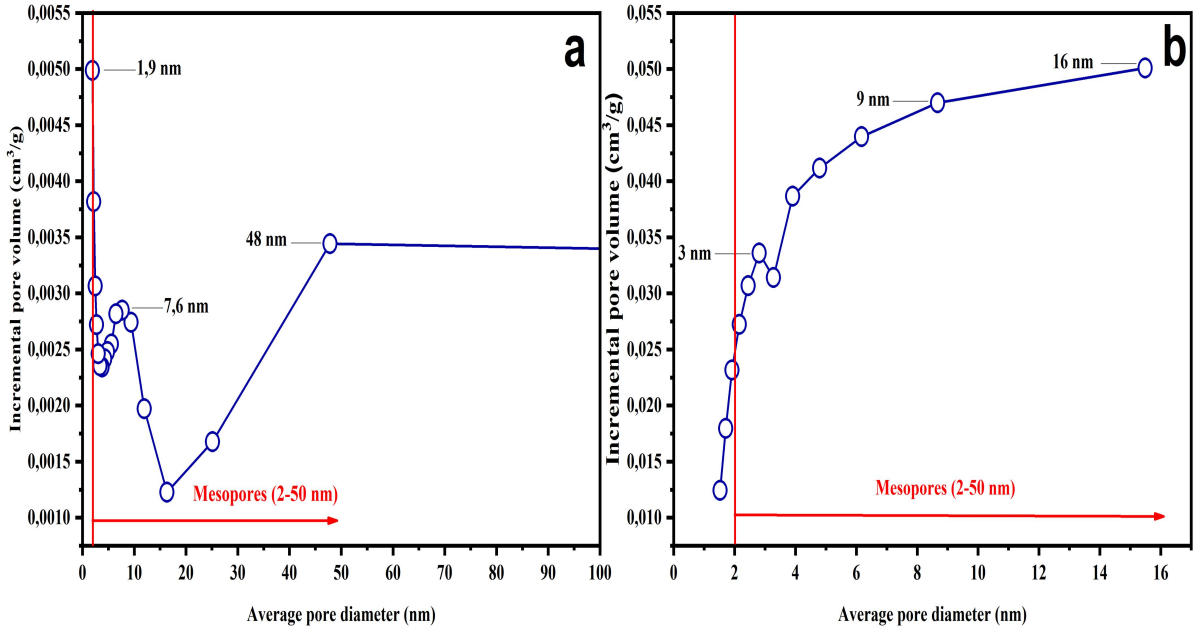

Figure II.1.15. The pore size distribution of (a) CCB-650 and (b) CC-$ZnCl_2$-AC.

Figure II.1.14 displays the nitrogen adsorption–desorption isotherms of the two synthesized materials, CCB-650 and CC-$ZnCl_2$-AC. Based on the IUPAC classification (Thommes et al., 2015), the obtained isotherms for CCB-650 and CC-$ZnCl_2$-AC correspond to Type IV with an H3-type hysteresis loop. These patterns indicate that both samples possess a well-developed hierarchical mesoporous structure, characterized by slit-shaped pores or plate-like particles.

As depicted in Figure II.1.15, the pore size distributions fall within the mesoporous range (2–50 nm).

The specific surface area (S_{BET}) and total pore volume (V_{Total}) of CC-$ZnCl_2$-AC, recorded as 1183.23 m^2/g and 0.455 cm^3/g, respectively, were significantly greater than those obtained for CCB-650 biochar, which exhibited values of 365.57 m^2/g and 0.199 cm^3/g. CCB-650, produced by direct carbonization of Cypress cones without $ZnCl_2$ activation, exhibited a low specific surface area and pore volume. These results highlight the crucial role of $ZnCl_2$ in promoting pore formation and developing the porosity of the resulting activated carbon. Therefore, $ZnCl_2$ has been confirmed as an effective activating agent for converting CC into activated carbon (Ma, Wang et al. 2015; Saied, Shaban et al. 2024). Generally, materials possessing a larger specific surface area tend to demonstrate superior adsorption capacity and enhanced solute diffusion compared to those with smaller S_{BET} values.

II.1.5.5. pH point of zero charge

The pH point of zero charge (pHpzc) was determined following the procedure outlined in earlier research by (Naima, Ammar et al. 2022).

- Aqueous NaCl solutions were prepared at a molar concentration of 0.01 M.
- The initial pH of each solution is adjusted by adding NaOH or HCl.
- Mixing 30 mg of each adsorbent into 30 ml of NaCl adjusted solutions (from pH 2 to pH 12). The mixtures were continuously agitated for 24 h at ambient temperature using a mechanical shaker.
- Each sample was subjected to filtration at the end of the test, followed by measurement of the final solution pH using a pH meter.
- The pH_{pzc} value of CCB-650 and CC-$ZnCl_2$-AC was defined graphically by plotting the intersection point of the curve ΔpH (pHi − pHf) versus pHi.

The point of zero charge (pHpzc) refers to the pH at which a material's surface exhibits no net electrical charge. This parameter plays a key role in adsorption, as it governs the interaction of the adsorbent surface with surrounding ions and molecules in solution. Figure II.1.16 presents the pHpzc values for the supports, where the surface charge is zero. The results show a pHpzc of 6.9 for CCB-650 and 6.18 for CC-$ZnCl_2$-AC. These findings imply that CCB-650 and CC $ZnCl_2$-AC exhibit a negatively charged surface when the solution pH exceeds the pHpzc (pH > pHpzc), whereas their surfaces become positively charged at pH values below the pHpzc (pH <pHpzc).

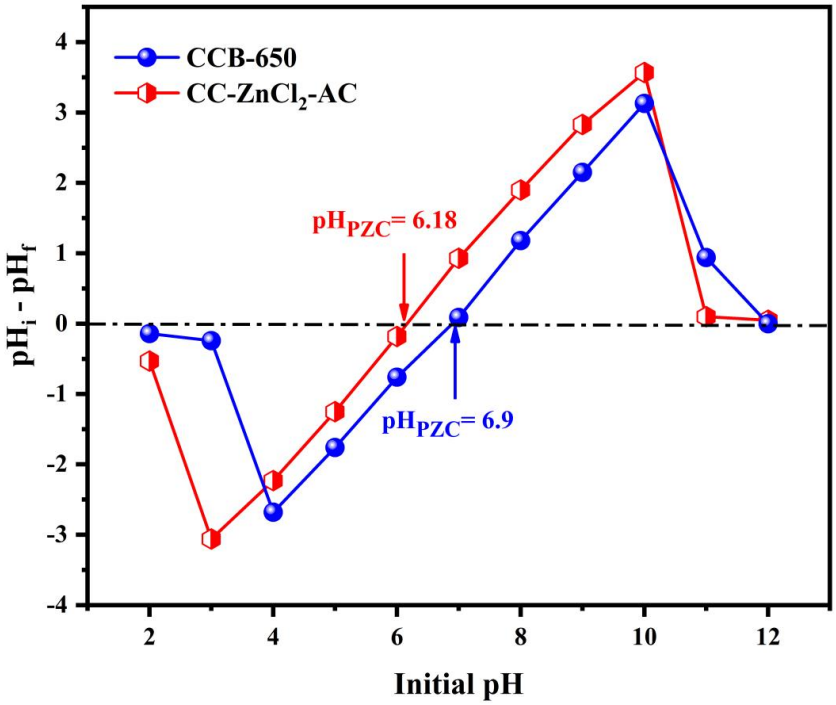

Figure II.1.16. pH point of zero charge (pH_{pzc}) of CCB-650 and CC-$ZnCl_2$-AC.

II.1.6. Conclusion

In this chapter, we present the characteristics of the synthesized adsorbent derived from cypress cones. The various samples were examined through a range of physicochemical analyses, as well as spectroscopic and microscopic techniques. FTIR analysis identified key functional groups like O–H, C=C, C–O, and C–H, demonstrating that the material's surface chemistry is well-suited for capturing a wide range of contaminants. The XRD analysis indicated that the CCB-650 material exhibit an amorphous structural nature,Whereas the activated carbon CC-ZnCl2-AC displayed a crystalline stucture. The SEM micrographs display distinct morphological variations that are directly influenced by the degree of carbonization and the chemical treatment applied. BET characterization indicated that the activated carbon CC-$ZnCl_2$-AC exhibits a significantly greater specific surface area compared to the CCB-650 biochar. The investigation of the pH point of zero charge provided essential information on the surface properties and the interaction behavior of the adsorbents with diverse adsorbates under varying environmental conditions.

References

Abubakar, I., M. Saeed, et al. (2024). "Physicochemical Properties of Biochar Prepared from Guinea Corn Straw as a Function of Different Pyrolysis Temperatures." J Envi Sci Agri Res **2**(4): 1-8 DOI: doi.org/10.61440/JESAR.2024.v2.37.

Almeida-Naranjo, C. E., M. Frutos, et al. (2024). "Characterization and performance of peanut shells in caffeine and triclosan removal in batch and fixed-bed column tests." Molecules **29**(12): 2923 DOI: https://doi.org/10.3390/molecules29122923.

Azzaz, A., S. Jellali, et al. (2019). "Investigations on a dye desorption from modified biomass by using a low-cost eluent: hysteresis and mechanisms exploration." International Journal of Environmental Science and Technology **16**(11): 7393-7408 DOI:https://doi.org/10.1007/s13762-018-2171-3.

Bedin, K. C., A. L. Cazetta, et al. (2018). "Porosity enhancement of spherical activated carbon: Influence and optimization of hydrothermal synthesis conditions using response surface methodology." Journal of environmental chemical engineering **6**(1): 991-999 DOI: https://doi.org/10.1016/j.jece.2017.12.069.

Benaoune, S., A. Merzougui, et al. (2025). "Dual-activated tamarix gallica-derived carbons for enhanced glyphosate adsorption: A comparative study of phosphoric and sulfuric acid activation." Materials **18**(3): 511 DOI: https://doi.org/10.3390/ma18030511.

Bouguenoun, I., M.-C. De Pauw-Gillet, et al. (2016). "Effet inflammatoire des extraits de Cupressus sempervirens planté dans l'Est de l'Algérie: du modèle murin à la stimulation des cellules BEAS-2B par l'allergène majeur Cup s 1." Revue Française d'Allergologie **56**(1): 10-19 DOI: https://doi.org/10.1016/j.reval.2015.09.005.

Bounaas, M., A. Bouguettoucha, et al. (2019). "High efficiency of methylene blue removal using a novel low-cost acid treated forest wastes, Cupressus semperirens cones: experimental results and modeling." Particulate Science and Technology **37**(4): 504-513 DOI: https://doi.org/10.1080/02726351.2017.1401569.

Chebbi, M., S. Ounoki, et al. (2023). "Synthesis and characterization of pine cones biochar for the removal of an antibiotic (Metronidazole) from aqueous solutions." Journal of Industrial and Engineering Chemistry **126**: 327-339 DOI: https://doi.org/10.1016/j.jiec.2023.06.023.

El-Kelany, S. M., E. K. Radwan, et al. (2024). "Insights into the adsorption of emerging organic contaminant by low-cost readily separable modified jute fiber." Environmental Science and Pollution Research **31**(52): 61763-61780 DOI: https://doi.org/10.1007/s11356-024-35295-2.

Elnour, A. Y., A. A. Alghyamah, et al. (2019). "Effect of pyrolysis temperature on biochar microstructural evolution, physicochemical characteristics, and its influence on biochar/polypropylenecomposites."Appliedsciences**9**(6):1149DOI:https://doi.org/10.3390/app9061149.

Gupta, M., H. Gupta, et al. (2018). "Adsorption of Cu (II) by low cost adsorbents and the cost analysis." Environmental Technology & Innovation **10**: 91-101 DOI: https://doi.org/10.1016/j.eti.2018.02.003.

Hadey, C., M. Allouch, et al. (2022). "Preparation and characterization of biochars obtained from biomasses for combustible briquette applications." The Scientific World Journal **2022**(1): 2554475 DOI:

Hamadneh, I., A. Al-Mobydeen, et al. (2021). "Arsenite adsorption on biochar-based nano copper oxide composites using mediterranean cypress cones: Equilibrium, kinetic and thermodynamic studies." Desalination and Water Treatment **221**: 260-269 DOI: https://doi.org/10.5004/dwt.2021.27043.

Hamida, K., H. Rehali, et al. (2024). "A low cost bio-composite derived from potato plant waste (PPW-ZnO) for the removal of Rhodamine B." Reaction Kinetics, Mechanisms and Catalysis **137**(2): 1189-1207 DOI: https://doi.org/10.1007/s11144-024-02567-4.

Ialeff, K. A., A. Debib, et al. (2021). "Phenolic content and antibacterial activity of Cupressus sempervirens leaves extracts against phytopathogenic bacteria Pectobacterium atrosepticum causative agent of soft rot on potato and clinical bacteria strains." Tropical Journal of Natural Product Research **5**: 866-872 DOI: http://doi.org/10.26538/tjnpr/v5i5.12.

Islam, M. A., M. K. Nazal, et al. (2024). "High performance adsorptive removal of emerging contaminant paracetamol using a sustainable biobased mesoporous activated carbon prepared from palm leaves waste." Journal of Analytical and Applied Pyrolysis **180**: 106546 DOI: https://doi.org/10.1016/j.jaap.2024.106546.

khadidja, H. (2025). Elaboration et caractérisation d'un composite à base biochar et ses applications à la photocatalyse et l'adsorption des polluants, Faculté des Sciences et technologie,University de Biskra.

Kim, K. H., J.-Y. Kim, et al. (2012). "Influence of pyrolysis temperature on physicochemical properties of biochar obtained from the fast pyrolysis of pitch pine (Pinus rigida)." Bioresource Technology **118**: 158-162 DOI: https://doi.org/10.1016/j.biortech.2012.04.094.

Kolar, P. and H. Jin (2019). "Baseline characterization data for raw rice husk." Data in brief **25**: 104219 DOI: https://doi.org/10.1016/j.dib.2019.104219.

Larous, S. and A.-H. Meniai (2016). "Adsorption of Diclofenac from aqueous solution using activated carbon prepared from olive stones." International Journal of Hydrogen Energy **41**(24): 10380-10390 DOI: https://doi.org/10.1016/j.ijhydene.2016.01.096.

Lima, D. R., A. Hosseini-Bandegharaei, et al. (2019). "Efficient acetaminophen removal from water and hospital effluents treatment by activated carbons derived from Brazil nutshells." Colloids and Surfaces A: Physicochemical and Engineering Aspects **583**: 123966 DOI: https://doi.org/10.1016/j.colsurfa.2019.123966.

Ma, Y., Q. Wang, et al. (2015). "A comprehensive study on activated carbon prepared from spent shiitake substrate via pyrolysis with ZnCl2." Journal of porous materials **22**(1): 157-169 DOI: https://doi.org/10.1007/s10934-014-9882-8.

Mazen S. F. Al-Hazeef, A. Amel, et al.(2024). "Valorizing date palm spikelets into activated carbon-derived composite for methyl orange adsorption: advancing circular bioeconomy in wastewater treatment—a comprehensive study on its equilibrium, kinetics, thermodynamics, and mechanisms." Environmental Science and Pollution Research **31**: 50493–50512 DOI: https://doi.org/10.1007/s11356-024-34581-3.

Melliti, A., M. Touihri, et al. (2024). "Sustainable removal of caffeine and acetaminophen from water using biomass waste-derived activated carbon: Synthesis, characterization, and modelling." Chemosphere **355**: 141787 DOI: https://doi.org/10.1016/j.chemosphere.2024.141787.

Naima, A., F. Ammar, et al. (2022). "Development of a novel and efficient biochar produced from pepper stem for effective ibuprofen removal." Bioresource Technology **347**: 126685 DOI: https://doi.org/10.1016/j.biortech.2022.126685.

Nampeera, J., Y. K. Recepoğlu, et al. (2024). "Valorization of olive tree pruning waste for potential utilization in lithium recovery from aqueous solutions." Biomass Conversion and Biorefinery **14**(4): 4975-4987 DOI: https://doi.org/10.1007/s13399-022-02647-2.

Saied, M. E., S. A. Shaban, et al. (2024). "Efficient adsorption of acetaminophen from the aqueous phase using low-cost and renewable adsorbent derived from orange peels." Biomass Conversion and Biorefinery **14**(2): 2155-2172 DOI: https://doi.org/10.1007/s13399-022-02541-x.

Salem, D. B., A. Ouakouak, et al. (2023). "Easy separable, floatable, and recyclable magnetic-biochar/alginate bead as super-adsorbent for adsorbing copper ions in water media." Bioresource Technology **383**: 129225 DOI: https://doi.org/10.1016/j.biortech.2023.129225.

Sathyabama, K. and S. Firdous (2025). "Effect of Pyrolysis Temperature on the Physicochemical Properties and Structural Characteristics of Agricultural Wastes-Derived Biochar." ACS omega **10**(33): 37013-37024 DOI: https://doi.org/10.1021/acsomega.5c00120.

Tang, H., D. Yan, et al. (2017). "Sulfur-doped carbon spheres with hierarchical micro/mesopores as anode materials for sodium-ion batteries." Electrochimica Acta **241**: 63-72 DOI: https://doi.org/10.1016/j.electacta.2017.04.112.

Tran, H. N., F. Tomul, et al. (2020). "Innovative spherical biochar for pharmaceutical removal from water: Insight into adsorption mechanism." Journal of hazardous materials **394**: 122255 DOI: https://doi.org/10.1016/j.jhazmat.2020.122255.

Uddin, M. K. and A. Nasar (2020). "Walnut shell powder as a low-cost adsorbent for methylene blue dye: isotherm, kinetics, thermodynamic, desorption and response surface methodology examinations." Scientific reports **10**(1): 7983 DOI: https://doi.org/10.1038/s41598-020-64745-3.

Wasewar, K. L., M. Atif, et al. (2008). "Adsorption of zinc using tea factory waste: kinetics, equilibrium and thermodynamics." CLEAN–Soil, Air, Water **36**(3): 320-329 DOI: https://doi.org/10.1002/clen.200700139.

Yanan, C., Z. Srour, et al. (2023). "Adsorption of paracetamol and ketoprofenon activated charcoal prepared from the residue of the fruit of Butiacapitate: Experiments and theoretical interpretations." Chemical Engineering Journal **454**: 139943 DOI: https://doi.org/10.1016/j.cej.2022.139943.

Zhao, S.-X., N. Ta, et al. (2017). "Effect of temperature on the structural and physicochemical properties of biochar with apple tree branches as feedstock material." Energies **10**(9): 1293 DOI: https://doi.org/10.3390/en10091293.

Chapter 2:

Adsorption of Paracetamol and Diclofenac onto CCB-650

II.2. Adsorption of Paracetamol and Diclofenac onto CCB-650

II.2.1. Introduction

In this chapter, we studied the adsorption of pharmaceutical compounds (paracetamol and diclofenac) onto biochars from cypress cones. In this context, the effects of several operational factors, including contact time, initial solution pH, adsorbent dosage, initial pollutant concentration, and ionic strength, were investigated on the removal efficiency and adsorption capacity of the pollutants. Adsorption kinetic and isotherm models were applied to understand the adsorption process better and determine the maximum adsorption capacity of the adsorbent for both pollutants.

II.2.2. Preparation of synthetic solutions

Distilled water was used to prepare synthetic solutions. Stock solutions of paracetamol and diclofenac at 500 mg/L were prepared from analytical-grade reagents. These stock solutions were used to prepare calibration standards and the required dilutions for the adsorption experiments.

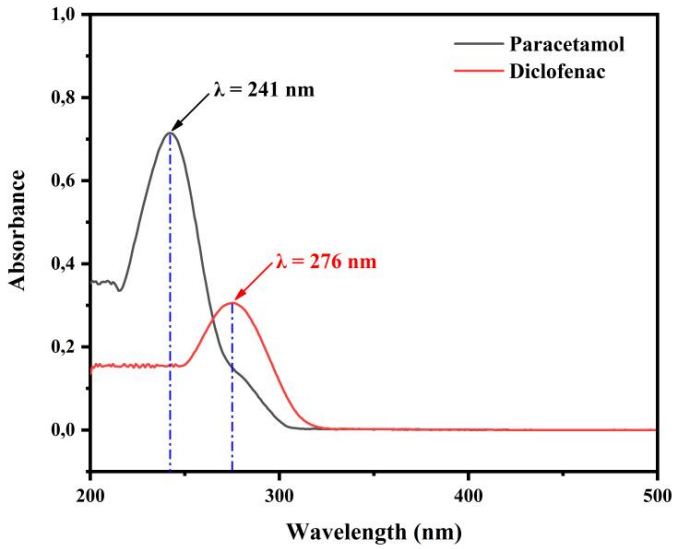

Figure.II.2.1. Typical UV-Vis spectrum of each single solution of PCM and DCF.

II.2.3. Investigation of Operational Conditions Influencing PCM and DCF Adsorption

Adsorption studies using an adsorbent dosage of 1 g/L of CCB-650 were conducted in 30 mL of drug solution (C_0 = 25 mg/L, pH = 5.4, T = 25 ± 5 °C) under magnetic stirring. Subsequently, the mixture (absorbent-adsorbate) was separated using a 0.2 µm syringe filter. A UV-Vis spectrophotometer (PhotoLab DR-6000) was used to measure the residual concentrations of PCM and DCF at λ = 241 nm and λ = 276 nm, respectively.

II.2.3.1. Investigation of Adsorption Kinetics

To identify the most efficient adsorbent among the three biochars produced at varying carbonization temperatures, adsorption kinetic experiments for both pollutants were carried out using the three biochars (CCB-450, CCB-550, and CCB-650) under the same operational conditions. The biochar exhibiting the highest removal efficiency was considered the most effective.

Figure II.2.2 shows that biochar produced at 650°C exhibits high efficiency in removing both paracetamol and diclofenac, achieving removal rates of 97.75% and 62.17%, respectively, after an equilibrium time of 180 minutes and an adsorbent dose of 1 g/L. Given these promising outcomes, it is advisable to conduct a detailed investigation into the adsorption kinetics and the influence of other operational parameters for the CCB-650 biochar.

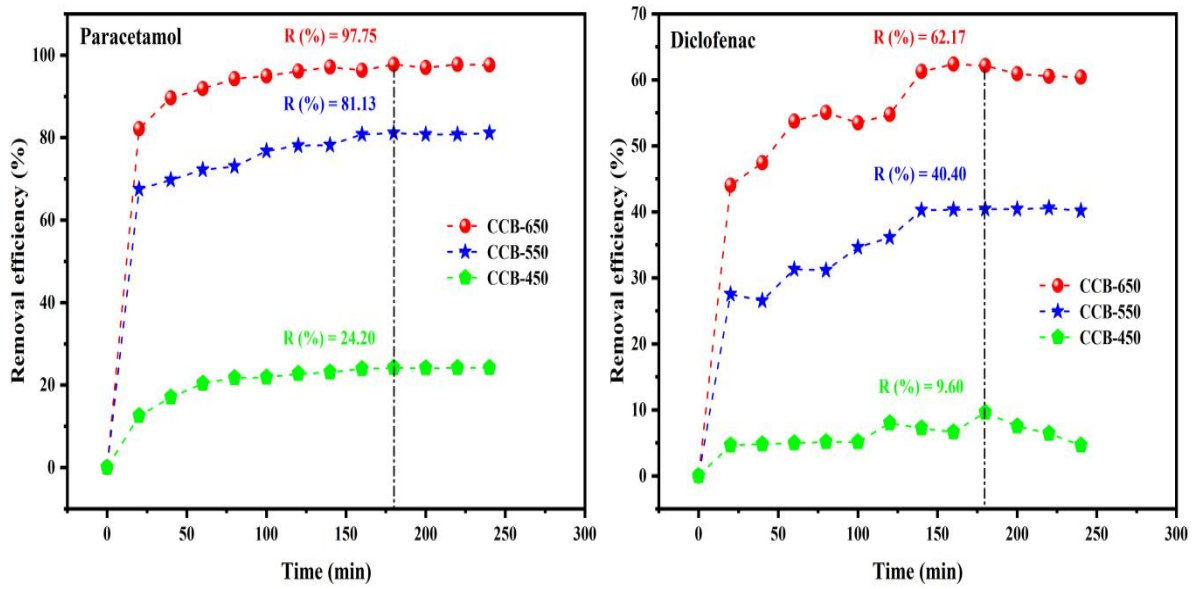

Figure II.2.2. Comparison between the evolutions of the adsorption efficiency of paracetamol and diclofenac on the prepared biochars as a function of time.

Evaluating the effect of contact time between CCB-650 and paracetamol or diclofenac is fundamental for a comprehensive understanding of adsorption mechanisms and for accurate kinetic modelling. The influence of this parameter on the removal efficiency of paracetamol and diclofenac is depicted in Figure II.2.3 and Figure II.2.4, respectively.

The findings demonstrate that adsorption capacity increases with extended contact time, reaching near-optimal values within the first 60 min: 22.98 mg/g for paracetamol and 13.44 mg/g for diclofenac. Nevertheless, the highest removal efficiencies were obtained at an equilibrium time of 180 min, with removal rates of 97.75% and 62.17%, and maximum

adsorption capacities of 24.44 mg/g and 15.58 mg/g for paracetamol and diclofenac, respectively. The experimental kinetic data were analysed and fitted using non-linear pseudo-first-order (PFO), pseudo-second-order (PSO), and Elovich models, as well as the linear intra-particle diffusion model. The modelling outcomes are presented in Table II.2.1.

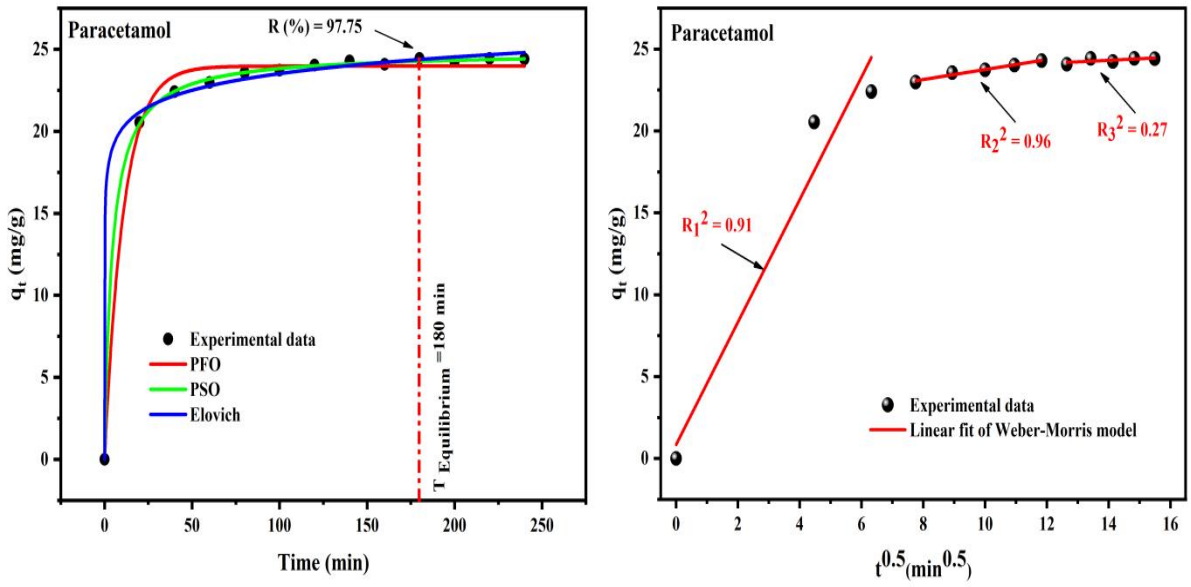

Figure II.2.3. Kinetics of paracetamol adsorption (Nonlinear fitting and Linear fitting of Weber-Morris model).

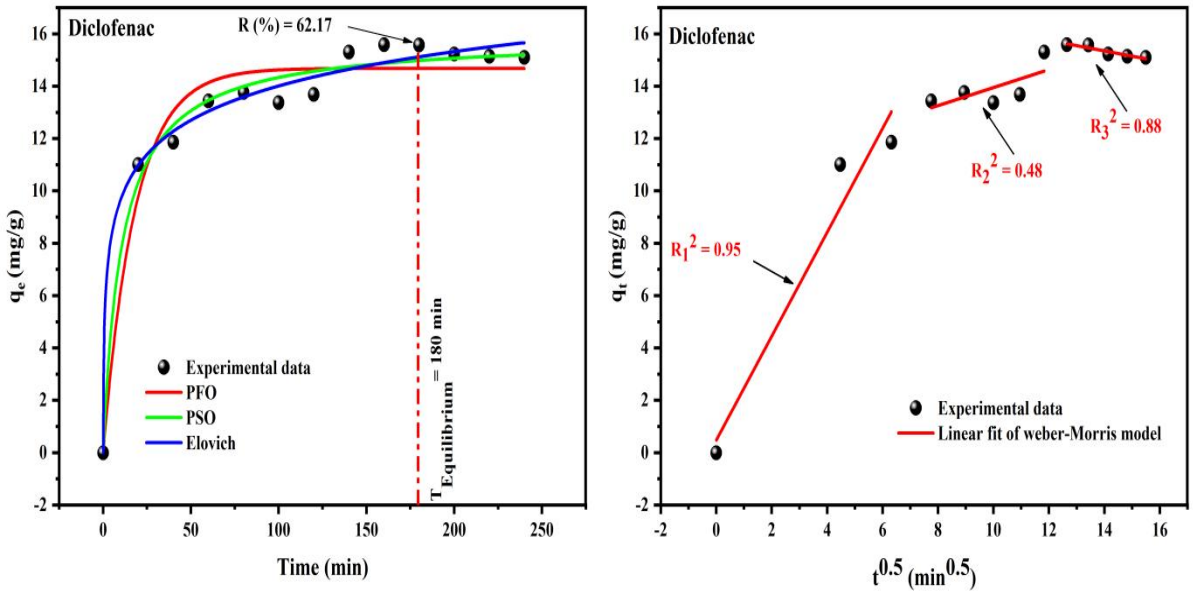

Figure II.2.4. Kinetics of diclofenac adsorption (Nonlinear fitting and Linear fitting of Weber-Morris model).

Table II.2.1. Kinetic model parameters for the adsorption of paracetamol and diclofenac on CCB-650.

Model	Parameter	Unit	Paracetamol	Diclofenac
Pseudo-first-order	q_e	mg/g	23.97	14.684
	k_1	1/min	0.091	0.054
	R^2	-	0.98	0.955
	χ^2	-	0.26	0.835
Pseudo-second-order	q_e	mg/g	24.85	15.86
	k_2	g/mg min	0.009	0.005
	R^2	-	0.999	0.981
	χ^2	-	0.054	0.352
Elovich	α	mg/g min	1.4×10^5	7.484
	β	g/mg	0.68	0.413
	R^2	-	0.992	0.830
	χ^2	-	0.406	1.194
Intraparticle diffusion				
First step	k_{IP1}	mg/g.min$^{0.5}$	3.359	1.985
	C_1	mg/g	2.979	0.483
	R_1^2	-	0.88	0.950
Second step	k_{IP2}	mg/g.min$^{0.5}$	0.309	0.344
	C_2	mg/g	20.665	10.510
	R_2^2	-	0.96	0.483
Third step	k_{IP3}	mg/g.min$^{0.5}$	0.094	0.026
	C_3	mg/g	22.98	18.157
	R_3^2	-	0.45	0.883

Considering the values of the correlation coefficient (R^2) and the chi-square statistic (χ^2), the pseudo-second-order (PSO) model proved to be the most suitable for describing the adsorption kinetics. Specifically, the model yielded R^2 values of 0.999 and 0.981, χ^2 values of 0.054 and 0.352 for paracetamol and diclofenac, respectively.

The transfer of paracetamol and diclofenac molecules to the surface and into the pores of CCB-650 was analysed using the intra-particle diffusion model. The results indicate that the adsorption of both can be divided into three distinct stages.

The adsorption process begins with liquid-film diffusion, characterized by a relatively high intra-particle diffusion rate constant, during which pharmaceutical molecules are swiftly transported from the aqueous phase to the external surface of CCB-650 through the boundary layer. This is followed by a second phase, in which intra-particle diffusion becomes the rate-limiting step, as paracetamol and diclofenac molecules gradually migrate into the biochar's internal structure and interact with available active sites. The final phase signifies the attainment of adsorption equilibrium.

II.2.3.2. Effect of adsorbent dosage

To achieve efficient contaminant removal while maintaining economic feasibility, it is essential to optimize the amount of adsorbent applied. The influence of varying CCB-650 dosages on the adsorption behaviour of paracetamol and diclofenac was systematically evaluated, as illustrated in Figure II.2.5. The experimental findings reveal a positive correlation between the amount of adsorbent used and the removal efficiency of both contaminants, which the increase in the amount of the available binding active site can explain. Conversely, a higher adsorbent dosage reduces the adsorption capacities of PCM and DCF. This might be due to the rise in the number of free binding sites on the adsorbent surface (El Naga, El Saied et al. 2019).

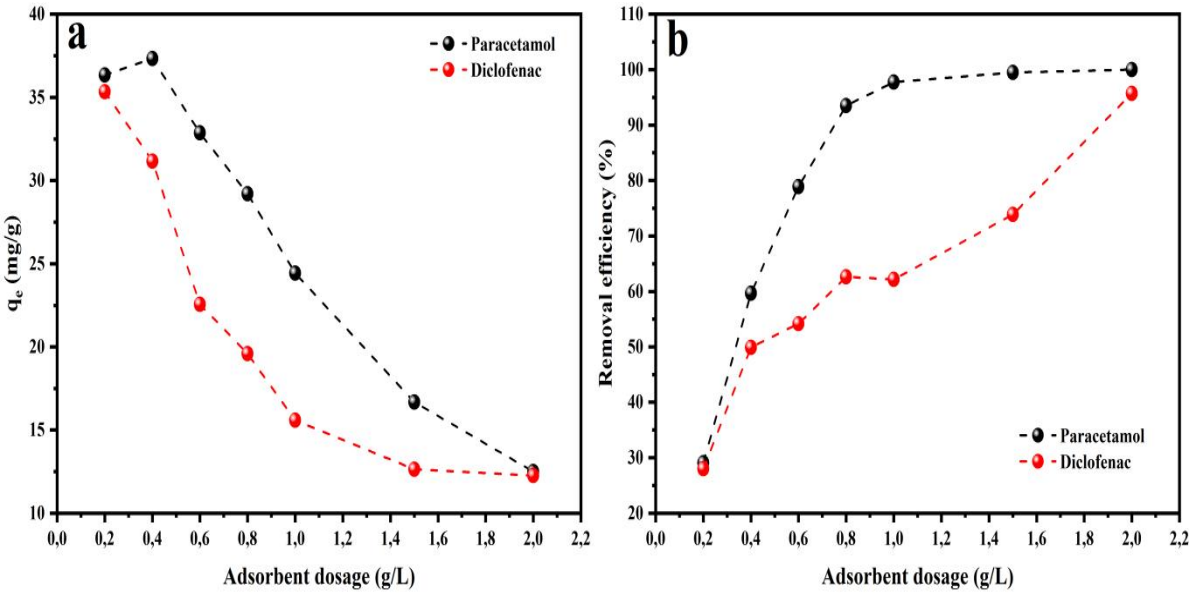

Figure II.2.5. Effect of CCB-650 dose on a) the adsorption capacity and b) the removal efficiency of paracetamol and diclofenac.

II.2.3.3. Effect of pH medium

The pH of a solution is a key factor in the adsorption process, as it influences the adsorbent surface charge and the ionic state of the adsorbate species (S, Guy et al. 2022). Figure II.2.6 (a) demonstrates the effect of solution pH on the adsorption capacity of paracetamol and diclofenac.

The adsorption capacity of CCB-650 for PCM ranges from 24.2 to 24.71 mg/g as the solution pH increases from 2 to 8, indicating no significant variation across this pH range. However, from pH 9 to 12, the adsorption capacity decreases. The observed pattern is attributed to the interactions between the functional groups on the adsorbent surface and paracetamol molecules. According to the CCB-650 characterization result (Figure II.1.16), the pHpzc of the adsorbent is 6.9. This indicates that the CCB-650 has a negative charge at pH values above 6.9 and a positive charge at pH values below 6.9. On the other hand, paracetamol is a weak acid (pKa = 9.38) that can exist in both ionized and non-ionized forms depending on the pH of the medium. This compound remains in solution at pH below 9.38 as a neutral (non-ionized) species. Moreover, it becomes ionized and dissociates when pH exceeds pKa (Mokhtaryan, Khodabakhshi et al. 2023). A slight variation in adsorption capacity was observed between pH 2 and 8. PCM molecules remain neutral over this pH range, facilitating hydrophobic interactions. Moreover, although PCM is in a non-ionic state, the oxygen in its amide group may carry a partial negative charge, potentially enhancing its adsorption onto the positively charged CCB-650 surface when the ($pH < pH_{PZC}$) (Sumalinog, Capareda et al. 2018). At an alkaline pH, the drug is converted to its anion form. Simultaneously, the adsorbent acquires a negative charge under the pH conditions ($pH > pH_{PZC}$), leading to electrostatic repulsion that decreases adsorption uptake (Wong, Lim et al. 2018). Furthermore, the observed reduction in adsorption capacity could be attributed to the competition between hydroxide ions (OH^-) and PCM anions for the active binding sites on CCB-650 (Islam, Nazal et al. 2024). The results showed that the adsorption capacity of diclofenac was relatively high at pH 2 and 3. It was then dramatically decreased at pH = 4. The ionization behaviour of diclofenac (DCF), a weak acid with a pKa of 4.15, determines its surface charge at different pH values. Above this pKa value, DCF predominantly exists in its deprotonated, anionic form, acquiring a negative charge. Conversely, under acidic conditions ($pH < 4.15$), DCF remains largely in its neutral molecular form, while the CCB-650 surface tends to exhibit a positive charge. Interestingly, the observed enhancement in DCF uptake within the pH range of 2 to 4 cannot be entirely attributed to electrostatic interactions,

suggesting the involvement of additional adsorption mechanisms. As the pH exceeds 4, the removal efficiency of DCF progressively declines, likely due to increased electrostatic repulsion between the negatively charged adsorbent and the anionic form of DCF. At highly alkaline conditions (pH ≥ 10), the adsorbent CCB-650 demonstrates minimal adsorption performance, attributed to the strong mutual repulsion between the negatively charged surface and DCF anions (Thi Minh Tam, Liu et al. 2020).

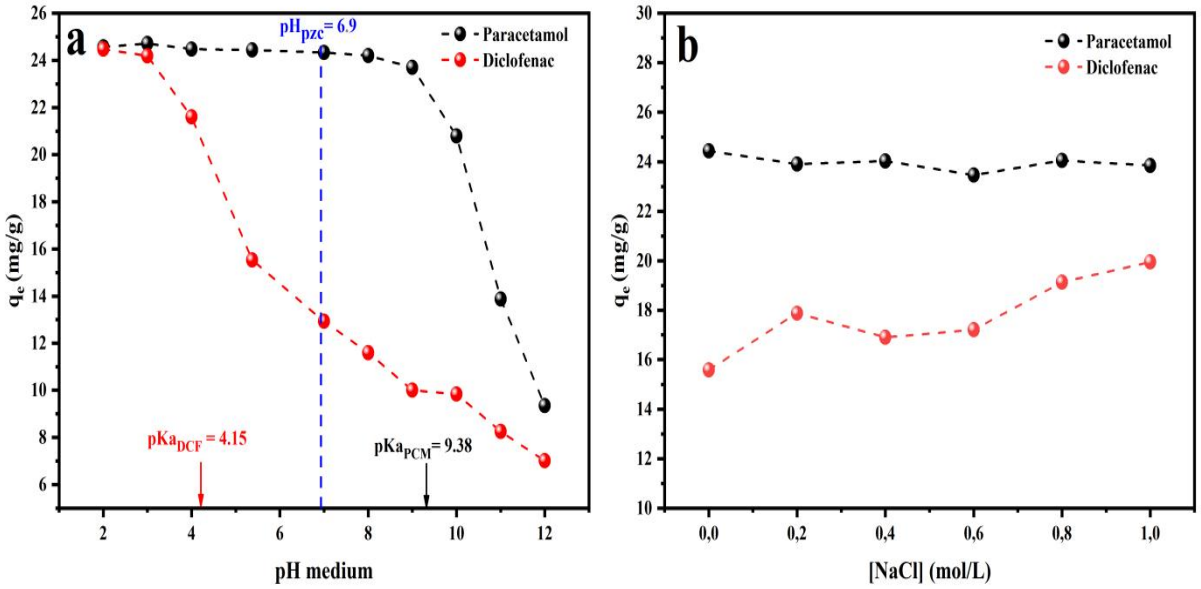

Figure II.2.6. a) Effect of pH medium, b) Effect of ionic stength on the removal of paracetamol and diclofenac onto CCB-650.

II.2.3.4. Effect of ionic strength

Ionic strength is a factor that frequently has a significant impact on the adsorption process of an adsorbent due to the presence of many substances, including organic pollutants dissolved in cationic, anionic, or neutral forms of ions, atoms or molecules in the water (Quesada, Cusioli et al. 2019). NaCl was chosen to explore the impact of ionic strength (Figure II.2.6 (b)) on the removal of PCM and DCF by CCB-650, due to its widespread presence in wastewater and other water sources. Findings indicated that there was no discernible change in PCM adsorption capacity with increasing Na^+ concentration from 0.2 to 1 M. Other researchers who examined PCM adsorption (Quesada, Cusioli et al. 2019; Tran, Tomul et al. 2020) reached the same conclusion and confirmed the negligible effect of ionic force. This occurred because Na^+ and PCM interact with different adsorption sites, eliminating the possibility of competitive adsorption (Qihang Wang 2023). The presence of NaCl notably enhanced DCF's adsorption capacity. This improvement may be attributed to the elevated ionic strength, which likely reduced the solubility of hydrophobic organic

compounds by increasing their activity coefficients, thereby promoting more favourable adsorption conditions(Tam, Liu et al. 2020).

II.2.3.5. Investigation of the adsorption isotherm

Assessing the influence of initial pollutant concentration on the adsorption of pharmaceutical compounds onto CCB-650 biochar is essential for determining the maximum adsorption capacity and for gaining insight into the underlying removal mechanisms. In this study, the initial concentrations of paracetamol and diclofenac were varied within the ranges of 15–300 mg/L and 15–40 mg/L, respectively, under constant agitation for 180 minutes. The resulting adsorption data were analyzed using three isotherm models: the Langmuir model, which assumes homogeneous monolayer adsorption with no interaction between adsorbed molecules(Kecili and Hussain 2018); the Freundlich model, which describes heterogeneous multilayer adsorption with adsorbate–adsorbate interactions (Mokhtaryan, Khodabakhshi et al. 2023) ; and the Temkin model, which considers multilayer chemisorption processes (Chen, Hossain et al. 2022). The parameters were calculated using a non-linear regression. Figure II.2.7 illustrates the adsorption isotherms of PCM and DCF on CCB-650, while Table II.2.2 reports the fitting parameters and correlation coefficients for each model, highlighting their respective predictive accuracy.

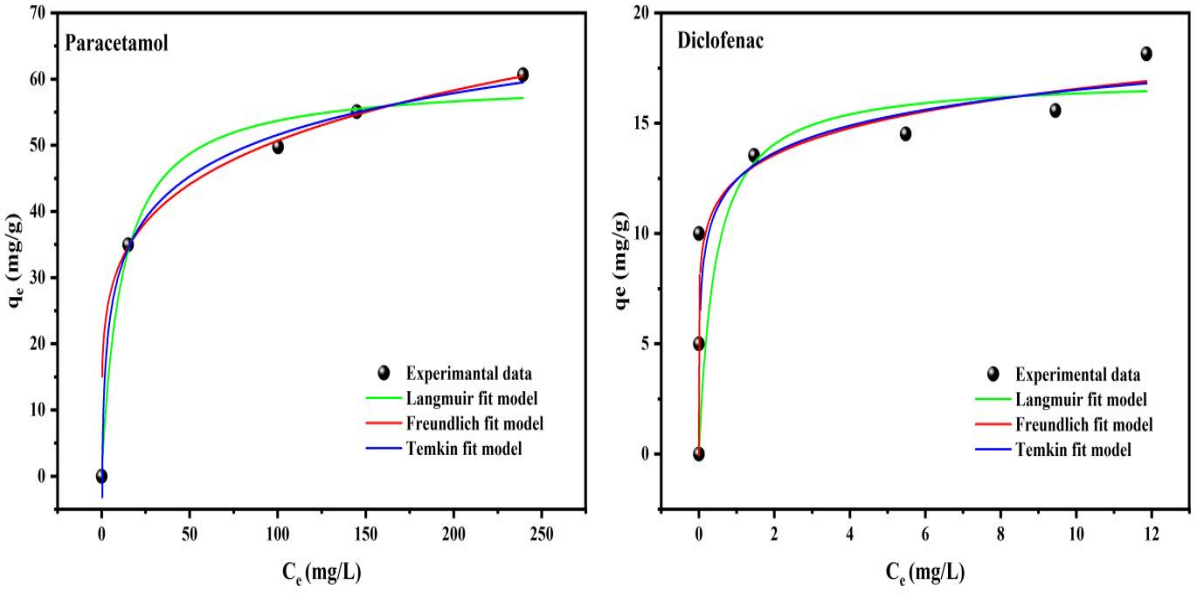

Figure II.2.7. Paracetamol and diclofenac adsorption isotherms onto CCB-650.

The adsorption data for paracetamol showed good correlation with all three isotherm models, with each model yielding a coefficient of determination (R^2) greater than 0.9. Among them, the Freundlich isotherm provided the best fit (R^2 = 0.996), followed by Temkin (R^2 =

0.990) and Langmuir (R^2 = 0.987) models. For diclofenac, the adsorption behaviour was best represented by the Freundlich isotherm, although the correlation was relatively weak (R^2 = 0.726). The Temkin (R^2 = 0.483) and Langmuir (R^2 = 0.476) models display lower correlations. Therefore, the results suggest that paracetamol and diclofenac predominantly adsorb heterogeneously onto CCB-650 and follow a multilayer adsorption mechanism.

Table II.2.2. Parameters of isotherm for paracetamol and diclofenac adsorption onto CCB-650.

Model	*Parameter*	*Unit*	*Paracetamol*	*Diclofenac*
Langmuir	Q^0_{max} K_L R^2 χ^2	mg/g L/mg - -	59.865 0.087 0.987 9.786	17.041 2.351 0.476 2.603
Freundlich	n K_F R^2 χ^2	mg/g (mg/g) / $(mg/L)^{1/n}$ - -	4.975 20.078 0.996 0.653	0.123 12.457 0.726 1.608
Temkin	B K_T R^2 χ^2	- L/mg - -	9.073 2.946 0.99 1.703	1.768 1132 0.483 25.69

II.2.3.6.Thermodynamic study

To optimise adsorption processes for real-world applications, it is essential to assess how temperature variations influence performance. In this study, the impact of temperature on the distribution coefficient (Kc) for paracetamol and diclofenac was examined at a fixed dye concentration of 25 mg/L for both drugs.

The thermodynamic properties of paracetamol and diclofenac adsorption onto CCB-650 were determined using the Van't Hoff equation shown in Eq.I.2.17, and plotting ln K_C vs 1/T as shown in Figure II.2.8, where K_C is the thermodynamic equilibrium constant, which was calculated according to **Eq.I.2.14**. ΔG (KJ/ mol) is the Gibbs free energy, ΔH (KJ/ mol) is the enthalpy; ΔS (J /mol. K) is the entropy; R is the gas constant (8.314 J /mol .K); and T (K) is the absolute temperature. The parameters ΔH° and ΔS° were calculated from the slope

and intercept of the linear plot, while Δ G° was calculated using the Gibbs free energy equation **Eq.I.2.17**.

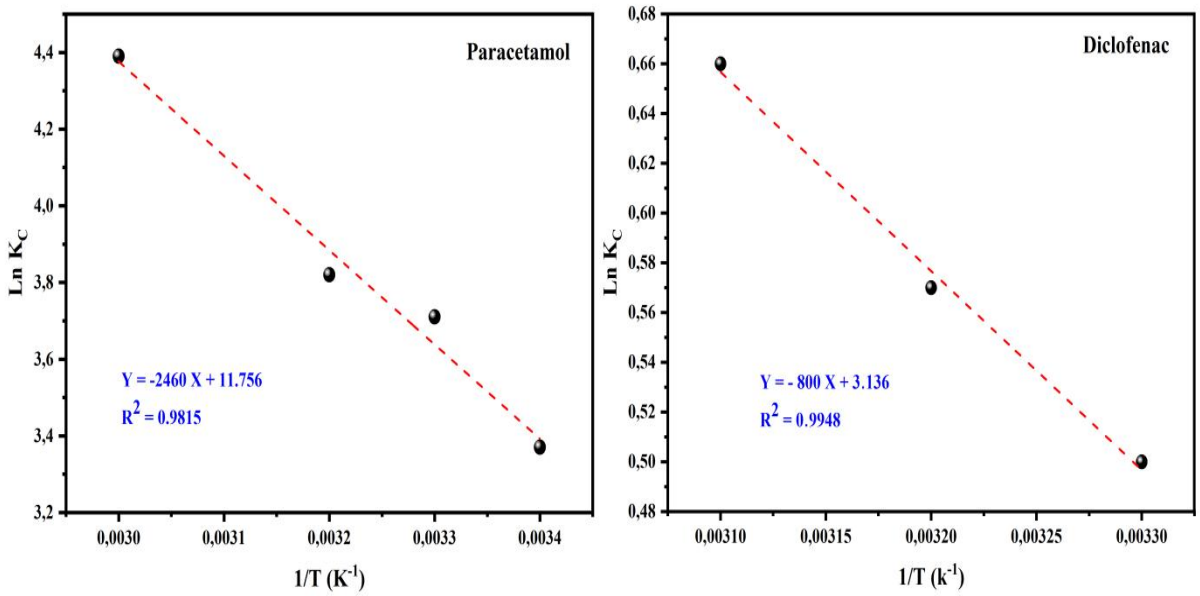

Figure II.2.8. Van't Hoff plot for paracetamol and diclofenac removal on CCB-650.

According to Table II.2.3, the increase in the K_C constant with temperature suggests an endothermic process. This interpretation is supported by the positive enthalpy change (ΔH° > 0 kJ/mol). Additionally, the negative Gibbs free energy values (ΔG°) across the studied temperatures indicate that adsorption occurs spontaneously, despite the positive ΔS°, which indicates increased randomness at the solid-solution interface during adsorption. The value of ΔH° also helps distinguish between physisorption and chemisorption (values below 40 kJ/mol are typical for physical interactions, while higher values suggest chemical bonding (Ninh, Dat et al. 2023; Mabrouk, Fizer et al. 2024). In the current work, the relatively low enthalpy values recorded for both PCM (20.452 kJ/mol) and DCF (6.651 kJ/mol) adsorption are consistent with a predominantly physical adsorption mechanism.

Table II.2.3. Thermodynamic parameters of paracetamol and diclofenac adsorption on CCB-650.

Pollutants	T (°K)	K_C	Van't Hoff equation	Thermodynamic parameters		
				$\Delta G°$ (KJ/mol)	$\Delta H°$ (KJ/mol)	$\Delta S°$ (J / (mol. k))
Paracetamol	**291**	80.96	Y = - 2460 X +11.75 R^2 = 0.9815	-7.990	20.452	97.739
	303	45.81		-9.162		
	313	40.66		-10.140		
	323	29.15		-11.117		
Diclofenac	**298**	1.927	Y = - 800 X +3.136 R^2 = 0.9948	-1.639	6.651	26.07
	308	1.772		-1.378		
	318	1.646		-1.117		

II.2.4. Conclusion

The effectiveness of the adsorption procedure for the medications paracetamol and diclofenac onto CCB-650 in a single-system configuration under various operating conditions has been the focus of this chapter. The best fits to the experimental kinetic and equilibrium data were the pseudo-second-order (PSO) and the Freundlich models, respectively, as determined by adsorption experiments. The adsorption of paracetamol and diclofenac on CCB-650 was shown to be favourable, endothermic, and consistent with physisorption from a thermodynamic perspective.

References

Chen, X., M. F. Hossain, et al. (2022). "Isotherm models for adsorption of heavy metals from water-A review." Chemosphere **307**: 135545 DOI: https://doi.org/10.1016/j.chemosphere.2022.135545.

El Naga, A. O. A., M. El Saied, et al. (2019). "Fast removal of diclofenac sodium from aqueous solution using sugar cane bagasse-derived activated carbon." Journal of Molecular Liquids **285**: 9-19 DOI: https://doi.org/10.1016/j.molliq.2019.04.062.

Islam, M. A., M. K. Nazal, et al. (2024). "High performance adsorptive removal of emerging contaminant paracetamol using a sustainable biobased mesoporous activated carbon prepared from palm leaves waste." Journal of Analytical and Applied Pyrolysis **180**: 106546 DOI: https://doi.org/10.1016/j.jaap.2024.106546.

Kecili, R. and C. M. Hussain (2018). Mechanism of adsorption on nanomaterials. Nanomaterials in chromatography, Elsevier**:** 89-115.

Mabrouk, S., M. Fizer, et al. (2024). "Grape seeds waste activated carbon as an adsorber of paracetamol drug residue: Experimental and theoretical approaches." Journal of Molecular Liquids: 125325 DOI: https://doi.org/10.1016/j.molliq.2024.125325.

Mokhtaryan, S., A. Khodabakhshi, et al. (2023). "New activated carbon derived from Gundelia tournefortii seeds for effective removal of acetaminophen from aqueous solutions: Adsorption performance." Arabian Journal of Chemistry **16**(11): 105253 DOI: https://doi.org/10.1016/j.arabjc.2023.105253.

Ninh, P. T. T., N. D. Dat, et al. (2023). "Two-stage preparation of highly mesoporous carbon for super-adsorption of paracetamol and tetracycline in water: Important contribution of pore filling and π-π interaction." Environmental Research **218**: 114927 DOI: https://doi.org/10.1016/j.envres.2022.114927.

Qihang Wang, D. H., Chengyu Li, Zijia Sun, Jun Mu (2023). "Honeycomb-like cork activated carbon modified with carbon dots for high-efficient adsorption of Pb(Ⅱ) and rhodamine B." Industrial Crops and Products **196** DOI: https://doi.org/10.1016/j.indcrop.2023.116485.

Quesada, H. B., L. F. Cusioli, et al. (2019). "Acetaminophen adsorption using a low‐cost adsorbent prepared from modified residues of Moringa oleifera Lam. seed

husks." Journal of Chemical Technology & Biotechnology **94**(10): 3147-3157 DOI: https://doi.org/10.1002/jctb.6121.

S, d. R. G., M. Guy, et al. (2022). "A comparative study of chemical treatment by MgCl2, ZnSO4, ZnCl2, and KOH on physicochemical properties and acetaminophen adsorption performance of biobased porous materials from tree bark residues." Colloids and Surfaces A: Physicochemical and Engineering Aspects **642**: 128626 DOI: https://doi.org/10.1016/j.colsurfa.2022.128626.

Sumalinog, D. A. G., S. C. Capareda, et al. (2018). "Evaluation of the effectiveness and mechanisms of acetaminophen and methylene blue dye adsorption on activated biochar derived from municipal solid wastes." Journal of environmental management **210**: 255-262 DOI: https://doi.org/10.1016/j.jenvman.2018.01.010.

Tam, N. T. M., Y.-g. Liu, et al. (2020). "Synthesis of porous biochar containing graphitic carbon derived from lignin content of forestry biomass and its application for the removal of diclofenac sodium from aqueous solution." Frontiers in Chemistry **8**: 274 DOI: https://doi.org/10.3389/fchem.2020.00274.

Thi Minh Tam, N., Y. Liu, et al. (2020). "Efficient removal of diclofenac from aqueous solution by potassium ferrate-activated porous graphitic biochar: ambient condition influences and adsorption mechanism." International Journal of Environmental Research and Public Health **17**(1): 291 DOI: https://doi.org/10.3390/ijerph17010291.

Tran, H. N., F. Tomul, et al. (2020). "Innovative spherical biochar for pharmaceutical removal from water: Insight into adsorption mechanism." Journal of hazardous materials **394**: 122255 DOI: https://doi.org/10.1016/j.jhazmat.2020.122255.

Wong, S., Y. Lim, et al. (2018). "Removal of acetaminophen by activated carbon synthesized from spent tea leaves: equilibrium, kinetics and thermodynamics studies." Powder Technology **338**: 878-886 DOI: https://doi.org/10.1016/j.powtec.2018.07.075.

Chapter 3:

Adsorption of Paracetamol and Diclofenac onto CC-$ZnCl_2$-AC

II.3. Adsorption of Paracetamol and Diclofenac onto CC-$ZnCl_2$-AC

II.3.1. Introduction

The synthesised activated carbon is an adsorbent derived from cypress cones, activated with zinc chloride and subsequently pyrolysed at 650 °C. The main objective of preparing this activated carbon is to enhance its textural properties and thereby improve its adsorption capacity for the two pharmaceutical pollutants. To achieve this, experimental tests were conducted using synthetic solutions of distilled water enriched with paracetamol and diclofenac to evaluate the retention of these contaminants by the prepared activated carbon. Various operational parameters were investigated, including contact time, pH, ionic strength, adsorbent dosage, and pharmaceutical concentration. Kinetic and isotherm adsorption models were employed to gain deeper insight into the adsorption behaviour and to estimate the adsorbent's maximum capacity for each pollutant.

II.3.2. Investigation of Operational Conditions Influencing PCM and DCF Adsorption

Adsorption experiments were carried out using a CC-$ZnCl_2$-AC adsorbent dosage of 1 g/L in 30 mL of pharmaceutical solutions (C_0 100 mg/L, pH 5.4, temperature 25 ± 5 °C) under continuous magnetic stirring. After adsorption, the adsorbent–adsorbate mixture was separated using a 0.2 µm syringe filter. The remaining concentrations of PCM and DCF in solution were then quantified using a UV-Vis spectrophotometer (PhotoLab DR-6000) at 241 nm and 276 nm, respectively.

II.3.2.1. Investigation of Adsorption Kinetics

To evaluate the adsorption performance, 30 mL of paracetamol or diclofenac solution was treated with 1 g/L of CC-$ZnCl_2$-AC under continuous magnetic stirring. The contact time ranged from 0 to 240 min. As illustrated in Figures II.3.1 and II.3.2, the adsorption process showed a progressive increase in both removal efficiency and adsorption capacity with increasing contact time. Equilibrium was established at 180 minutes for paracetamol and at 240 minutes for diclofenac. The maximum removal rates achieved were 95.5% for paracetamol and 90.9% for diclofenac, respectively. The adsorption capacity increased rapidly at first, then levelled off. This behaviour is attributed to the availability of adsorption sites (Mabrouk, Fizer et al. 2024) and the influence of mass transfer forces. During the initial phase, many active sites on the adsorbent surface remained unoccupied, while the concentration gradient of PCM and DCF between the solution and the adsorbent was high. As adsorption progressed, spatial resistance around the active sites became more pronounced, reducing the

concentration gradient. Consequently, the adsorption capacity of adsorbates progressively reached saturation (Xie, Liu et al. 2023).

The kinetic data were adjusted to pseudo-first-order, pseudo-second-order, Elovich, and intra-particle diffusion models. The calculated parameters are summarized in Table II.3.1 .The experimental dataset of adsorption kinetics was well described by the three selected models (with $R^2 \geq 0.99$).

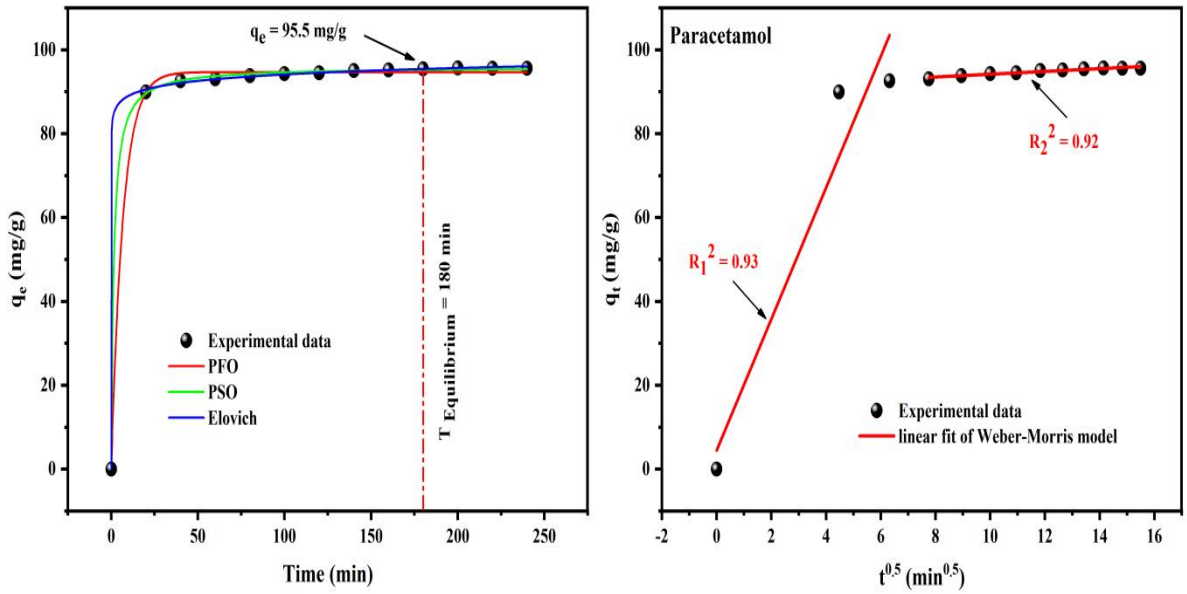

Figure II.3.1. Kinetics of paracetamol adsorption (Nonlinear fitting and Linear fitting of Weber-Morris model).

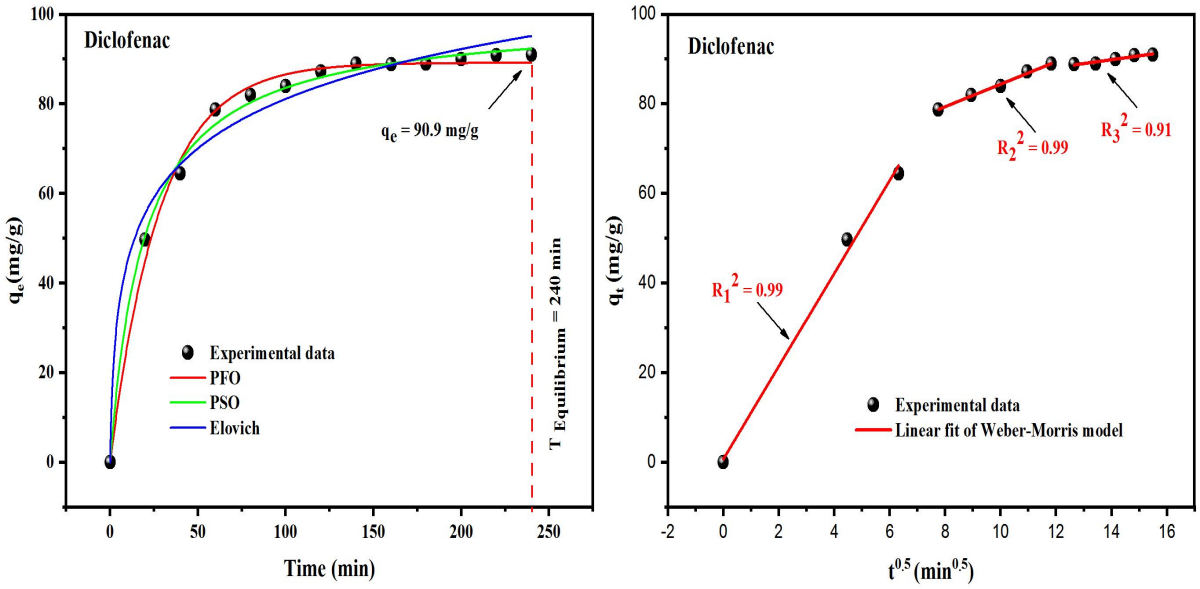

Figure II.3.2. Kinetics of diclofenac adsorption (Nonlinear fitting and Linear fitting of Weber-Morris model).

The Intraparticle diffusion model was applied to investigate the mass-transfer mechanism governing the diffusion of PCM and DFC molecules into CC-$ZnCl_2$-AC. The relationship between the amount adsorbed at time t and $t^{0.5}$ was analyzed through curve fitting, as illustrated in Fig. 3(c,d). The results reveal that paracetamol adsorption proceeds through two successive phases, whereas diclofenac uptake occurs via three sequential steps, confirming that the overall adsorption behavior follows a complex, multistage mechanism. Based on the intraparticle diffusion rate constants summarized in Table 3, the values for paracetamol decrease markedly from the first to the second stage $K_{int,\ 1}$ (15.663) > $K_{int,\ 2}$ (0.330) (mg/g.$min^{1/2}$).. The elevated rate constant observed in the initial stage indicates a fast transport of paracetamol molecules from the bulk solution to the outer surface of the activated carbon. Subsequently, the adsorption rate becomes controlled by diffusion into the mesoporous structure of CC-$ZnCl_2$-AC, accompanied by adsorption at internal active sites. This stage represents the gradual approach to equilibrium, as intraparticle diffusion slows considerably.

In contrast, the diffusion kinetics of diclofenac sodium are characterized by three decreasing rate constants arranged in the order $k_{IP1} > k_{IP2} > k_{IP3}$, suggesting a rapid initial uptake followed by progressively slower adsorption stages. The first phase is dominated by liquid film diffusion, with a relatively high diffusion constant (k_{IP1} = 3.359 mg/g.$min^{0.5}$), during which diclofenac molecules are swiftly transported across the boundary layer to the external surface of CC-$ZnCl_2$-AC (Saied, Shaban et al. 2024). In the second phase, intraparticle diffusion governs the adsorption rate as diclofenac molecules penetrate deeper into the porous network and interact with internal binding sites. The final stage corresponds to the establishment of adsorption equilibrium. Notably, the magnitude of the boundary layer thickness constant (C) indicates a significant boundary layer influence, where an increase in layer thickness can restrict solute transfer from the solution while simultaneously favoring diffusion within the adsorbent structure (Ahmad, Soomro et al. 2021).

Table II.3.1. Kinetic model parameters for the adsorption of paracetamol and diclofenac on CC-$ZnCl_2$-AC.

Model	Parameter	Unit	Paracetamol	Diclofenac
Pseudo-first-order	q_e	mg/g	94.67	89.16
	k_1	1/min	0.147	0.035
	R^2	-	0.998	0.993
	χ^2	-	0.965	4.352
Pseudo-second-order	q_e	mg/g	95.94	99.72
	k_2	g/mg min	0.007	5.19^{-4}
	R^2	-	0.999	0.996
	χ^2	-	0.122	0.035
Elovich	α	mg/g min	6.9×10^{16}	24.80
	β	g/mg	0.452	0.062
	R^2	-	0.999	0.981
	χ^2	-	0.094	13.55
Intraparticle diffusion				
First step	k_{IP1}	$mg/g.min^{0.5}$	15.663	10.372
	C_1	mg/g	4.513	0.752
	R_1^2	-	0.932	0.995
Second step	k_{IP2}	$mg/g.min^{0.5}$	0.330	2.509
	C_2	mg/g	90.867	59.311
	R_2^2	-	0.929	0.994
Third step	k_{IP3}	$mg/g.min^{0.5}$		0.858
	C_3	mg/g		77.822
	R_3^2	-		0.913

II.3.2.2. Effect of adsorbent dosage

To achieve efficient contaminant removal while maintaining economic viability, it is essential to determine the optimal adsorbent dosage. The influence of varying CC-$ZnCl_2$-AC quantities on paracetamol and diclofenac adsorption was evaluated, as depicted in Figure II.3.3. The findings indicate that elevating the adsorbent mass from 0.2 g/L to 2 g/L enhanced the paracetamol removal rate from 27.26% to 99.07% and diclofenac from 23.74% to 100%. However, this increase in dosage led to a reduction in the specific adsorption capacity (qe, mg g^{-1}). It was found that as the adsorbent dosage increased, the adsorption capacity per unit mass declined, whereas the overall adsorption efficiency improved for both pharmaceuticals. The enhanced removal efficiency can be attributed to the increased available surface area, which provides more active sites for contaminant attachment (Shirani, Song et al. 2020). Conversely, the reduction in adsorption capacity arises because the adsorption sites are not

fully saturated at higher dosages, resulting in a lower amount adsorbed per gram of adsorbent (Seymen, Eroğlu et al. 2025). This demonstrates that a higher adsorbent dose increases the number of active sites, thus promoting greater overall contaminant removal.

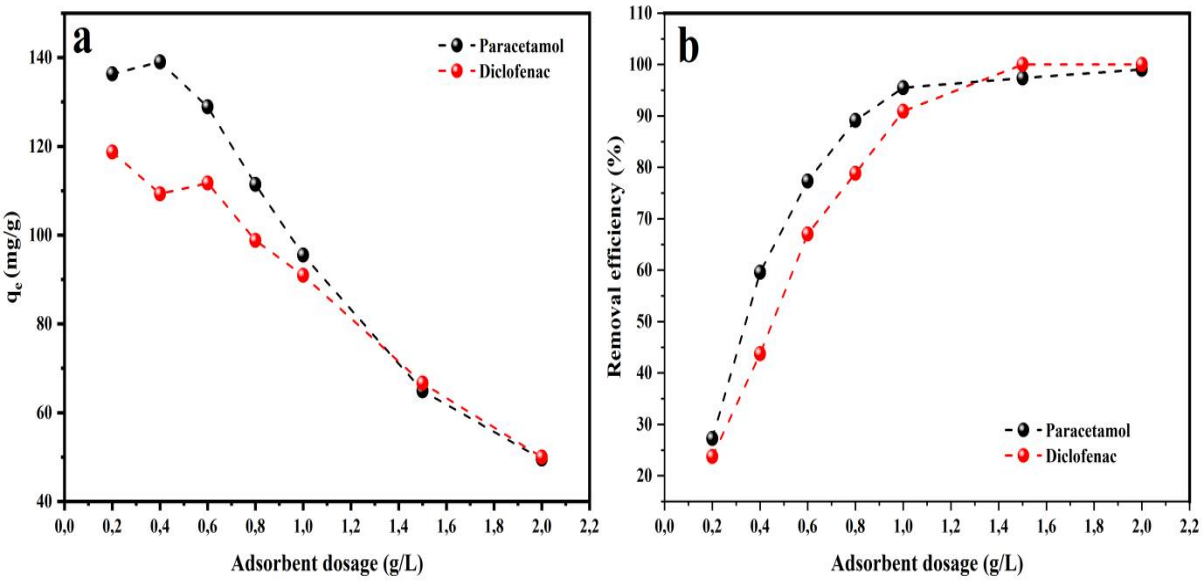

Figure II.3.3. Effect of CC-$ZnCl_2$-AC dose on a) the adsorption capacity and b) the removal efficiency of paracetamol and diclofenac.

II.3.2.3. Effect of pH medium

The effects of a change in the pH value of the solution on the adsorption performance of paracetamol and Diclofenac were investigated in Figure II.3.4 (a). The adsorption diagram of paracetamol indicates that the adsorption performance remains relatively stable between pH 2 and pH 9. A noticeable decline in adsorption capacity is observed only above pH 10. The point of zero charge (pHpzc) of the adsorbent was determined to be 6.18. Paracetamol (PCM), a weakly acidic compound with a pKa of 9.38, can exist in both neutral and anionic forms depending on the pH of the surrounding medium. Below its pKa, PCM primarily remains in its neutral molecular state, whereas it shifts to its deprotonated anionic form (PCM-) at pH levels above 9.38 (Melliti, Touihri et al. 2024). However, across the pH range of 2 to 10, minimal variation in adsorption capacity suggests that adsorption is more governed by textural characteristics, such as pore size, than by surface charge interactions. This stability in adsorption is likely due to PCM maintaining its neutral form within this pH range, enabling hydrophobic forces to play a more prominent role (Sumalinog, Capareda et al. 2018). Conversely, at alkaline pH values exceeding 10, PCM converts to its anionic form, and the adsorbent surface also carries a negative charge, resulting in electrostatic repulsion that inhibits adsorption efficiency (Sajid, Bari et al. 2022) .

In contrast, Diclofenac shows that maximum uptake occurred under acidic conditions, specifically between pH 2 and pH 4. In this pH range, Diclofenac (DCF) mainly exists in its neutral molecular form, as the pH is below its pKa, while the surface of CC-$ZnCl_2$-AC is positively charged because the pH is below its point of zero charge (pH_{PZC}). This trend confirms that the increased adsorption capacity at lower pH is primarily linked to the reduced solubility of DCF. Within the pH range of 4.2 to 6.18, DCF gradually acquires a stronger negative charge. However, the simultaneous increase in its solubility offsets the electrostatic attraction, thereby decreasing adsorption capacity (Cuccarese, Brutti et al. 2021). In alkaline media, hydroxide ions compete with DCF ions for available adsorption sites, leading to weaker interactions and decreased adsorption efficiency (Jagadeesan, Solayman et al. 2025). Moreover, given that DCF predominantly exists in its anionic form at pH values above its pKa (Al-Hazmi, Alayyafi et al. 2024).Consequently, the reduction in adsorption can also be attributed to electrostatic repulsion between the negatively charged adsorbent surface and the anionic DCF species. (Kocabıyık, Üner et al. 2024) obtained similar findings, noting that at acidic pH levels (below 4.20), the interaction between the positively charged adsorbent and the neutral form of DCF is much stronger than the repulsive forces observed between the negatively charged adsorbent surface and anionic DCF species at higher pH values.

These results underscore the crucial role of solution pH in maximizing the adsorption efficiency of CC-$ZnCl_2$-AC for DCF and PCM removal, with a marked decrease in performance under highly alkaline conditions.

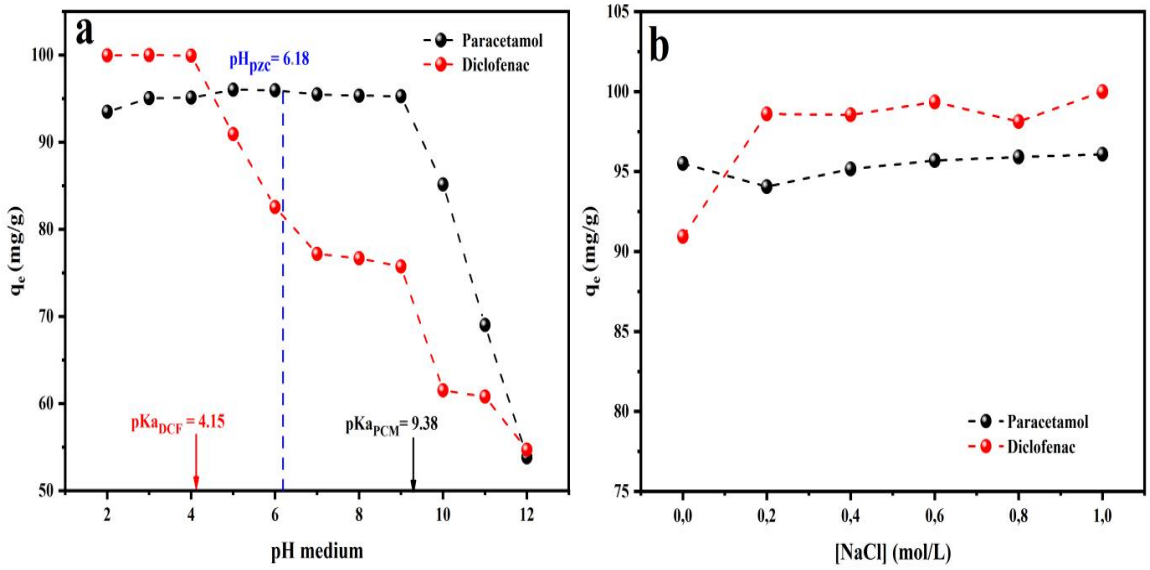

Figure II.3.4. a) Effect of pH medium, b) Effect of ionic stength on the removal of paracetamol and diclofenac on CC-$ZnCl_2$-AC.

II.3.2.4. Effect of ionic strength

In real water or wastewater systems, pharmaceutical substances coexist with different concentrations of dissolved salts. These salts modify the electrostatic and hydrophobic interactions between the pharmaceuticals and the adsorbent's active sites, thereby enhancing or diminishing adsorption efficiency (El-Kelany, Radwan et al. 2024).

In this part, we studied the effect of ionic strength on the adsorption capacity of paracetamol and diclofenac onto the surface of the modified CC Various concentrations of NaCl solution (ranging from 0.1 M to 1 M) were prepared, using a concentration of 100 mg/L of pharmaceuticals and a modified CC dosage of 1 g/L.The adsorption capacity of CC-$ZnCl_2$-AC for paracetamol did not change significantly, as illustrated in Figure II.3.4 (b), indicating that Na^+ ions had a minimal effect on PCM adsorption. This slight variation can be attributed to the fact that sodium ions (Na^+) and PCM interact with different adsorption sites on the adsorbent surface, thereby ruling out any competitive adsorption between them (khadidja 2025), According to (El-Kelany, Radwan et al. 2024), if changes in ionic strength do not influence the adsorption behavior, the process is probably dominated by hydrogen bonding, n–π, and π–π interactions. In the case of diclofenac adsorption, the addition of NaCl significantly boosted DCF uptake. This enhancement is attributed to the 'salting-out' effect, which reduced DCF's solubility in the aqueous phase. As a result, a greater amount of DCF was adsorbed via organic carbon partitioning. Moreover, the salting-out effect also suppressed the leaching of organic carbon from the adsorbent into the solution, thereby maintaining a higher concentration of organic carbon within the adsorbent matrix. This retained organic content further contributed to the improved adsorption performance (Yan, Zhang et al. 2019).

II.3.2.5. Investigation of the adsorption isotherm

To effectively develop an adsorption system capable of eliminating PCM and DCF contaminants and to gain insights into their interaction with CC-$ZnCl_2$-AC, it is essential to establish a link between the equilibrium data derived from experiments. For this purpose, various isotherm models, namely Langmuir, Freundlich, and Temkin, were employed to analyse the experimental adsorption behaviour (as illustrated in Figure II.3.5). The adsorption parameters for each model were determined through a nonlinear optimization method. The resulting values from fitting the experimental data to these models are summarized in Table II.3.2.

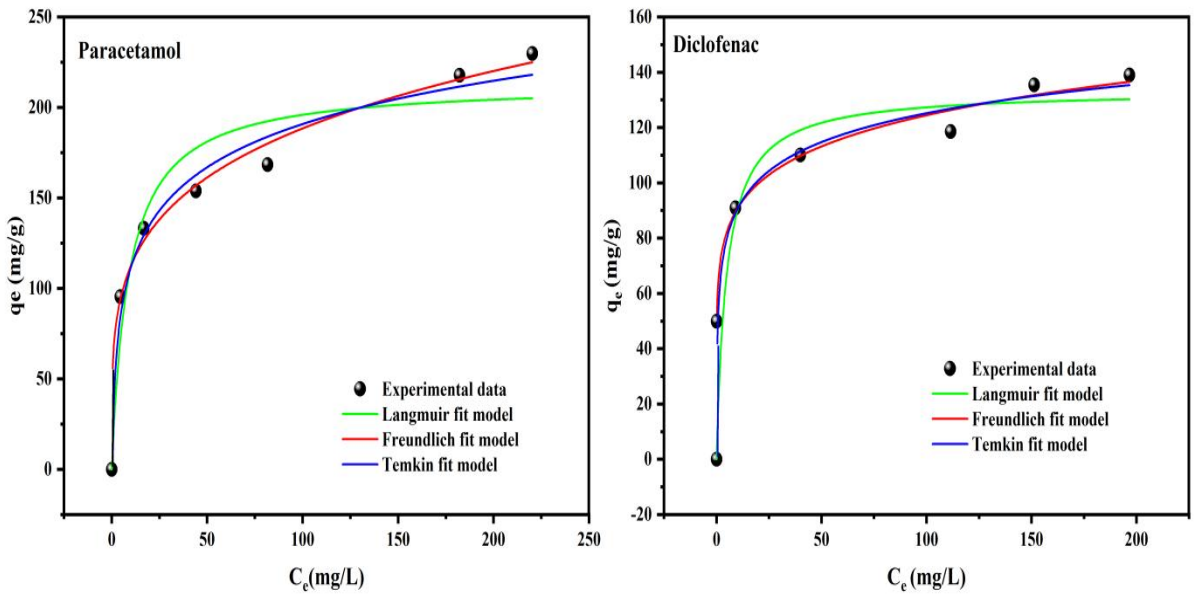

Figure II.3.5. Paracetamol and diclofenac adsorption isothers onto CC-$ZnCl_2$-AC.

The results indicated that the adsorption of both PCM and DCF was best described by the Freundlich model, with high correlation coefficients of 0.98 and 0.94, respectively, demonstrating multilayer adsorption on a heterogeneous surface (Alakayleh 2025). The maximum adsorption capacity (q_m) obtained from the Langmuir model was 213.35 and 133.41 mg g^{-1} for PCM and DFC, indicating that CC-$ZnCl_2$-AC is a better adsorbent for PCM adsorption than DFC.

Table II.3.2. Parameters of isotherm for paracetamol and diclofenac adsorption onto CC-$ZnCl_2$-AC.

Model	*Parameter*	*Unit*	*Paracetamol*	*Diclofenac*
Langmuir	Q^0_{max} K_L R^2 χ^2	mg/g L/mg - -	213.386 0.112 0.93 500.71	133.412 0.208 0.817 559.588
Freundlich	n K_F R^2 χ^2	mg/g (mg/g) / $(mg/L)^{1/n}$ - -	0.224 67.12 0.982 55.92	0.136 66.246 0.946 27.651

Temkin	B K_T R^2 χ^2	- L/mg - -	34.472 2.539 0.975 28.51	15.035 41.334 0.83 520.74

II.3.2.6. Thermodynamic study

In this work, thermodynamic analyses were performed at three temperatures: 298.15 K, 308 K, and 318 K. It was observed that the adsorption capacity of CC-$ZnCl_2$-AC for paracetamol decreased with increasing temperature, whereas the capacity for diclofenac increased under the same conditions. The findings in Figure II.3.6 showed coefficients of determination (R^2) of approximately 0.97 for paracetamol and 0.99 for diclofenac, indicating strong agreement between the experimental data and the van't Hoff model and thereby confirming the model's suitability for describing the thermodynamic behavior observed in this study.

The calculated standard Gibbs free energy (ΔG°) values were negative for both pharmaceuticals, confirming that adsorption occurred spontaneously (Bernal, Giraldo et al. 2020). Additionally, the negative enthalpy change (ΔH°) for PCM indicated an exothermic adsorption process, while the positive ΔH° for DCF adsorption pointed to an endothermic mechanism. Since the ΔH° values were below 40 kJ/mol, the adsorption processes for both compounds can be classified as physical in nature (Shirani, Song et al. 2020). Furthermore, the negative entropy change (ΔS°) for PCM suggests reduced disorder at the interface between the adsorbent and solution as the temperature increased. In contrast, DCF adsorption was associated with a positive ΔS°, reflecting an increase in randomness at the solid–liquid interface during uptake by CC-$ZnCl_2$-AC. These results are compiled in Table II.3.3.

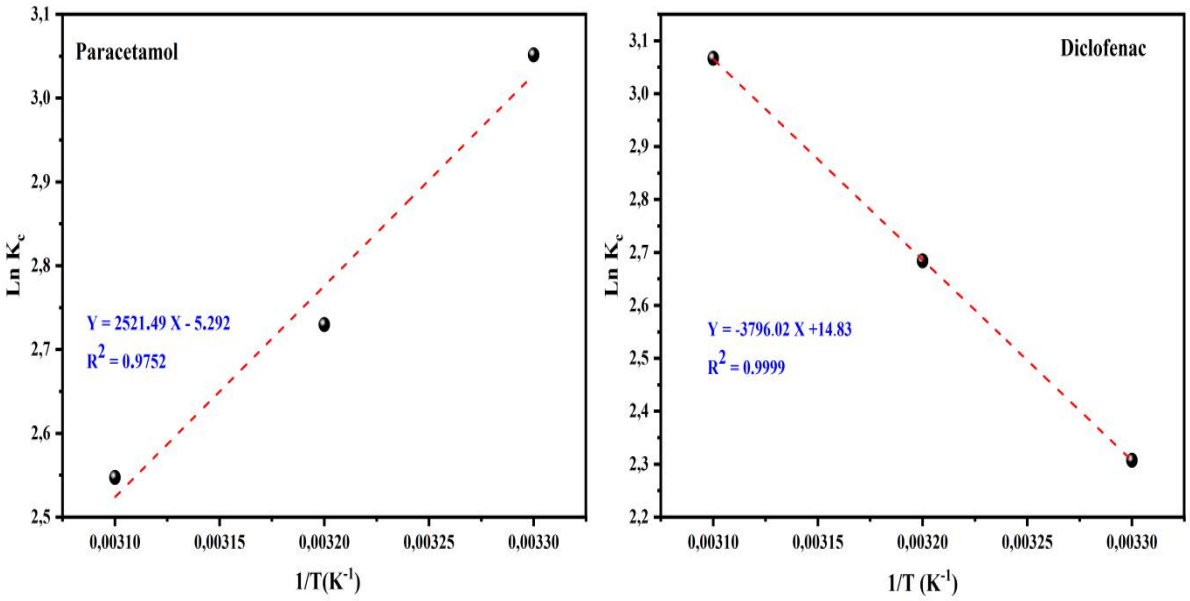

Figure II.3.6. Van't Hoff plot for paracetamol and diclofenac removal on CC-$ZnCl_2$-AC.

Table II.3.3. Thermodynamic parameters of paracetamol and diclofenac adsorption on CC-$ZnCl_2$-AC.

Pollutants	T(°K)	K_C	Van't Hoff equation	Thermodynamic parameters		
				$\Delta G°$ (KJ/mol)	$\Delta H°$ (KJ/mol)	$\Delta S°$ (J / (mol. k))
Paracetamol	**298**	21.14	Y = 2521.49 X - 5.292 R^2 = 0.9752	-7.914	-21.026	-44.002
	308	15.32		-7.474		
	318	12.77		-7.034		
Diclofenac	**298**	1.92	Y = -3796.02 X +14.83 R^2 = 0.9999	-5.184	31.559	123.32
	308	1.77		-6.417		
	318	1.64		-7.650		

II.3.3. Conclusion

In this chapter, the effectiveness of the activated carbon (CC-$ZnCl_2$-AC) was studied for the removal of paracetamol and diclofenac from synthetic distilled water solutions in a single system. The pseudo-second-order model accurately described the adsorption kinetics of PCM and DCF on CC-$ZnCl_2$-AC, whereas the Freundlich isotherm provided the best fit to the equilibrium data. Thermodynamic analysis indicated that the adsorption of PCM and DCF onto CC-$ZnCl_2$-AC was spontaneous, with PCM exhibiting exothermic behaviour and DCF endothermic behaviour.

References

Ahmad, M. B., U. Soomro, et al. (2021). "Adsorption of Indigo Carmine dye onto the surface-modified adsorbent prepared from municipal waste and simulation using deep neural network." Journal of hazardous materials **408**: 124433 DOI: 10.1016/j.jhazmat.2020.124433

Al-Hazmi, G. A., A. A. Alayyafi, et al. (2024). "Guava seed activated carbon loaded calcium alginate aerogel for the adsorption of diclofenac sodium: Characterization, isotherm, kinetics, and optimization via Box-Behnken design." International Journal of Biological Macromolecules **262**: 129995 DOI: https://doi.org/10.1016/j.ijbiomac.2024.129995.

Alakayleh, Z. (2025). "Sulfuric acid-activated carbon from guava leaves for paracetamol adsorption." Results in Engineering **25**: 103685 DOI: https://doi.org/10.1016/j.rineng.2024.103685.

Bernal, V., L. Giraldo, et al. (2020). "Thermodynamic analysis of acetaminophen and salicylic acid adsorption onto granular activated carbon: Importance of chemical surface and effect of ionic strength." Thermochimica Acta **683**: 178467 DOI: https://doi.org/10.1016/j.tca.2019.178467.

Cuccarese, M., S. Brutti, et al. (2021). "Removal of diclofenac from aqueous solutions by adsorption on thermo-plasma expanded graphite." Scientific reports **11**(1): 3427 DOI: https://doi.org/10.1038/s41598-021-83117-z.

El-Kelany, S. M., E. K. Radwan, et al. (2024). "Insights into the adsorption of emerging organic contaminant by low-cost readily separable modified jute fiber." Environmental Science and Pollution Research **31**(52): 61763-61780 DOI: https://doi.org/10.1007/s11356-024-35295-2.

Jagadeesan, D., H. Solayman, et al. (2025). "Hierarchical Ultra Microporous Aluminum Based Metal Organic Aerogels for Water Purification: Kinetic, Isotherm, and Regeneration Insights into Diclofenac Adsorption." Water Research X: 100424 DOI: https://doi.org/10.1016/j.wroa.2025.100424.

khadidja, H. (2025). Elaboration et caractérisation d'un composite à base biochar et ses applications à la photocatalyse et l'adsorption des polluants, Faculté des Sciences et technologie,University de Biskra.

Kocabıyık, B., O. Üner, et al. (2024). "Diclofenac sodium adsorption in aqueous media by activated carbon obtained from einkorn (Triticum monococcum L.) husk." Adsorption **30**(6): 1033-1046 DOI: https://doi.org/10.1007/s10450-024-00479-2.

Mabrouk, S., M. Fizer, et al. (2024). "Grape seeds waste activated carbon as an adsorber of paracetamol drug residue: Experimental and theoretical approaches." Journal of Molecular Liquids: 125325 DOI: https://doi.org/10.1016/j.molliq.2024.125325.

Melliti, A., M. Touihri, et al. (2024). "Sustainable removal of caffeine and acetaminophen from water using biomass waste-derived activated carbon: Synthesis, characterization, and modelling." Chemosphere **355**: 141787 DOI: https://doi.org/10.1016/j.chemosphere.2024.141787.

Saied, M. E., S. A. Shaban, et al. (2024). "Efficient adsorption of acetaminophen from the aqueous phase using low-cost and renewable adsorbent derived from orange peels." Biomass Conversion and Biorefinery **14**(2): 2155-2172 DOI: https://doi.org/10.1007/s13399-022-02541-x.

Sajid, M., S. Bari, et al. (2022). "Adsorption characteristics of paracetamol removal onto activated carbon prepared from Cannabis sativum Hemp." Alexandria Engineering Journal **61**(9): 7203-7212 DOI: https://doi.org/10.1016/j.aej.2021.12.060.

Seymen, S. T., H. A. Eroğlu, et al. (2025). "Comprehensive study on efficient diclofenac sodium removal using walnut and pistachio shell activated carbon: ANN, kinetics, isotherms, thermodynamics and DFT calculations." Biomass and Bioenergy **202**: 108216 DOI: https://doi.org/10.1016/j.biombioe.2025.108216.

Shirani, Z., H. Song, et al. (2020). "Efficient removal of diclofenac and cephalexin from aqueous solution using Anthriscus sylvestris-derived activated biochar." Science of The Total Environment **745**: 140789 DOI: https://doi.org/10.1016/j.scitotenv.2020.140789.

Sumalinog, D. A. G., S. C. Capareda, et al. (2018). "Evaluation of the effectiveness and mechanisms of acetaminophen and methylene blue dye adsorption on activated biochar derived from municipal solid wastes." Journal of environmental management **210**: 255-262 DOI: https://doi.org/10.1016/j.jenvman.2018.01.010.

Xie, J., M. Liu, et al. (2023). "Ultra-efficient adsorption of diclofenac sodium on fish-scale biochar functionalized with H3PO4 via synergistic mechanisms." Environmental pollution **322**: 121226 DOI: https://doi.org/10.1016/j.envpol.2023.121226.

Yan, J., X. Zhang, et al. (2019). "Adsorption behavior of diclofenac-containing wastewater on three kinds of sewage sludge." Water Science and Technology **80**(4): 717-726 DOI: https://doi.org/10.2166/wst.2019.315.

Chapter 4:

Adsorption of Paracetamol and Diclofenac onto CC-$ZnCl_2$-AC in binary mixture

II.4. Adsorption of Paracetamol and Diclofenac onto CC-$ZnCl_2$-AC in binary mixture

II.4.1. Introduction

Eliminating different pharmaceutical contaminants simultaneously from wastewater has become a crucial environmental issue. In this regard, the shift from conventional methods for removing single pollutants to implementing a system that simultaneously removes multiple contaminants is required. The current chapter begins by exploring the combined effect of diclofenac and paracetamol removal using activated carbon produced from cypress cones (CC-$ZnCl_2$-AC). This adsorbent was selected for its demonstrated effectiveness in adsorbing both contaminants. In this chapter, a kinetic study investigating the effects of pH, ionic strength, adsorbent dosage, initial concentration, and a thermodynamic study were conducted.

II.4.2. Binary experiments

Binary equilibrium experiments of diclofenac and paracetamol were performed using an adsorbent dosage of 1 g/L in contact with 30 mL of solution. The competitive adsorption of the binary component system was carried out using three different binary concentration ratios [50:100 mg/L, 100:100 mg/L, 100:50 mg/L] in a DCF-to-PCM and PCM-to-DCF sequence. After that, the adsorbent was removed by filtration, and the residual pharmaceutical concentration in the liquid phase was determined by spectrophotometry. The equilibrium concentrations of diclofenac (C_D) and paracetamol (C_P), in the binary system, were determined by **Eq.II.4.1** and **Eq.II.4.2**, respectively (Pauletto, Lütke et al. 2021)

$$C_D = \frac{K_{P2}Abs_1 - K_{P1}Abs_2}{K_{D1}K_{P2} - K_{D2}K_{P1}} \quad \textbf{Eq.II.4.1}$$

$$C_P = \frac{K_{D1}Abs_2 - K_{D2}Abs_1}{K_{D1}K_{P2} - K_{D2}K_{P1}} \quad \textbf{Eq.II.4.2}$$

Where k_{D1}, k_{D2}, k_{P1}, and k_{P2} are the calibration constants for diclofenac and paracetamol at the two wavelengths k_1 (276 nm) and k_2 (241 nm). Abs_1 and Abs_2 are the measured absorbances of each pharmaceutical compound.

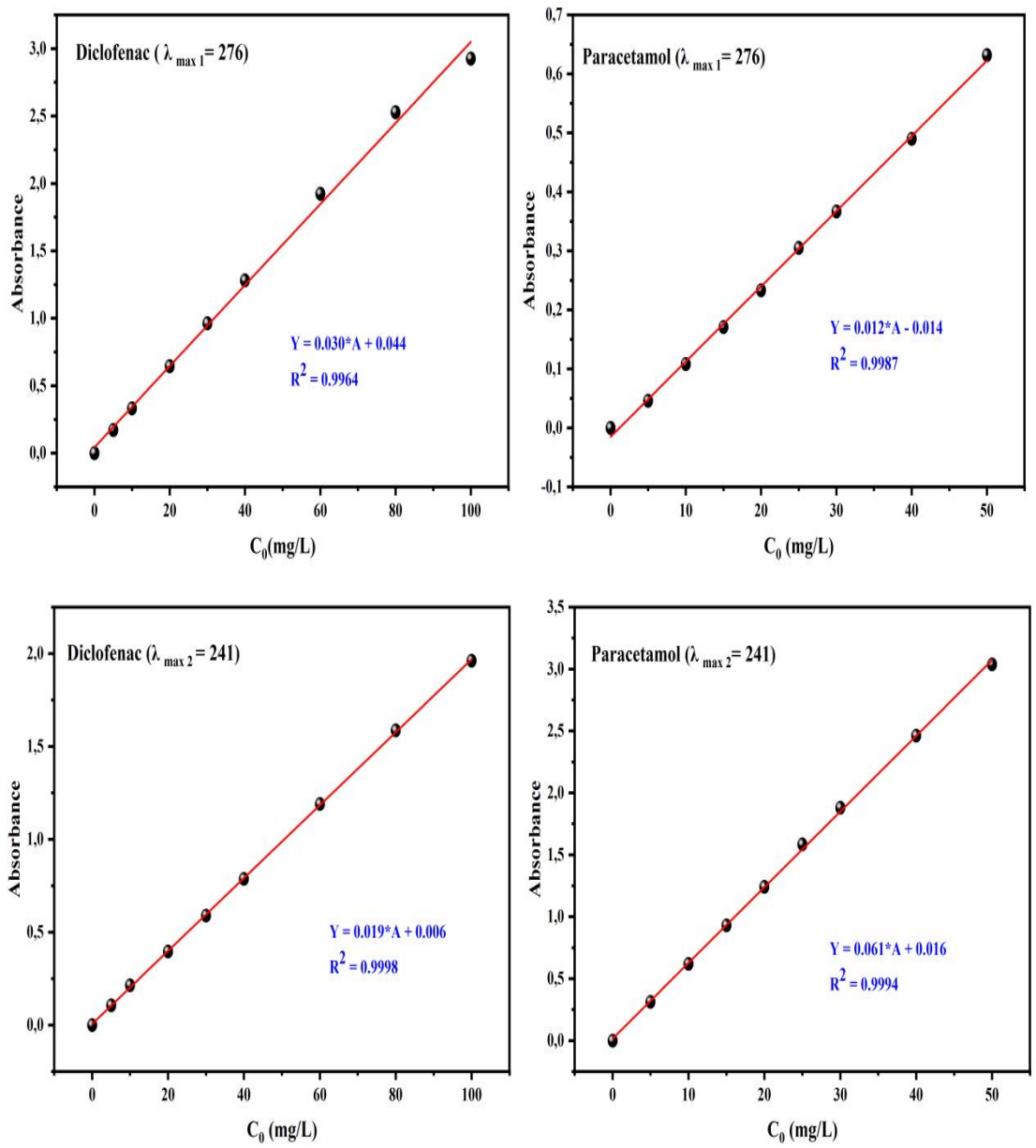

Figure II.4.1. Calibration curves of paracetamol and diclofenac at $\lambda_{max\ 1}$ and $\lambda_{max\ 2}$.

II.4.3. Investigation of Operational Conditions Influencing PCM and DCF Adsorption

II.4.3.1. Effect of contact time

The influence of contact time on the adsorption behavior of DCF and PCM in a binary mixture onto CC-$ZnCl_2$-AC was investigated over 0-240 minutes. According to Figure II.4.2, the uptake of both drugs increased significantly during the initial phase of interaction, followed by a gradual reduction in the adsorption rate, eventually stabilizing at equilibrium around 180 minutes. The increase in the amount adsorbed in the first stage is due to the ample

vacant active sites on CC-$ZnCl_2$-AC and an adequate concentration of pollutant molecules (Wakejo, Maged et al. 2024). After a lapse of some time, all the reaction sites progressively become occupied by the drugs, and consequently, the surface of the CC-$ZnCl_2$-AC has become saturated, which implies that the adsorption becomes less efficient during this stage (Bentahar, Dbik et al. 2017).

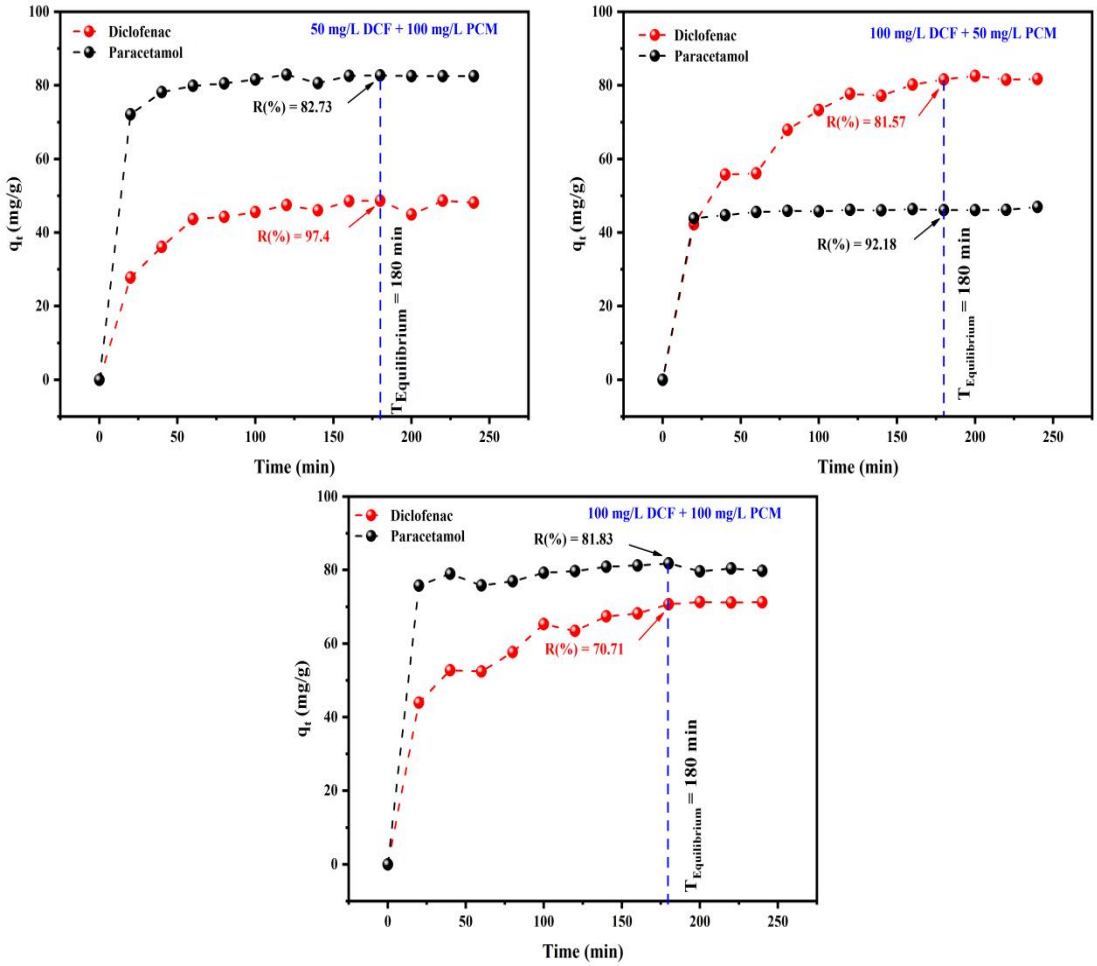

Figure II.4.2. Effect of contact time on the adsorption behavior of diclofenac and paracetamol in binary mixture onto CC-$ZnCl_2$-AC at different concentration ratios.

The experimental kinetic data were analyzed using non-linear kinetic models, such as the pseudo-first-order (PFO) and pseudo-second-order (PSO) models, in binary sorption experiments. The employed kinetic models were evaluated based on the coefficient of determination (R^2) and the closeness of the experimental equilibrium capacity (qe,exp) to the model-predicted equilibrium capacity (qe, cal). In all cases, PSO showed the highest R^2 and acceptable equilibrium capacity (model predicted qe close to experimental qe) values as

shown in Table II.4.1. Therefore, the PSO model best described the kinetic behavior of binary sorption of DCF and PCM onto CC-$ZnCl_2$-AC. To evaluate the impact of combining DCF and PCM at a 100:100 mg/L concentration ratio, a comparison was made with their individual adsorption performances, as discussed in Chapter 3. The findings revealed a noticeable decline in removal efficiency when both compounds were present simultaneously: DCF and PCM achieved removal rates of 90.9% and 95.5% respectively, in their single-component systems, whereas these values dropped to 70.71% and 81.83% in the binary mixture. This decrease in the case of a binary mixture could be attributed to the rivalry of DCF and PCM to occupy the sorption sites, meaning that the pollutants compete with each other to occupy the available sites on CC-$ZnCl_2$-AC (Spaolonzi, da Silva et al. 2025).

Table II.4.1. Kinetic model parameters for the adsorption of paracetamol and diclofenac in binary mixture onto CC-$ZnCl_2$-AC at different concentration ratios.

		Pseudo first-order kinetic model				Pseudo second-order kinetic model			
		q_e (mg/g)	k_1	R^2	χ^2	q_e (mg/g)	k_2	R^2	χ^2
Diclofenac (with paracetamol)	50:100 mg/L	47.30	0.038	0.989	2.034	52.29	0.001	0.990	1.830
	100:50 mg/L	80.61	0.026	0.972	16.548	92.65	3.903	0.987	7.261
	100:100 mg/L	67.94	0.036	0.947	21.723	75.72	0.0007	0.981	7.652
Paracetamol (with diclofenac)	50:100 mg/L	46.01	0.151	0.998	0.248	46.59	0.016	0.999	0.068
	100:50 mg/L	81.69	0.104	0.997	1.431	83.91	0.003	0.999	0.376
	100:100 mg/L	79.50	0.151	0.994	2.876	80.64	0.008	0.996	2.017

II.4.3.2. Effect of adsorbent dosage

The quantity of adsorbent utilized plays a crucial role in both the effectiveness of pollutant removal and the overall cost-efficiency in real-world scenarios. As illustrated in Figure II.4.3, the removal performance of DCF and PCM in binary mixtures is closely linked to the amount of CC-$ZnCl_2$-AC applied. A gradual increase in CC-$ZnCl_2$-AC dosage from 0.2 g/L to 2.0 g/L significantly enhanced the elimination rates of both compounds across different concentration ratios. Specifically, for the [50:100 mg/L] mixture, DCF and PCM removals rose from 26.1% and 47.89% to complete removal (100%) and 98.48%, respectively. In the case of the [100:50 mg/L] ratio, efficiencies improved from 25.53% and 43.56% to 98.65% and 98.96%. Likewise, at the highest ratio tested [100:100 mg/L], removal increased from 16.98% and 40.2% to 98.47% and 97.68%, indicating a clear positive correlation between CC-$ZnCl_2$-AC dose and adsorption performance for both pharmaceuticals. This is due to the greater availability of the active sites or surface area at higher concentrations of the adsorbent (Ashrafi, Bagherian et al. 2018). However, adsorption capacity per unit mass (mg/g) often declines due to site overlap and aggregation at high dosages, reducing the available surface area per unit mass. Nevertheless, each pharmaceutical compound has an optimal adsorbent dosage beyond which further additions yield only minor improvements in removal performance. Therefore, it is crucial to optimize the dosage to ensure high removal efficiency while utilizing the adsorbent material effectively (Mahmoud, Mahgoub et al. 2024).

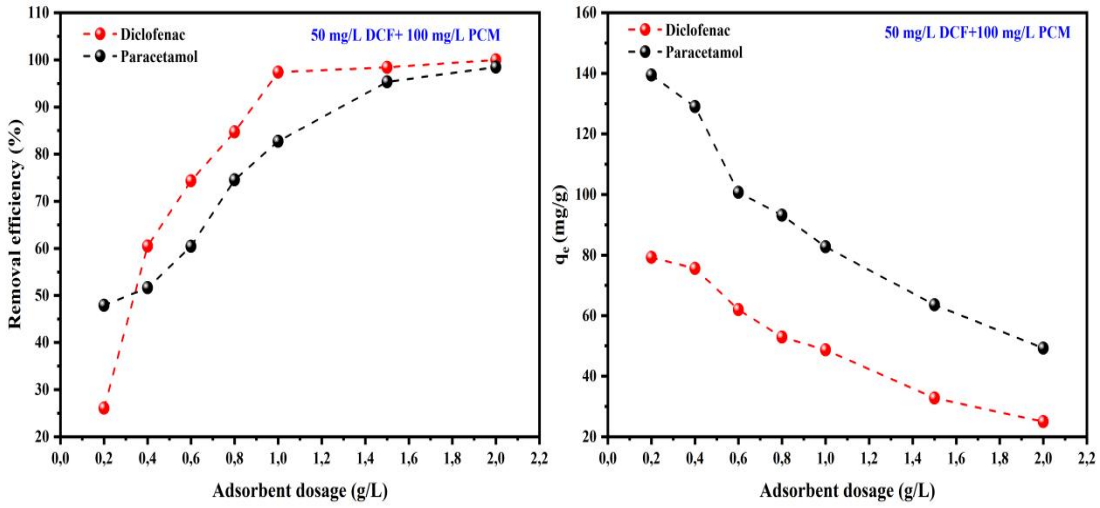

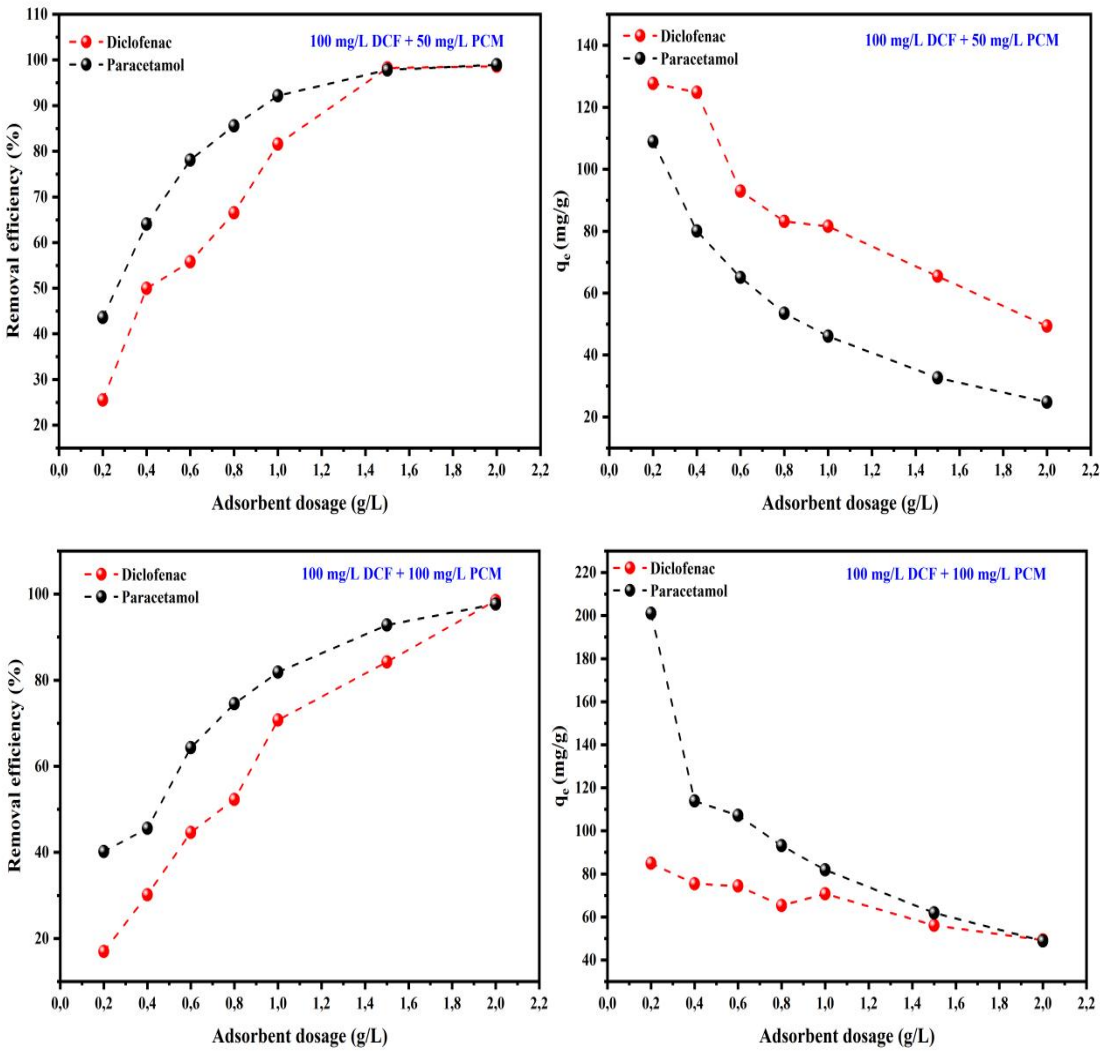

Figure II.4.3. Effect of CC-$ZnCl_2$-AC dose on the removal efficiency and the adsorption capacity of diclofenac and paracetamol in binary mixture at different concentration ratios.

II.4.3.3. Effect of pH medium

Among the various factors influencing adsorption, solution pH is pivotal. It significantly influences the solution's chemical environment, alters the adsorbent's surface properties and reactivity, and determines the extent of competition between hydrogen ions and the target molecules. Furthermore, it impacts the equilibrium constant of the adsorption process (Azri, Chebbi et al. 2024). The influence of solution pH on the adsorption of DCF and PCM was studied using CC-$ZnCl_2$-AC as the adsorbent, and the results are shown in Figure II.4.4. The efficiency of DCF and PCM removal was assessed over a pH range of 2.0 to 10.0. The adsorption diagram of paracetamol indicates that the adsorption performance remains relatively stable between pH 2 and pH 9. A noticeable decline in adsorption capacity

is observed only above pH 9.

In contrast, Diclofenac shows that maximum uptake occurred under acidic conditions, specifically between pH 2 and pH 4. Similarly, adsorption decreases after pH 9. The experimental results showed that both the individual adsorption systems of DCF and PCM (each at 100 mg/L) and the binary system at a 100:100 mg/L ratio exhibited similar responses to changes in solution pH in terms of DCF and PCM removal efficiency.

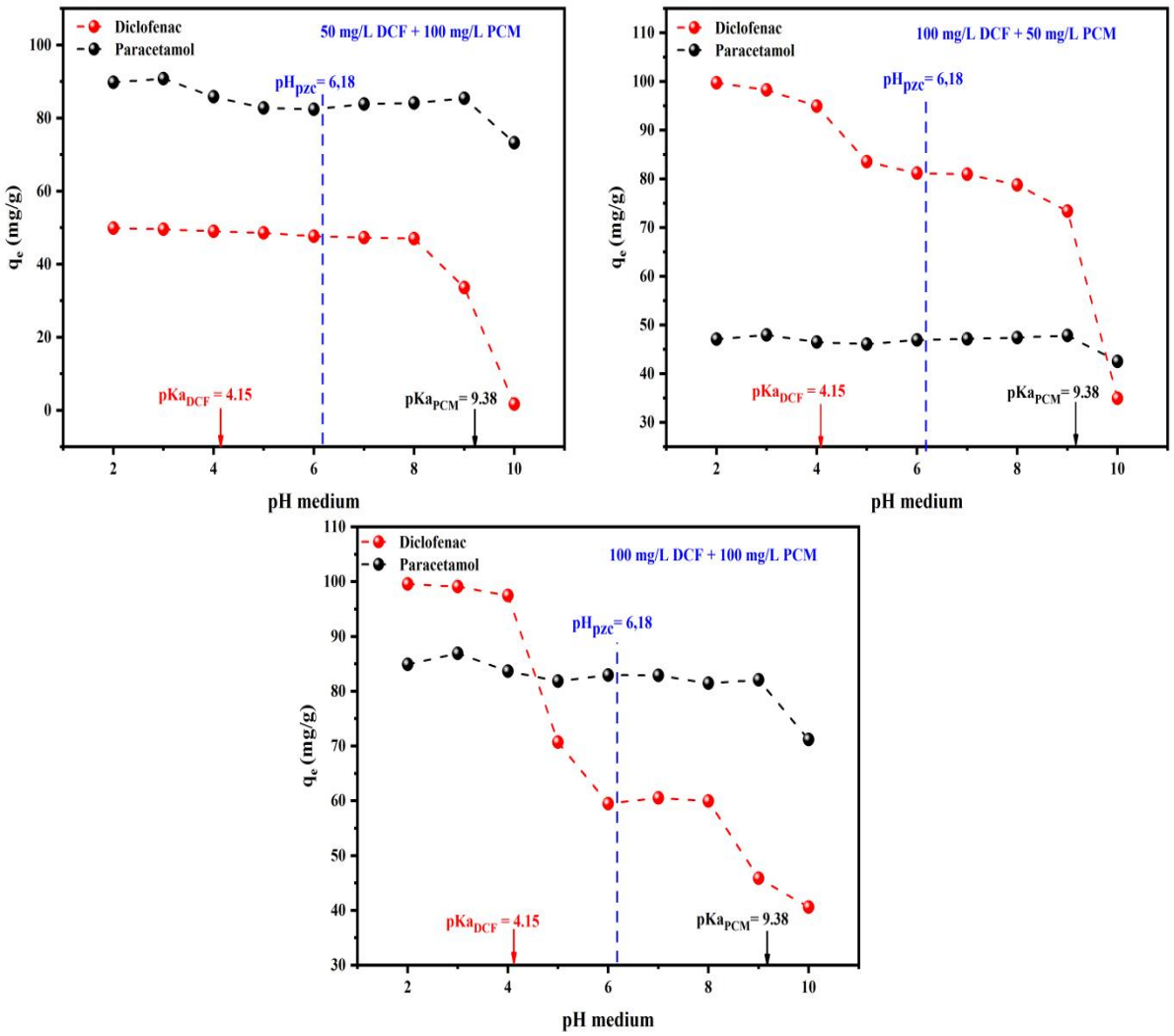

Figure II.4.4. Effect of pH medium on the removal of diclofenac and paracetamol onto CC-$ZnCl_2$-AC in binary mixture at different concentration ratios.

II.4.3.4. Effect of ionic strength

Ionic strength plays a significant role in governing adsorption behavior in aqueous systems. Figure II.4.5 illustrates how varying ionic strength affects the adsorption of DCF and

PCM onto CC-$ZnCl_2$-AC at pH 5.4 in binary mixtures. In the concentration ratios: [100:100 mg/L] and [100:50 mg/L]. The adsorption of PCM remained largely unaffected by changes in ionic strength, indicating that Na^+ ions and PCM likely occupy separate sites on the adsorbent surface, minimizing any competitive interference. Conversely, DCF adsorption increased modestly as NaCl concentration rose from 0.2 M to 1 M. This enhancement can be attributed to a reduction in electrostatic repulsion between DCF molecules and the adsorbent surface, which facilitates greater uptake (Medina, Aguiar et al. 2021). A similar pattern was observed in the single-component system for both pollutants. However, in a mixture with a [50 DCF:100 PCM mg/L] ratio, PCM adsorption increased, while DCF uptake remained essentially unchanged.

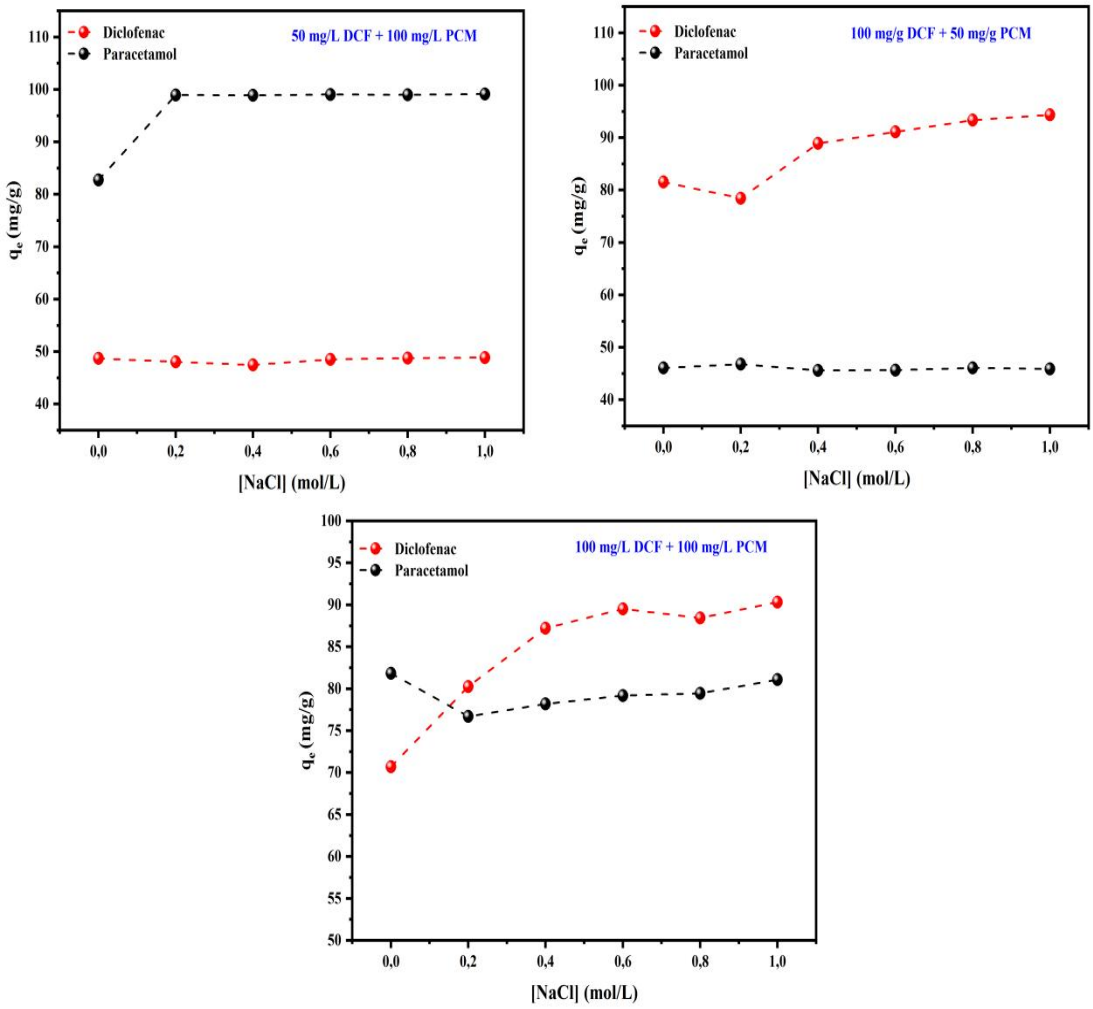

Figure II.4.5. Effect of ionic strength on the removal of diclofenac and paracetamol onto CC-$ZnCl_2$-AC in binary mixture at different concentration ratios.

II.4.3.5. Effect of concentration

To explore competitive behavior between PCM and DCF during adsorption, a series of binary experiments was conducted in which the initial concentration (Co) of one compound was fixed at 100 mg/L. In contrast, the concentration of the other was varied from 80 to 300 mg/L. As illustrated in Figure II.4.6, the data indicate that as the concentration of one drug increases, the adsorption efficiency of the other declines. This antagonistic interaction was more pronounced for DCF, whose removal dropped significantly from 75.15% to 30.86%. In contrast, PCM exhibited a more moderate decrease, with efficiency declining slightly from 82.05% to 75.02%.

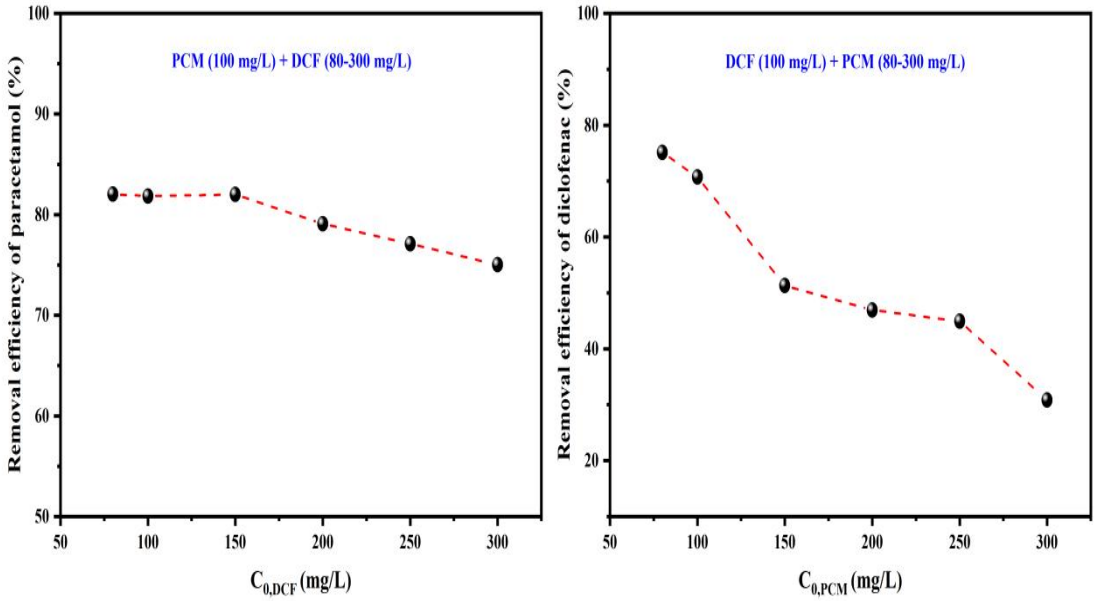

Figure II.4.6. Effect of concentration on the removal of diclofenac and paracetamol onto CC-$ZnCl_2$-AC in binary mixture.

II.4.3.6. Thermodynamic study

The thermodynamic study was carried out to reveal the nature of the adsorption of DCF and PCM drugs onto CC-$ZnCl_2$-AC in a binary mixture. The thermodynamic parameters, such as the Gibbs energy change (ΔG °), the enthalpy change (ΔH °) and the entropy change (ΔS °) were determined. The obtained results are illustrated in Table II.4.2. According to these results, we have found that the value of ΔG° at different temperatures is negative for both contaminants in the binary mixture, showing the feasibility of the process of adsorption of both pharmaceuticals onto the prepared adsorbent and its spontaneous nature in the

considered experimental conditions (Boukhelkhal, Benkortbi et al. 2019). The adsorption of DCF was characterized by a positive ΔH°, indicating an endothermic process. In contrast, the adsorption of PCM exhibited a negative ΔH°, signifying that the process releases heat and is thus exothermic. In the literature, magnitudes of ΔH below 40 kJ mol^{-1} are reported to indicate physisorption mechanisms (Shikuku, Zanella et al. 2018). The calculated ΔH values in the present work indicate that physisorption is the adsorption mechanism for DCS and PCM on CC-$ZnCl_2$-AC in the binary system. Moreover, the positive ΔS° observed for DCF implies that its adsorption led to greater molecular disorder at the solid–liquid boundary. On the other hand, a negative ΔS° for PCM indicates that the system became more ordered at the adsorbent–solution interface as the temperature rose.

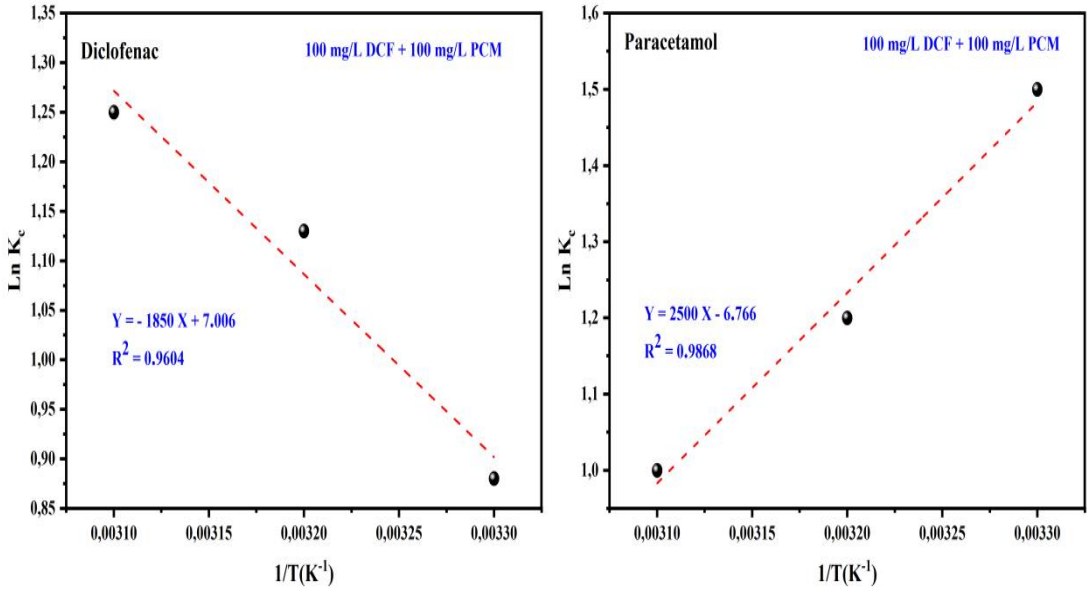

Figure II.4.7. Van't Hoff plot for diclofenac and paracetamol removal onto CC-$ZnCl_2$-AC in binary mixture.

Table II.4.2. Thermodynamic parameters of diclofenac and paracetamol adsorption onto CC-$ZnCl_2$-AC in binary mixture.

Pollutants	T(°K)	K_C	Van't Hoff equation	Thermodynamic parameters		
				$\Delta G°$ (KJ/mol)	$\Delta H°$ (KJ/mol)	$\Delta S°$ (J / (mol. k))
Diclofenac	**298**	2.414	Y = - 1850 X + 7.006 R^2 = 0.9604	-2.195	15.089	58.247
	308	3.099		-2.775		
	318	3.498		-3.355		
Paracetamol	**298**	4.503	Y = 2500 X - 6.766 R^2 = 0.9868	-4.037	-20.785	-56.252
	308	3.345		-3.475		
	318	2.735		-2.913		

II.4.4. Conclusion

The adsorption of paracetamol and diclofenac in the binary system shows a decrease in removal efficiency, suggesting that competition occurs for vacant adsorption sites on the surface of CC-$ZnCl_2$-AC. The equilibrium data were well fit by the nonlinear Freundlich isotherm model. The process was spontaneous, exothermic for PCM and endothermic for DCF, according to thermodynamic analysis. The adsorption values additionally indicated that a mostly physical mechanism was at work.

References

Ashrafi, M., G. Bagherian, et al. (2018). "Removal of brilliant green and crystal violet from mono-and bi-component aqueous solutions using NaOH-modified walnut shell." Analytical and Bioanalytical Chemistry Research **5**(1): 95-114 DOI: https://sid.ir/paper/354353/en.

Azri, N., R. Chebbi, et al. (2024). "Single and binary adsorption of paracetamol and diclofenac onto biochar produced from pepper stem: Which adsorption properties change in the binary system?" Colloids and Surfaces A: Physicochemical and Engineering Aspects **694**: 134136 DOI: https://doi.org/10.1016/j.colsurfa.2024.134136.

Bentahar, S., A. Dbik, et al. (2017). "Adsorption of methylene blue, crystal violet and congo red from binary and ternary systems with natural clay: Kinetic, isotherm, and thermodynamic." Journal of environmental chemical engineering **5**(6): 5921-5932 DOI: https://doi.org/10.1016/j.jece.2017.11.003.

Boukhelkhal, A., O. Benkortbi, et al. (2019). "Use of an anionic surfactant for the sorption of a binary mixture of antibiotics from aqueous solutions." Environmental Technology **40**(25): 3328-3336 DOI: https://doi.org/10.1080/09593330.2018.1472301.

Mahmoud, R., S. M. Mahgoub, et al. (2024). "Activated carbon alginate as adsorbent for simultaneous removal of almotriptan and paracetamol from binary solutions." Sustainable Chemistry and Pharmacy **41**: 101708 DOI: https://doi.org/10.1016/j.scp.2024.101708.

Medina, F. M. O., M. B. Aguiar, et al. (2021). "Insights of competitive adsorption on activated carbon of binary caffeine and diclofenac solutions." Journal of environmental management **278**: 111523 DOI: https://doi.org/10.1016/j.jenvman.2020.111523.

Pauletto, P. S., S. F. Lütke, et al. (2021). "Adsorption mechanisms of single and simultaneous removal of pharmaceutical compounds onto activated carbon: Isotherm and thermodynamic modeling." Journal of Molecular Liquids 336: 116203 DOI: https://doi.org/10.1016/j.molliq.2021.116203.

Shikuku, V. O., R. Zanella, et al. (2018). "Single and binary adsorption of sulfonamide antibiotics onto iron-modified clay: linear and nonlinear isotherms, kinetics, thermodynamics,

and mechanistic studies." Applied Water Science **8**(6): 175 DOI: https://doi.org/10.1007/s13201-018-0825-4.

Spaolonzi, M. P., M. G. C. da Silva, et al. (2025). "Enhanced adsorption of emerging contaminants by green carbon nanotubes in binary and ternary systems." Surfaces and Interfaces 69: 106809 DOI: https://doi.org/10.1016/j.surfin.2025.106809.

Wakejo, W. K., A. Maged, et al. (2024). "Tuneable functionalized biochar for simultaneous removal of pharmaceuticals from binary mixture." Colloids and Surfaces A: Physicochemical and Engineering Aspects **681**: 132718 DOI: https://doi.org/10.1016/j.colsurfa.2023.132718.

Chapter 5:

Machine learning approaches of adsorption of pharmaceutical compounds

II.5. Machine learning approaches of adsorption of pharmaceutical compounds

II.5.1. Introduction

Currently, artificial intelligence is widely utilized across a broad range of sectors, including chemical synthesis, stock market forecasting, media recommendation systems, medical diagnosis, and environmental monitoring and research. The process of using an algorithm to learn from data and make predictions without specific programming instructions is referred to as machine learning (Kooh, Thotagamuge et al. 2022)

In recent years, significant progress has been made in developing machine learning ensemble models to predict complicated, nonlinear processes like adsorption (Abbasi, Moghaddam et al. 2022). The use of machine learning (ML) offers a promising approach to addressing the challenges involved in predicting how different organic pollutants are adsorbed onto carbon-based materials (Wang, Wang et al. 2024)

II.5.2. Types of Machine Learning Techniques

Machine Learning algorithms are generally classified into four types: Supervised learning, Unsupervised learning, Semi-supervised learning, and Reinforcement learning(Sarker 2021).

II.5.2.1. Supervised learning

In supervised learning, a collection of examples or training data is provided along with the correct outputs. Based on this data, the algorithm improves its performance by adjusting its responses to match the given inputs. This method is often referred to as learning from examples or exemplars. Supervised learning is commonly used in scenarios where predictions are made using past data. Tasks in supervised learning can be divided into two types: classification, where the output consists of distinct labels, and regression, where the outputs are continuous(Jafar Alzubi 2018).

II.5.2.2. Unsupervised learning

Unsupervised learning refers to algorithms that operate without predefined correct answers or guidance from a teacher, unlike supervised learning. These algorithms independently explore and identify patterns or structures within the data. They extract a limited set of features from the data and, when new information is presented, they use these learned features to classify the data. This approach is commonly applied in clustering and dimensionality reduction tasks (Mahesh 2018).

II.5.2.3. Semi-supervised learning

Semi-supervised learning (SSL) lies between supervised and unsupervised learning, utilizing a dataset that is only partially labeled. The key goal of SSL is to address the limitations of both approaches. Supervised learning relies on large amounts of labeled data to classify new data, which can be costly and time-intensive. In contrast, unsupervised learning doesn't require labeled data but groups data based on similarities using clustering or maximum likelihood methods. However, it struggles to accurately categorize unknown data. To tackle these challenges, SSL was introduced by researchers. It can make use of a small amount of labeled data and still generalize to classify unlabeled or test data effectively. SSL builds models using a few labeled examples for training(Y C A Padmanabha Reddy 2018)

II.5.2.4. Reinforcement learning

Reinforcement Learning (RL) is a method in which an AI agent learns by engaging with its environment through trial and error, gradually refining its behavior based on the feedback it receives from past actions. This approach has proven to be highly effective for tackling complex decision-making challenges, especially in scenarios where creating precise models of the system is either impractical or prohibitively expensive. In recent years, RL has gained recognition as a powerful tool for advancing technology in areas where traditional methods fall short (Ashish Kumar Shakya 2023).

II.5.3. Adsorption modeling of data via machine learning

Developing a nonlinear correlation between operating conditions and the adsorption efficiency of biochar for pollutant removal significantly supports the design of high-performance adsorption systems, including adsorption columns and adsorption beds. Owing to the cost-effectiveness, efficiency, and strong predictive capabilities of machine learning techniques, optimizing the adsorption of pollutants onto biochar has become achievable. Common machine learning algorithms used to enhance the adsorption performance of biochar by optimizing operating parameters include Random Forest (RF), Support Vector Machine (SVM), Artificial Neural Network (ANN), and Adaptive Neuro-Fuzzy Inference System (ANFIS). Linear regression, as a basic machine learning approach, can also be employed to optimize pollutant adsorption processes on biochar. However, because of its inherent drawbacks, such as limited robustness, more advanced machine learning methods with greater predictive and explanatory capabilities are increasingly utilized. These include RF, SVM, and

Kernel Extreme Learning Machine (KELM), which provide improved optimization of biochar adsorption processes (Zhang, Chen et al. 2023).

II.5.3.1. Artificial Neural Networks (ANNs) Algorithm

Artificial Neural Networks (ANNs) are increasingly applied in environmental engineering and science because of their capability to identify underlying relationships within complex multivariable systems and support accurate predictive modeling. In many treatment-based studies, ANN models are mainly employed to establish correlations between operational variables and process performance. Beyond prediction, ANNs can also quantify the influence of each input factor by calculating their respective weights, thereby revealing the contribution of individual parameters to the observed outputs using experimental datasets. This evaluation of parameter significance provides valuable insight for improving and optimizing treatment systems (Salawu, Han et al. 2022).

II.5.3.2. Random Forest Regression (RFR)

Random forest regression (RFR) is widely employed as a machine learning approach for the classification and modeling of complex nonlinear systems using advanced statistical algorithms. This technique is considered highly effective because it can process a very large number of input variables to predict and assess adsorption performance (Beigzadeh, Bahrami et al. 2020). Random Forest (RF) operates as an ensemble learning method based on the integration of multiple decision trees to enhance prediction accuracy and minimize model variance. The model is developed through the random generation of numerous trees using bootstrap resampling, while the final prediction is obtained by averaging the outputs of all trees. Moreover, during tree construction, RF randomly selects subsets of variables, which helps decrease correlation among trees and improves the overall generalization performance of the model (Soares, de Oliveira Carvalho et al. 2020).

II.5.4. Data collection, model development, and performance evaluation

The quantity and reliability of experimental adsorption data are essential for developing predictive models with high accuracy and precision. Therefore, adsorption data were obtained through laboratory experiments carried out under different operating conditions. The experimental investigations focused on evaluating the adsorption performance of the CC-$ZnCl_2$-AC adsorbent material toward paracetamol and diclofenac removal.

In the present study, approximately 100 experimental runs were conducted under various conditions of contact time, adsorbent dosage, temperature, pH, initial pollutant

concentration, and NaCl concentrations. The obtained experimental results were compiled to establish the adsorption dataset used in the modeling analysis.

Before starting the modeling procedure, the collected experimental dataset was divided into training and testing subsets. Subsequently, normalization techniques were applied to both subsets in order to minimize the influence of variable scaling and improve prediction performance.

Through this methodology, predicted adsorption values were generated and compared with the experimental observations to evaluate the prediction errors. Two machine learning models, namely Artificial Neural Network (ANN) and Random Forest Regression (RFR), were employed to predict the adsorption behavior.

The performance of the developed models was evaluated using several statistical indicators, including the coefficient of determination (R^2), relative error (RE), and root mean square error (RMSE). The most suitable predictive model was selected based on the highest R^2 value and the lowest error values, indicating better agreement between the predicted and experimental adsorption data.

Table II.5.1. Performance evaluation of ANN and RFR models using statistical parameters for PCM and DCF adsorption.

Output	Model	Paracetamol				Diclofenac			
		MAE	R^2	RE	RMSE	MAE	R^2	RE	RMSE
Removal (%)	ANN	3.16	0.823	4.23	6.08	4.614	0.936	12.11	6.693
	RFR	0.84	0.982	2.98	2.30	0.161	0.999	0.26	0.223
Capacity (mg/g)	ANN	4.10	0.971	3.39	5.38	6.594	0.897	8.58	8.503
	RFR	4.01	0.976	3.25	4.76	2.398	0.988	2.54	3.215

The mathematical expressions of these statistical parameters are given as follows:

Coefficient of determination:

$$R^2 = 1 - \frac{\sum_{i=1}^{n} \left(y_i - \hat{y}_i\right)^2}{\sum_{i=1}^{n} \left(y_i - \bar{y}_i\right)^2} \qquad \textbf{Eq.II.5.1}$$

Relative error:

$$RE = \left|\frac{y_i - \hat{y}_i}{\hat{y}_i}\right| \quad \textbf{Eq.II.5.2}$$

Root mean squared error:

$$RMSE = \sqrt{\frac{1}{n}\sum_{i=1}^{n}\left(y_i - \hat{y}_i\right)^2} \quad \textbf{Eq.II.5.3}$$

Mean absolute error:

$$MAE = \frac{1}{n}\sum_{i=1}^{n}\left|y_i - \hat{y}_i\right| \quad \textbf{Eq.II.5.4}$$

Where:

y_i: The experimental adsorption values.

$\hat{y}_i$: The predicted values obtained from the models.

$\bar{y}_i$: The average of the experimental values.

n: The total number of data point.

Table II.5.1. illustrates the values of the investigated statistical parameters employed to evaluate the reliability of ANN and RFR models. The results demonstrate that the Random Forest Regression (RFR) model consistently outperformed the Artificial Neural Network (ANN) model. RFR achieved higher coefficient of determination and lower prediction errors for paracetamol and diclofenac and both outputs. This suggests that the ensemble learning approach of RFR was more capable of handling the nonlinear adsorption system and complex interactions among process variables.

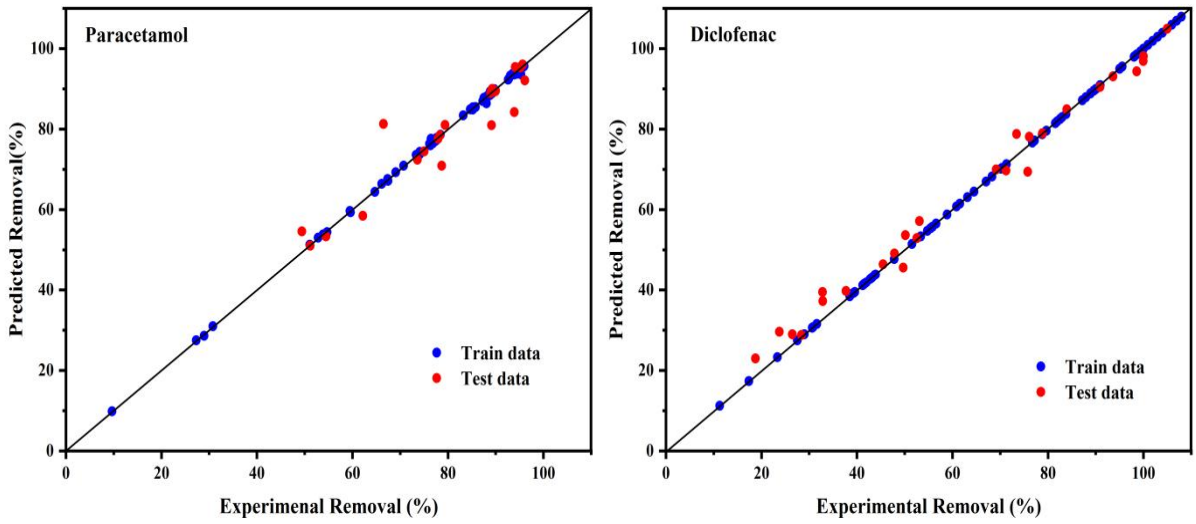

Figure II.5.1. Predicted versus experimental values for the removal efficiency of PCM and DCF adsorption systems.

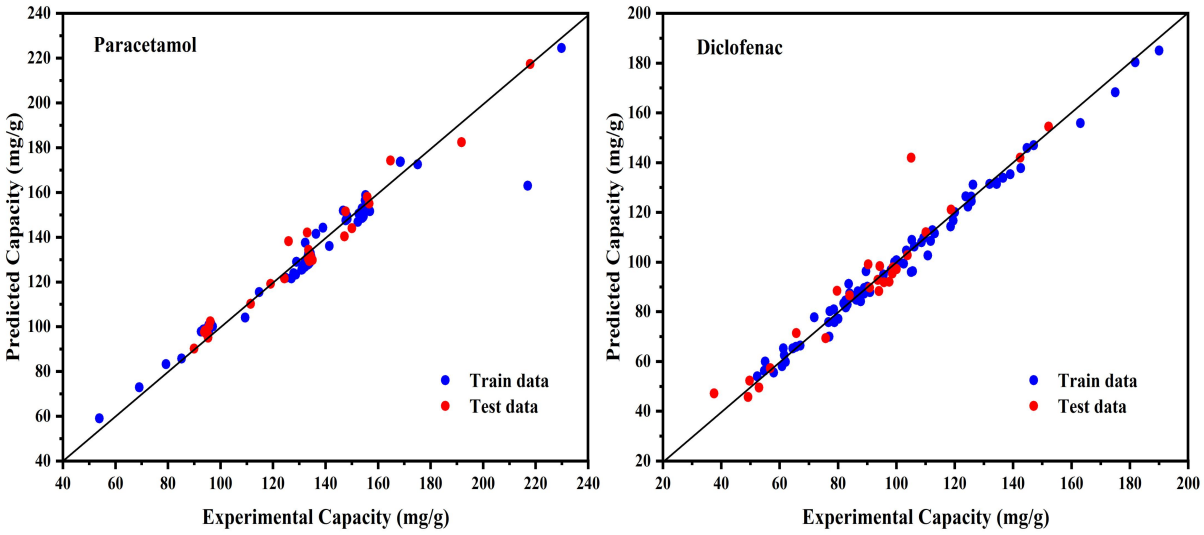

Figure II.5.2. Predicted versus experimental values for the adsorption capacity of PCM and DCF adsorption systems.

The predictive effectiveness of the machine learning models was assessed through parity plots relating predicted outputs to experimental observations (Figure II.5.1). The identity line (y = x) signifies perfect concordance between predicted and measured values. Accordingly, the degree of clustering of the data points around this line provides a visual measure of the models' prediction accuracy and generalization performance.

For the prediction of paracetamol removal efficiency, the parity plot demonstrates that the predicted values generally align with the identity line, indicating that the model effectively captured the relationship between the operating variables and the removal performance. The training data points are tightly clustered around the parity line, reflecting a high degree of agreement between predicted and experimental values. In contrast, the testing data exhibit a relatively greater dispersion, particularly within the medium and high removal efficiency ranges, suggesting reduced predictive accuracy under certain conditions. The observed deviations from the identity line indicate the presence of prediction errors for specific experimental cases. This increased scatter may be attributed to the inherent complexity of modeling paracetamol removal efficiency. Nevertheless, the overall distribution of points confirms that the model possesses satisfactory predictive capability.

The parity plot of paracetamol adsorption capacity reveals a stronger agreement between predicted and experimental values. The majority of the data points are concentrated

near the identity line, and both the training and testing datasets display comparable distributions. Only minor deviations are observed at higher adsorption capacities, while the overall scatter is noticeably lower than that observed for paracetamol removal efficiency. These results indicate that the developed model predicts adsorption capacity with greater accuracy and consistency, suggesting that adsorption capacity is a more predictable response variable than removal efficiency in the paracetamol adsorption process using CC-$ZnCl_2$-AC.

The parity plot of diclofenac removal efficiency exhibits a high degree of agreement between the predicted and experimental values, demonstrating the model's ability to accurately represent the adsorption process. The majority of the data points are closely clustered around the identity line ($y = x$), indicating excellent prediction accuracy. Furthermore, the training and testing datasets show a substantial overlap. The agreement between predictions and observations is maintained throughout nearly the entire range of removal efficiencies, with only a few isolated deviations from the parity line. These findings highlight the strong predictive capability of the model and its effective generalization performance.

Similarly, the parity plot for diclofenac adsorption capacity (mg g^{-1}) reveals excellent predictive accuracy. Most of the predicted values coincide closely with the corresponding experimental measurements and are concentrated near the identity line. The dispersion of the data points remains very low across the entire adsorption-capacity range, indicating a high level of prediction precision. In addition, the comparable distributions of the training and testing datasets suggest that the model is not significantly affected by overfitting. The consistent agreement observed, even at elevated adsorption capacities, confirms the robustness and stability of the model in describing the adsorption-capacity behavior of diclofenac systems.

The predictive performance obtained for diclofenac is superior to that of paracetamol, as evidenced by the closer clustering of the data points around the identity line in the parity plots. In addition, the prediction of adsorption capacity demonstrates slightly higher accuracy than that of removal efficiency, particularly in the case of paracetamol adsorption. Furthermore, the strong similarity between the training and testing data distributions suggests that the model exhibits good generalization capability and is not significantly affected by overfitting.

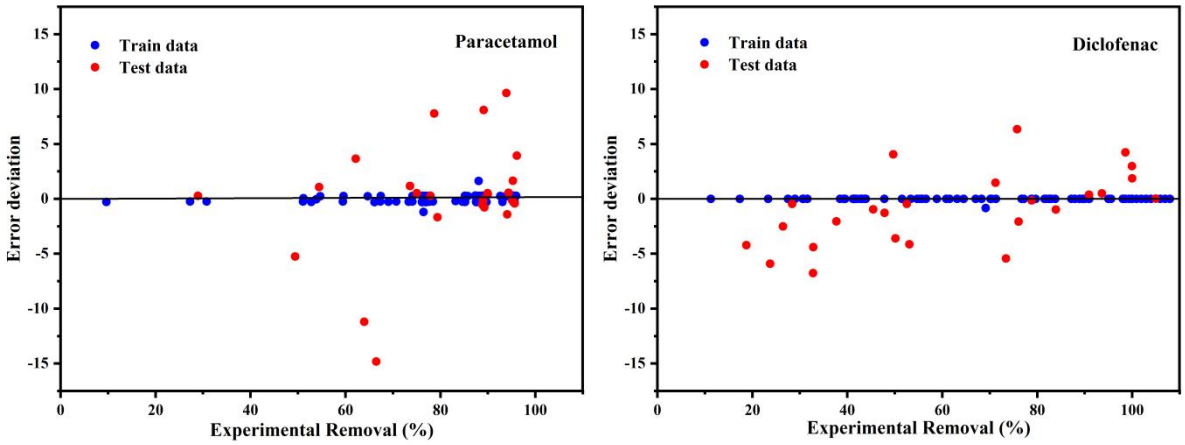

Figure II.5.3. Error deviation plots for PCM and DCF removal prediction model

The error deviation distributions for paracetamol (PCM) and diclofenac (DCF) removal reveal that most training residuals are clustered around zero, reflecting the strong fitting ability of the developed models. For PCM, the testing dataset exhibits a wider spread of errors and several pronounced deviations, indicating reduced prediction consistency and limited generalization capability. Conversely, DCF shows a more compact and balanced error distribution centered near zero, highlighting its greater stability and predictive reliability.

II.5.5.Conclusion

The results demonstrate that the Random Forest Regression (RFR) model consistently outperformed the Artificial Neural Network (ANN) model. The parity plots demonstrate strong agreement between predicted and experimental values for both PCM and DCF adsorption systems. In general, DCF exhibited superior prediction accuracy compared with PCM, as shown by the tighter clustering of data points around the parity line. Moreover, adsorption capacity predictions showed slightly lower dispersion than removal efficiency predictions, particularly for PCM. The close overlap between training and testing datasets confirms the robustness and generalization capability of the developed machine learning models.

References

Abbasi, E., M. R. A. Moghaddam, et al. (2022). "A systematic and critical review on development of machine learning based-ensemble models for prediction of adsorption process efficiency." Journal of Cleaner Production **379**: 134588.

Ashish Kumar Shakya , G. P., Sohom Chakrabarty (2023). "Reinforcement learning algorithms: A brief survey." Expert Systems With Applications DOI: https://doi.org/10.3390/s24082461

Beigzadeh, B., M. Bahrami, et al. (2020). "A new approach in adsorption modeling using random forest regression, Bayesian multiple linear regression, and multiple linear regression: 2, 4-D adsorption by a green adsorbent." Water Science and Technology **82**(8): 1586-1602 DOI : https://doi.org/10.2166/wst.2020.440.

Jafar Alzubi, A. N., Akshi Kumar (2018). "Machine Learning from Theory to Algorithms: An Overview." Journal of Physics: Conference Series.

Kooh, M. R. R., R. Thotagamuge, et al. (2022). "Machine learning approaches to predict adsorption capacity of Azolla pinnata in the removal of methylene blue." Journal of the Taiwan Institute of Chemical Engineers **132**: 104134 DOI: https://doi.org/10.1016/j.jtice.2021.11.001

Mahesh, B. (2018). "Machine Learning Algorithms - A Review." International Journal of Science and Research DOI: https://doi.org/10.21275/ART20203995.

Salawu, O. A., Z. Han, et al. (2022). "Shrimp waste-derived porous carbon adsorbent: Performance, mechanism, and application of machine learning." Journal of hazardous materials **437**: 129266 DOI:https://doi.org/10.1016/j.jhazmat.2022.129266.

Sarker, I. H. (2021). "Machine Learning: Algorithms, Real‐World Applications and Research Directions." SN Computer Science DOI : https://doi.org/10.1007/s42979-021-00592-x.

Soares, A. P. d. M. R., F. de Oliveira Carvalho, et al. (2020). "Random Forest as a promising application to predict basic-dye biosorption process using orange waste." Journal of environmental chemical engineering **8**(4): 103952 DOI: https://doi.org/10.1016/j.jece.2020.103952

Wang, Z., Q. Wang, et al. (2024). "How Machine learning boosts the understanding of organic pollutant adsorption on carbonaceous Materials: A comprehensive review with statistical insights." Separation and Purification Technology: 127790 DOI: https://doi.org/10.1016/j.seppur.2024.127790Get rights and content

Y C A Padmanabha Reddy , P. V., B Eswara Reddy (2018). "Semi-supervised learning: a brief review." International Journal of Engineering & Technology.

Zhang, W., R. Chen, et al. (2023). "Synthesis optimization and adsorption modeling of biochar for pollutant removal via machine learning." Biochar **5**(1): 25 DOI: https://doi.org/10.1007/s42773-023-00225-x.

General Conclusion

General conclusion

This research work explores water treatment through the development of activated carbons obtained from cypress cones biomass. By focusing on both environmental protection and water resource conservation, the study highlights the potential to convert agricultural residues into valuable materials for removing synthetic pharmaceuticals. The utilization of these biomaterials is based on the development of two categories of adsorbents prepared by distinct techniques. In the first approach, the biomass of cypress cones was subjected to single-step pyrolysis at different temperatures, yielding biochars labelled CCB-450, CCB-550, and CCB-650. In the second approach, the biomass was processed in two stages: first, chemically modified with zinc chloride, and second, carbonized at 650 °C. The prepared adsorbents were subjected to various analyses, including SEM-EDS, XRD, FTIR, and the BET method, to determine their physicochemical properties and ensure high removal capacity for the pharmaceuticals tested.

The experimental results demonstrated that the removal efficiencies of the two pharmaceuticals were superior for CCB-650 compared to the other biochars, and that the removal efficiency increased progressively with increasing pyrolysis temperature.

The kinetic behaviour of the two pharmaceuticals on CCB-650 was investigated at an initial concentration of 25 mg/L. The equilibrium attainment time was found to vary according to the specific adsorbate–adsorbent interaction. For the biochar CCB-650, equilibrium adsorption of both pharmaceuticals was achieved within 3 h. Analysis of the kinetic data revealed that the pseudo-second-order model provided the best fit to the experimental results with R^2 values of 0.999 and a χ^2 of 0.054 for paracetamol, and an R^2 of 0.981 and χ^2 of 0.352 for diclofenac.

The removal efficiency of the two pollutants increased with the adsorbent dosage, which can be ascribed to the enhanced availability of adsorption sites. The pH of the medium exerted no significant influence on paracetamol adsorption under acidic and neutral conditions. However, a pronounced effect was observed under basic conditions. In contrast, diclofenac exhibited its highest removal efficiency in an acidic medium. Ionic strength showed negligible influence on patacetamol adsorption, owing to the distinct interaction of Na^+ and PCM with different adsorption sites. By contrast, NaCl significantly enhanced diclofenac uptake, likely because

increased ionic strength reduced the solubility of hydrophobic organic molecules. The Freundlich model provided good agreement with the experimental adsorption data for paracetamol and diclofenac, suggesting that adsorption predominantly occurs heterogeneously on the biochar surface and follows a multilayer adsorption mechanism. The maximum Langmuir adsorption capacities were 59.86 mg/g for paracetamol and 17.04 mg/g for diclofenac, respectively. The thermodynamic parameters of adsorption for the two pharmaceuticals on CCB-650 confirmed the physisorptive, spontaneous, and endothermic nature of the process.

In order to improve the adsorption performance at higher concentration ranges, an additional adsorbent was prepared through chemical treatment, named (CC-$ZnCl_2$-AC), and subsequently applied at an initial concentration of 100 mg/L for each pollutant. The adsorption kinetics of paracetamol and diclofenac on the CC-$ZnCl_2$-AC adsorbent established equilibrium after contact times of 3 h and 4 h, respectively. Fitting the kinetic data showed that the pseudo-second-order model was the most suitable, as reflected by R^2 values of 0.999 and 0.996, and χ^2 values of 0.122 and 0.035 for paracetamol and diclofenac, respectively.
Increasing the adsorbent dosage improved the elimination of paracetamol and diclofenac, though it also led to a decline in adsorption capacity. Paracetamol adsorption remained stable at acidic/neutral pH but declined in alkaline conditions, while diclofenac removal peaked in acidic medium. Ionic strength had little effect on paracetamol adsorption, while it significantly improved diclofenac adsorption. The adsorption behaviour of paracetamol and diclofenac was well described by the Freundlich isotherm, indicating a heterogeneous distribution of active sites and a multilayer adsorption mechanism. The maximum adsorption capacities obtained were 213.38 mg/g for paracetamol and 133.41 mg/g for diclofenac.
The thermodynamic study showed that the adsorption of paracetamol and diclofenac was spontaneous, with paracetamol being exothermic and diclofenac endothermic.

Pharmaceuticals adsorption was slightly more efficient on activated carbon (CC-$ZnCl_2$-AC) than on biochar (CCB-650), supporting the choice of CC-$ZnCl_2$-AC for the binary adsorption study of the two pollutants in a binary system. The reductions in equilibrium adsorption capacity and efficiency observed in the binary system are attributed to competitive interactions among pharmaceuticals on the surface of CC-$ZnCl_2$-AC, reflecting competition

for available adsorption sites. Nonlinear fitting of the equilibrium data revealed good agreement with the Freundlich isotherm model. Thermodynamic evaluation indicated that the process occurred spontaneously, exhibiting an exothermic character for DCF and an endothermic nature for PCM. Moreover, the adsorption parameters indicated that the mechanism was predominantly physical, consistent with the behaviour observed in the single system.

The comparative evaluation of statistical indicators and graphical analyses demonstrated that both machine-learning models, ANN and RFR, effectively predicted the adsorption behavior of PCM and DCF. The close agreement between experimental and predicted values confirmed the ability of these approaches to accurately capture adsorption trends. However, the RFR model exhibited superior predictive performance, as evidenced by higher R^2 values and lower MAE, RE, and RMSE for both removal efficiency and adsorption capacity. Overall, the results highlight the effectiveness of machine learning techniques for adsorption modeling and identify RFR as the most reliable and robust model for predicting the adsorption performance of PCM and DCF under the investigated conditions using CC-$ZnCl_2$-AC as an adsorbent.

Ultimately, this study contributes to ongoing research efforts aimed at developing more sustainable and environmentally friendly water treatment technologies, with the application of machine learning approaches to support the modeling of adsorption processes, the prediction of their behavior, and the optimization of their efficiency for pollutant removal. However, additional work is needed to improve the adsorbents' characteristics, optimize adsorption conditions, assess the performance of the prepared adsorbents at larger scales, and establish regeneration strategies to ensure long-term applicability. Moreover, evaluate their performance in real wastewater and multicomponent systems, investigate its application in fixed-bed column processes for continuous treatment, and explore magnetic biochar-based adsorbents to improve separation and recovery.

Abstract

The population extensively consumes pharmaceutical products, which are continuously discharged into the environment, constituting a significant source of aquatic contamination. This research investigates the removal of these pollutants using cost-effective adsorbents derived from locally available agricultural waste (Cypress cones). Additionally, machine learning models, namely Artificial Neural Networks (ANN) and Random Forest Regression (RFR), were employed to predict adsorption performance under different operating conditions. The results demonstrate the potential of integrating sustainable adsorbents with machine learning techniques to enhance and optimize water treatment processes. The adsorbents were prepared as CC-biochar at varying pyrolysis temperatures (450, 550, and 650 °C), along with a chemically modified carbon treated with zinc chloride to improve its adsorption capacity for the elimination of paracetamol and diclofenac in aqueous solutions in single- and binary-systems. Characterization results demonstrated that the adsorbents possess an amorphous structure with a porous morphology. Moreover, the specific surface area increased markedly with increasing pyrolysis temperature and chemical modification. The adsorption experiments revealed that CCB-650 exhibited superior performance compared to the other synthesized biochars, removing 59.86 mg/g of paracetamol and 17.04 mg/g of diclofenac. At the same time, activated carbon demonstrated higher efficiencies, with maximum adsorption capacities of 213.38 mg/g and 133.41 mg/g, respectively. The pseudo-second-order model accurately described the adsorption kinetics of PCM and DCF on each adsorbent, whereas the Freundlich isotherm provided the best fit to the equilibrium data. Thermodynamic analysis indicated that the adsorption of PCM and DCF onto CCB-650 was spontaneous and endothermic.In contrast, adsorption onto CC-$ZnCl_2$-AC was spontaneous, with PCM exhibiting exothermic behaviour and DCF endothermic behaviour in the single system. In addition, the adsorption efficiency of PCM and DCF was higher in the single-component system than in the binary mixture on CC-$ZnCl_2$-AC. The nonlinear Freundlich isotherm model provided a good fit to the equilibrium data. Although the adsorption kinetics of both contaminants followed the pseudo-second-order model, thermodynamic analysis confirmed that the process was spontaneous, exothermic for PCM and endothermic for DCF. The adsorption values further suggested that the mechanism was predominantly physical. The obtained results demonstrate the suitability of machine learning for adsorption modeling, with RFR exhibiting superior accuracy and robustness in predicting the adsorption performance of PCM and DCF on CC-$ZnCl_2$-AC.

Keywords: Adsorption, Machine learning, Cypress cones, Paracetamol, Diclofenac, CCB-650, CC-$ZnCl_2$-AC.

Résumé

La population consomme largement des produits pharmaceutiques qui sont continuellement rejetés dans l'environnement, constituant ainsi une source importante de contamination des milieux aquatiques. Cette étude examine l'élimination de ces polluants à l'aide d'adsorbants à faible coût dérivés de déchets agricoles localement disponibles (cônes de cyprès). En outre, des modèles d'apprentissage automatique, à savoir les réseaux de neurones artificiels (ANN) et la régression par forêts aléatoires (RFR), ont été utilisées pour prédire les performances d'adsorption dans différentes conditions opératoires. Les résultats démontrent le potentiel de l'intégration d'adsorbants durables et de techniques d'apprentissage automatique pour améliorer et optimiser les procédés de traitement des eaux. Les adsorbants ont été préparés sous forme de biochar de cônes de cyprès (CC-biochar) à différentes températures de pyrolyse (450, 550 et 650 °C), ainsi qu'un carbone chimiquement modifié traité par le chlorure de zinc afin d'améliorer sa capacité d'adsorption pour l'élimination du paracetamol et du diclofenac en solution aqueuse, en systèmes simple et binaire. Les résultats de caractérisation ont montré que les adsorbants présentent une structure amorphe avec une morphologie poreuse. De plus, la surface spécifique a montré une augmentation notable avec l'élévation de la température de pyrolyse et la modification chimique. Les expériences d'adsorption ont révélé que le CCB-650 présentait des performances supérieures par rapport aux autres biochars synthétisés, avec l'élimination de 59.86 mg/g de PCM et 17.04 mg/g de DCF, tandis que le charbon activé a démontré des efficacités plus élevées avec des capacités d'adsorption maximales de 213.38 mg/g et 133.41 mg/g, respectivement. Les cinétiques d'adsorption du PCM et du DCF sur chaque adsorbant ont été décrites avec précision par le modèle du pseudo-second ordre, tandis que l'isotherme de Freundlich a fourni le meilleur ajustement aux données d'équilibre. L'analyse thermodynamique a indiqué que l'adsorption du PCM et du DCF sur le CCB-650 était spontanée et endothermique, alors que l'adsorption sur le CC-$ZnCl_2$-AC était également spontanée, le PCM présentant un caractère exothermique et le DCF un comportement endothermique en système simple. De plus, l'efficacité d'adsorption du PCM et du DCF était relativement plus élevée dans le système monocomposant que dans le mélange binaire sur le CC-$ZnCl_2$-AC. Le modèle non linéaire de l'isotherme de Freundlich a donné un bon ajustement aux données d'équilibre. Bien que la cinétique d'adsorption des deux contaminants ait suivi le modèle du pseudo-second ordre, l'analyse thermodynamique a confirmé que le processus était spontané, exothermique pour le PCM et endothermique pour le DCF. Les valeurs d'adsorption ont en outre suggéré que le mécanisme impliqué était majoritairement de nature physique. Les résultats obtenus démontrent la pertinence des techniques d'apprentissage automatique pour la modélisation des processus d'adsorption, le modèle de régression par forêt aléatoire (RFR) ayant présenté une précision et une robustesse supérieures pour la prédiction des performances d'adsorption du (PCM) et (DCF) sur le charbon actif CC-$ZnCl_2$-AC.

Mots-clés : Adsorption, cônes de cyprès, Paracetamol, Diclofenac, CCB-650, CC-$ZnCl_2$-AC.

الملخص

يستهلك السكان المنتجات الصيدلانية على نطاق واسع، والتي تُطرح باستمرار في البيئة، مما يجعلها مصدرًا مهمًا لتلوث النظم المائية. يهدف هذا البحث إلى إزالة هذه الملوثات باستخدام مواد ممتزة منخفضة التكلفة مشتقة من مخلفات زراعية محلية متوفرة متمثلة في مخاريط السرو. بالإضافة إلى ذلك، تم استخدام نماذج التعلم الآلي، والمتمثلة في الشبكات العصبية الاصطناعية (ANN) والانحدار العشوائي للغابات (RFR)، للتنبؤ بأداء الامتزاز تحت ظروف تشغيل مختلفة. وتُبرز النتائج إمكانات دمج المواد الممتزة المستدامة مع تقنيات التعلم الآلي لتحسين عمليات معالجة المياه وتعزيز كفاءتها. حضرت المواد الماصة على شكل فحم حيوي من مخاريط السرو عند درجات حرارة انحلال حراري مختلفة CCB-450، CCB-650، CCB-550. بالإضافة الى CC-$ZnCl_2$-AC كربون معدل كيميائيا بواسطة كلوريد الزنك لتحسين قدرة الامتزاز لازالة الباراسيتمول(PCM) والديكلوفيناك (DCF)في المحاليل المائية في كل من الانظمة الاحادية والثنائية. أظهرت نتائج التوصيف أن المواد المازة تتميز ببنية غير متبلورة ذات شكل مسامي يختلف من مادة الى مادة. علاوة على ذلك، أظهرت مساحة السطح النوعية زيادة ملحوظة بين الفحم الحيوي والفحم الحيوي المعدل كيميائيا. من خلال نتائج الإمتزاز أظهر CCB-650 أداءا متفوقا مقارنة ب CCB-450و CCB-550 حيث أزال 59.86 ملغ/غ من الباراسيتمول و 17.04 ملغ/غ من الديكلوفيناك ، بينما أظهر الكربون المنشط كفاءة أعلى حيث قدرت كفاءة إمتزازالباراسيتمول والديكلوفيناك على التوالي ب 213.38 ملغ/غ و 133.41 ملغ/غ .

تم وصف حركية الإمتزاز للباراسيتمول والديكلوفيناك على كل من CCB-650 وCC-$ZnCl_2$-AC بدقة بواسطة نموذج الدرجة الثانية، في حين قدم منحنى فروندليش أفضل ملاءمة لبيانات التوازن. أشار التحليل الديناميكي الحراري الى أن إمتزاز الباراسيتمول و الديكلوفيناك على الفحم الحيوي CCB-650 كان تلقائيا وماصا للحرارة، في حين كان الامتزاز على الفحم المعدل كيميائيا CC-$ZnCl_2$-AC تلقائيا أيضا، حيث أظهر الباراسيتمول طابعا طاردا للحرارة أما بالنسبة للديكلوفيناك فكان سلوكا ماصا للحرارة في النظام البسيط. علاوة على ذلك، كانت كفاءة امتزاز كلا الملوثين أعلى نسبيا في النظام الأحادي مقارنة بالنظام الثنائي على الفحم المنشط كيميائيا. وقد طابق نموذج فروندليش غير الخطي بيانات التوازن بشكل جيد. وعلى الرغم من أن حركية إمتزاز كلا الملوثين اتبعت نموذج شبه الدرجة الثانية، إلا أن التحليل الديناميكي الحراري أكد أن العملية تلقائية وطاردة للحرارة بالنسبة للباراسيتمول وماصة للحرارة بالنسبة للديكلوفيناك. كما أشارت قيم الإمتزاز إلى أن الالية المعنية فيزيائية في الغالب. تُظهر النتائج المتحصل عليها ملاءمة تقنيات التعلم الآلي لنمذجة عمليات الامتزاز، حيث أظهر نموذج الانحدار العشوائي للغابات (RFR) دقةً ومتانةً أعلى في التنبؤ بأداء امتزاز الباراسيتامول والديكلوفيناك باستخدام الكربون المنشط CC-$ZnCl_2$-AC .

الكلمات المفتاحية: الامتزاز، التعلم الالي، مخاريط السرو (CC)، االباراسيتمول ، الديكلوفيناك، الفحم الحيوي CCB-650، الفحم المعدل كيميائيا CC-$ZnCl_2$-AC.

Annex

Name and formula

Reference code:	98-006-7848
Compound name:	Zinc Oxide
Common name:	Zinc Oxide
Chemical formula:	O_1Zn_1

Crystallographic parameters

Crystal system:	Hexagonal
Space group:	P 63 m c
Space group number:	186
a (Å):	3.2540
b (Å):	3.2540
c (Å):	5.2150
Alpha (°):	90.0000
Beta (°):	90.0000
Gamma (°):	120.0000
Calculated density (g/cm^3):	5.65
Volume of cell (10^6 pm^3):	47.82
Z:	2.00
RIR:	5.55

Subfiles and quality

Subfiles:	User Inorganic
Quality:	User From Structure (=)

Comments

Creation Date:	10-01-1995
Modification Date:	01-04-2007
Original ICSD space group:	P63MC. Zn O obtained from beta-Zn (O H) Cl. X-ray diffraction (powder)
Structure type:	ZnS(2H). Temperature factors available. Rietveld profile refinement applied

The structure has been assigned a PDF number (calculated powder diffraction data):
01-080-0074

Structure type:	ZnS(2H)
Recording date:	1/10/1995
Modification date:	4/1/2007
ANX formula:	AX
Z:	2
Calculated density:	5.65

R value: 0.0433
Pearson code: hP4
Wyckoff code: b2
Publication title: Microstructural characterization of nanocrystals of Zn O and Cu O obtained from basic salts
ICSD collection code: 67848
Structure: ZnS(2H)
Chemical Name: Zinc Oxide
Second Chemical Formula: Zn O

References

Structure: Martin de Vidales, J.L.;Vila, E.;Rojas, R.M.;Garcia-Martinez, O., *Solid State Ionics*, **63**, 442 - 449, (1993)

Peak list

No.	h	k	l	d [A]	2Theta[deg]	I [%]
1	0	1	0	2.81805	31.727	55.2
2	0	0	2	2.60750	34.365	41.3
3	0	1	1	2.47923	36.203	100.0
4	0	1	2	1.91389	47.466	23.0
5	1	1	0	1.62700	56.517	34.5
6	0	1	3	1.47949	62.752	31.4
7	0	2	0	1.40902	66.281	4.8
8	1	1	2	1.38033	67.843	26.5
9	0	2	1	1.36025	68.984	13.0
10	0	0	4	1.30375	72.432	2.1
11	0	2	2	1.23961	76.837	4.3
12	0	1	4	1.18325	81.234	2.2
13	0	2	3	1.09460	89.454	9.6

Structure

No.	Name	Elem.	X	Y	Z	Biso	sof	Wyck.
1	O1	O	0.33333	0.66667	0.38240	0.4700	1.0000	2b
2	ZN1	Zn	0.33333	0.66667	0.00000	0.4700	1.0000	2b

Stick Pattern

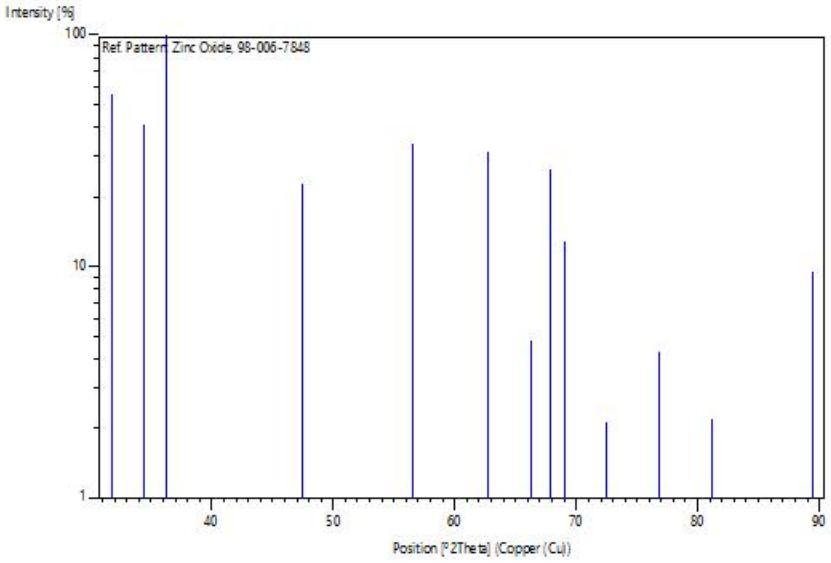
Intensity [%]
100
10
1
Ref. Pattern: Zinc Oxide, 98-006-7848
40
50
60
70
80
90
Position [°2Theta] (Copper (Cu))